Measurement of B meson production fraction ratios in proton-proton collisions at $\sqrt{s} = 13$ TeV using open-charm and charmonium decays

A. Hayrapetyan *et al.*[*]
(CMS Collaboration)

(Received 10 February 2026; accepted 29 May 2026; published 6 July 2026)

Production fraction ratios of B^+, B^0, and B_s^0 mesons are measured in proton-proton collisions at $\sqrt{s} =$ 13 TeV using a special dataset recorded in 2018 with high-rate triggers designed to collect an unbiased sample of 10^{10} b hadrons with the CMS experiment at the LHC. These data allow the study of the open-charm decays of B mesons ($B_{(s)} \to \pi D_{(s)}$) where the D meson decays into fully hadronic final states. By utilizing known branching fractions and precise theoretical calculations, production fraction ratios as functions of B meson transverse momentum (p_{T}) and rapidity (y) are measured using open-charm decays in the kinematic range of $8 < p_{\mathrm{T}} < 60$ GeV and $|y| < 2.25$. In addition, the same dataset is used to measure the relative production fraction ratios with the charmonium decay channels [$B_{(s)} \to XJ/\psi$ with X indicating a K^+, $K^*(892)^0$, or $\phi(1020)$ meson] where the J/ψ meson decays into a pair of muons. The open-charm results are used to normalize the relative production fraction ratios obtained from the charmonium samples. Measurements of the ratios of branching fractions of B meson decays to charmonium and open-charm final states are also reported, which will improve the world-average values of these ratios. Finally, we test isospin invariance in B meson production in proton-proton collisions and observe that it holds within the experimental precision.

DOI: 10.1103/36cv-vst3

I. INTRODUCTION

Studies of production fractions of various species of b hadrons have been a topic of intense experimental and theoretical interest since the CERN Large Electron-Positron (LEP) collider era. These fractions, defined as the ratios of the number of produced b hadron species to the total number of produced b hadrons, are closely related to the b quark fragmentation fractions. Specifically, the fractions f_u, f_d, and f_s are the production fractions for B^+, B^0, and B_s^0 mesons, respectively. Here and in what follows, charge-conjugate final states are implicitly included unless otherwise indicated, and K^{*0} and ϕ represent the $K^*(892)^0$ and $\phi(1020)$ mesons, respectively. Production fraction ratios (PFRs), namely f_s/f_u, f_s/f_d, and f_d/f_u, are also of interest. Measurements of the production fractions and PFRs have been performed in electron-positron (e^+e^-), proton-antiproton ($p\bar{p}$), and proton-proton (pp) collisions at various energies. Of particular interest are measurements of the last decade conducted at the CERN LHC by the LHCb [1–5], ATLAS [6], and CMS [7] experiments, as the results are used in a variety of ways. The b hadron production fraction measurements directly enter the precision measurements of branching fractions of B_s^0 meson decays, as the yields of B^+ or B^0 meson decays are used to normalize the B_s^0 measurements. The only measurements of branching fractions of B_s^0 decays that are not directly dependent on the b hadron production ratios have been performed by Belle on the $\Upsilon(5S)$ peak and are presently limited to about 20% precision [8]. Furthermore, the dominant systematic uncertainty in the most precise single measurement of the rare $B_s^0 \to \mu^+\mu^-$ decay, performed by the CMS Collaboration [9], is from the uncertainty in f_s/f_u.

The LHCb Collaboration has studied f_s/f_u and f_s/f_d as functions of the absolute rapidity ($|y|$) and transverse momentum (p_{T}) of the B mesons as well as the pp collision energy. While no evidence has been found for a dependence on $|y|$, there is a clear dependence on both the B p_{T} and the pp collision energy [1–5]. The latest LHCb result [5] finds that f_s/f_d decreases linearly versus B p_{T} in the $p_{\mathrm{T}} < 40$ GeV range accessible by this measurement for pp collisions at $\sqrt{s} = 13$ TeV. A recent CMS measurement [7] using data collected at $\sqrt{s} = 13$ TeV finds a similar dependence for f_s/f_u for $p_{\mathrm{T}} \lesssim 18$ GeV. By extending the measurement up to $p_{\mathrm{T}} < 70$ GeV, it is found that f_s/f_u reaches an asymptotic value around 18 GeV,

[*]Full author list given at the end of the article.

remaining constant above this value. This measurement was performed using the charmonium decay channels [$B^+ \to J/\psi(\mu^+\mu^-)K^+$, $B^0 \to J/\psi(\mu^+\mu^-)K^{*0}(K^+\pi^-)$, and $B_s^0 \to J/\psi(\mu^+\mu^-)\phi(K^+K^-)$]. The present world-average value of $\mathcal{B}(B_s^0 \to J/\psi\phi)$ is dominated by the LHCb measurement [5], which uses the PFR measured by LHCb as an input. As a result, while the f_s/f_u dependence on B p_T can be determined, the normalization is unknown, and therefore the CMS result is expressed in terms of the relative PFR, $\mathcal{R}_s$, defined as the ratio of efficiency-corrected yields of B_s^0 to B^+ mesons, which is proportional to f_s/f_u.

Another area of interest is testing the limits of isospin symmetry, which postulates the same production rate for B^+ and B^0, i.e., $f_d/f_u = 1$. In most applications of PFRs, e.g., when measuring various branching fractions, the isospin symmetry in production is assumed. While the isospin symmetry may be a good assumption in the case of isospin-singlet e^+e^- collisions at the Z or $\Upsilon(4S)$, it is less obvious for hadronic collisions, where the production process is much more complicated. Even in e^+e^- collisions, the $f_u = f_d$ assumption may not hold at the $\Upsilon(4S)$ resonance, where the majority of data are taken by B factories, due to the Coulomb interaction in the B^+B^- system near the production threshold, which is absent for the $B^0\bar{B}^0$ system. In fact, there are hints at about 2 standard deviations that $f_u \neq f_d$ for the $\Upsilon(4S)$ production of B mesons [10,11]. The CMS Collaboration provided the first test of isospin invariance in pp collisions by measuring the f_d/f_u ratio and demonstrating that it is flat in the entire $12 < p_T < 70$ GeV range of the measurement and consistent with unity ($f_d/f_u = 0.998 \pm 0.063$) within the 6% precision of the measurement [7].

In this paper, we extend the earlier CMS analysis [7], which used 2018 data collected in pp collisions at $\sqrt{s} =$ 13 TeV with dimuon triggers, by measuring f_s/f_d, f_s/f_u, and f_d/f_u in a dedicated dataset from the same year and collision energy, obtained with high-rate single-muon triggers designed to collect an unbiased sample of 10^{10} b hadrons [12]. This dataset, corresponding to an integrated luminosity of 41.6 ± 1.0 fb^{-1} [13], allows for a direct measurement of PFRs using the open-charm B meson decays $B^+ \to \pi^+\bar{D}^0(K^+\pi^-)$, $B^0 \to \pi^+D^-(K^+\pi^-\pi^-)$, and $B_s^0 \to \pi^+D_s^-(\pi^-\phi(K^+K^-))$ for the first time in CMS. Additionally, the relative PFR variables, $\mathcal{R}_s$ and $\mathcal{R}_s^d$, are measured simultaneously with charmonium decays [$B^+ \to J/\psi(\mu^+\mu^-)K^+$, $B^0 \to J/\psi(\mu^+\mu^-)K^{*0}(K^+\pi^-)$, and $B_s^0 \to J/\psi(\mu^+\mu^-)\phi(K^+K^-)$], where $\mathcal{R}_s$ and $\mathcal{R}_s^d$ are defined as the ratio of efficiency-corrected yields of B_s^0 to B^+ and B^0 mesons, respectively. We also derive the absolute normalization for $\mathcal{R}_s$ and $\mathcal{R}_s^d$ by combining the results from the open-charm and charmonium decays, which can be used for extraction of the PFRs using charmonium decays. Another product of this analysis is the measurement of three B branching fraction ratios. Representative Feynman diagrams for the open-charm and charmonium decays are shown in Fig. 1. Tabulated data for this analysis can be found in the HEPData database [14].

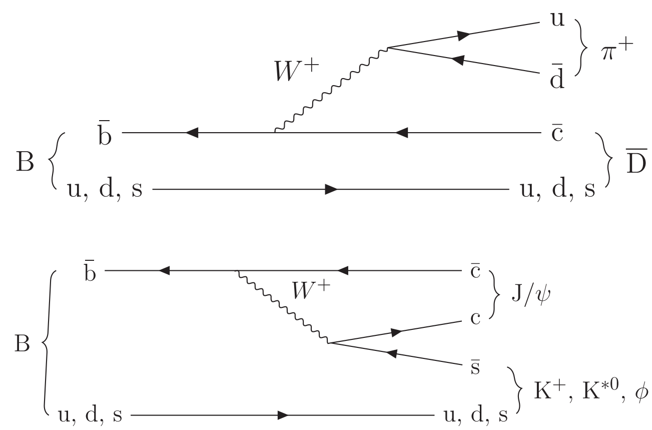

FIG. 1. Representative Feynman diagrams for the open-charm (upper) and charmonium (lower) decays of the B^+, B^0, and B_s^0 mesons.

The paper is organized as follows. After a brief description of the CMS detector in Sec. II, we discuss the data and simulated event samples in Sec. III and outline the analysis strategy in Sec. IV. The event reconstruction and B meson candidate selection are described in Sec. V, followed by the signal extraction in Sec. VI and the efficiency determination in Sec. VII. Systematic uncertainties are discussed in Sec. VIII, followed by the presentation of the results in Sec. IX. The paper is summarized in Sec. X.

II. THE CMS DETECTOR

The central feature of the CMS apparatus is a superconducting solenoid of 6 m internal diameter, providing a magnetic field of 3.8 T. Within the solenoid volume are a silicon pixel and strip tracker, a lead tungstate crystal electromagnetic calorimeter, and a brass and scintillator hadron calorimeter, each composed of a barrel and two end cap sections. Forward calorimeters extend the pseudorapidity (η) coverage provided by the barrel and end cap detectors. Muons are measured in gas-ionization detectors embedded in the steel flux-return yoke outside the solenoid.

During the 2018 LHC running period when the data used in this paper were recorded, the silicon tracker consisted of 1856 silicon pixels and 15 148 silicon strip detector modules. Details on the pixel detector can be found in Ref. [15]. The silicon tracker measures charged particles within the pseudorapidity range $|\eta| < 3$. For nonisolated particles of $1 < p_T < 10$ GeV, the track resolutions are typically 1.5% in p_T and 20–75 μm in the transverse impact parameter [16].

Muons are measured in the pseudorapidity range $|\eta| < 2.4$, with detection planes made using three technologies: drift tubes, cathode strip chambers, and resistive-plate chambers. The single-muon trigger efficiency exceeds 90% over the full pseudorapidity range, and the efficiency to reconstruct and identify muons is greater than 96%. Matching muons to tracks measured in the silicon tracker results in a relative transverse momentum resolution, for muons with p_{T} up to 100 GeV, of 1% in the barrel and 3% in the end caps [17].

Events of interest are selected using a two-tiered trigger system. The first level (L1), composed of custom hardware processors, uses information from the calorimeters and muon detectors to select events at a rate of around 100 kHz within a fixed latency of about 4 μs [18]. The second level, known as the high-level trigger (HLT), consists of a farm of processors running a version of the full event reconstruction software optimized for fast processing and reduces the event rate to a few kilohertz before data storage [19].

A more detailed description of the CMS detector, together with a definition of the coordinate system used and the relevant kinematic variables, can be found in Refs. [20,21].

III. DATA AND SIMULATED SAMPLES

A. The CMS B parking campaign

During the 2018 data taking period, CMS deployed a novel trigger and data processing strategy, referred to as "B parking," which enabled the collection and reconstruction of order 10^{10} unbiased b hadron decays [12]. The trigger strategy used to collect these data exploited the fact that b hadrons are predominantly produced in pairs at the LHC, and therefore one could use a semileptonic decay of one ("tag-side") b hadron to trigger on the event, while the other ("probe-side") b hadron can decay arbitrarily, i.e., its decay is *unbiased* by the trigger.

The B parking trigger requires a muon with a relatively high p_{T} and a significant displacement from the pp collision point. This triggering strategy is made possible by a relatively low rate of L1 single-muon triggers, combined with a gradual decrease of the L1 bandwidth and online computing resource usage as the instantaneous luminosity $\mathcal{L}$ decreases over the LHC fill. Specifically, as $\mathcal{L}$ decreases, the L1 and HLT trigger rates of the nominal CMS physics program also decrease. Therefore, the B parking trigger thresholds were tuned to use most of the available bandwidth and resources by switching on triggers with looser requirements as $\mathcal{L}$ goes down.

Table I summarizes the muon trigger requirements imposed at the L1 and HLT. The L1 trigger logic requires the presence of a muon within $|\eta| < 1.5$ and imposes a variable minimum p_{T} requirement. Additionally, for the full pseudorapidity range of $|\eta| < 2.4$, a single-muon L1 trigger with a fixed p_{T} threshold of 22 GeV is used. Since the muon displacement information is not available at L1, only p_{T} and $|\eta|$ thresholds are used to control the rate. At the HLT, the p_{T} threshold is refined, based on more precise momentum reconstruction compared to that at L1. Additionally, a requirement is imposed on the minimum two-dimensional muon track impact parameter significance $\mathrm{IP}_{\mathrm{sig}}^{\mathrm{beam}}$, defined as the distance of closest approach of the track to the beamline in the plane transverse to the beams, divided by its uncertainty. Overall, this strategy leads to an L1 rate of up to about 30 kHz and an HLT output rate of up to 5.4 kHz.

TABLE I. Summary of the single-muon B parking triggers used in this analysis.

Peak $\mathcal{L}$ (10^{34} cm^{-2} s^{-1})	L1 p_{T}^{μ} (GeV)	HLT p_{T}^{μ} (GeV)	HLT μ $\mathrm{IP}_{\mathrm{sig}}^{\mathrm{beam}}$	Peak HLT rate (kHz)
1.7	>12	>12	>6	1.5
1.5	>10	>9	>6	2.8
1.3	>9	>9	>5	3.0
0.9	>7	>7	>4	5.4

The B parking dataset corresponds to an integrated luminosity of 41.6 ± 1.0 fb^{-1} [13], about 20% less than the integrated luminosity of 59.8 fb^{-1} collected with the main physics triggers operating during the entire 2018 data taking.

B. Event simulation

Monte Carlo (MC) simulated samples are used to evaluate signal efficiencies, optimize the analysis, and model various background sources. Signal and background processes are generated using the PYTHIA 8.230 [22] package, including parton showering, fragmentation, and hadronization. The underlying event is also modeled with PYTHIA using the CP5 [23] tune. The parton distribution functions are taken from the NNPDF3.1 set [24]. To account for the effects of additional interactions in the same or adjacent bunch crossings (pileup), simulated minimum bias events are added to the hard scattering, with the pileup vertex multiplicity matching that observed in the data. Samples are interfaced with EVTGEN 1.3.0 [25], which is used to simulate the decays of heavy hadrons. Final-state photon radiation is modeled with PHOTOS 3.61 [26].

The following signal samples were generated with and without emulation of trigger conditions:

(i) $B^+ \to \pi^+ \bar{D}^0(K^+\pi^-)$,
(ii) $B^0 \to \pi^+ D^-(K^+\pi^-\pi^-)$,
(iii) $B_s^0 \to \pi^+ D_s^-(\pi^-\phi(K^+K^-))$,
(iv) $B^+ \to J/\psi(\mu^+\mu^-)K^+$,
(v) $B^0 \to J/\psi(\mu^+\mu^-)K^{*0}(K^+\pi^-)$, and
(vi) $B_s^0 \to J/\psi(\mu^+\mu^-)\phi(K^+K^-)$.

In addition, we simulated several background processes. In the open-charm channels, they are the Cabibbo-suppressed decays

(i) $B^+ \to K^+ \bar{D}^0(K^+\pi^-)$,
(ii) $B^0 \to K^+ D^-(K^+\pi^-\pi^-)$, and
(iii) $B_s^0 \to K^+ D_s^-(\pi^-\phi(K^+K^-))$.

In the charmonium channels, they are

(i) $B^+ \to J/\psi(\mu^+\mu^-)\pi^+$ and

(ii) $\Lambda_b^0 \to J/\psi(\mu^+\mu^-)pK^-$.

The CMS detector response is simulated using the GEANT4 package [27]. Simulated samples are reconstructed with the same software packages as used for collision data.

IV. ANALYSIS STRATEGY

Measurements of the PFRs of B mesons are performed in the open-charm and charmonium decay modes. As independent branching fraction measurements of B_s^0 meson decay modes with a precision better than about 20% are not available, the only way to extract the PFR for the B_s^0 meson is by using theoretical predictions. Precise theoretical calculations are currently available for the open-charm decays using the quantum chromodynamics factorization approach [28–30]. Since no reliable calculations exist for the charmonium modes, independent absolute measurements of f_s/f_d and f_s/f_u are impossible in this channel. Therefore, we utilize the measured PFRs in the open-charm channels and normalize the relative measurement of PFRs in the charmonium channels to those in order to extract the PFRs in the charmonium channels. Measurements of f_d/f_u can be directly performed in both channels as they do not involve B_s^0 decays. To ensure that our measurement of f_d/f_u is a test of isospin invariance, it is important to avoid assuming isospin invariance. The values of most B^0 and B^+ branching fractions are dominated by results from the B factories and often assume equal production of B^+B^- and $B^0\bar{B}^0$ pairs at the $\Upsilon(4S)$ from isospin invariance. There are indications that this assumption is not valid, and a recent evaluation has found $r^{\pm,0} \equiv \mathcal{B}(\Upsilon(4S) \to B^+B^-)/\mathcal{B}(\Upsilon(4S) \to B^0\bar{B}^0) = 1.057 \pm 0.023$ [11].

A. Open-charm measurement

The most recent and precise theoretical calculations of the branching fractions of the $B^0 \to K^+D^-$ and $B_s^0 \to \pi^+D_s^-$ decays [31] reveal a puzzling substantial discrepancy between the theory predictions and the experimental measurements in the individual decay channels. Nevertheless, the prediction for the ratio of these decays appears to be in good agreement with the experimental measurements [31], so we will rely on this theoretical framework to extract the f_s/f_d ratio.

At the same time, the prediction for the branching fraction of the Cabibbo-favored $B^0 \to \pi^+D^-$ decay is prone to a sizable additional uncertainty, as there is a nonfactorizable exchange diagram that contributes to this decay channel, which is absent in the case of the Cabibbo-suppressed $B^0 \to K^+D^-$ decay. The current theoretical estimate of the impact of this diagram on the corresponding branching fraction is 0.966 ± 0.056 [29], which contributes an additional ≈6% theoretical uncertainty. This presents an experimental challenge, given the lack of particle identification in CMS, as far as pion/kaon separation is concerned. Because of that, there is no difference in the experimental topology for the Cabibbo-suppressed and Cabibbo-favored decays, so the latter becomes a major background to the former, making it impractical to extract the $B^0 \to K^+D^-$ signal in bins of p_T or rapidity of the B^0 meson. We overcome this difficulty by measuring the $B^0 \to \pi^+D^-$ signal and then relating it to the theoretically clean $B^0 \to K^+D^-$ signal by using the world average of the ratio of these two branching fractions: $\mathcal{B}(B^0 \to K^+D^-)/\mathcal{B}(B^0 \to \pi^+D^-) = 0.0819 \pm 0.0020$ [32], which is known to a 2.4% precision and is independent of the f_s/f_d value. That allows for the extraction of the f_s/f_d value in a theoretically clean fashion by using the much more copious Cabibbo-favored decay channel without introducing a large theoretical uncertainty due to the nonfactorizable exchange diagram contribution.

The formula used for the f_s/f_d measurement is as follows (using notations of Ref. [5]):

$$\begin{aligned}
f_s/f_d &= \frac{\mathcal{B}(B^0 \to \pi^+D^-)}{\mathcal{B}(B_s^0 \to \pi^+D_s^-)} \frac{\mathcal{B}(D^- \to K^+\pi^-\pi^-)}{\mathcal{B}(D_s^- \to \pi^-\phi)\mathcal{B}(\phi \to K^+K^-)} \frac{N_{\text{corr}}(B_s^0 \to \pi^+D_s^-(\pi^-\phi(K^+K^-)))}{N_{\text{corr}}(B^0 \to \pi^+D^-(K^+\pi^-\pi^-))} \\
&= \frac{\mathcal{B}(B^0 \to K^+D^-)}{\mathcal{B}(B_s^0 \to \pi^+D_s^-)} \frac{\mathcal{B}(B^0 \to \pi^+D^-)}{\mathcal{B}(B^0 \to K^+D^-)} \frac{\mathcal{B}(D^- \to K^+\pi^-\pi^-)}{\mathcal{B}(D_s^- \to \pi^-\phi)\mathcal{B}(\phi \to K^+K^-)} \frac{N_{\text{corr}}(B_s^0 \to \pi^+D_s^-(\pi^-\phi(K^+K^-)))}{N_{\text{corr}}(B^0 \to \pi^+D^-(K^+\pi^-\pi^-))} \\
&= \Phi_{\text{PS}} \frac{|V_{us}|^2}{|V_{ud}|^2} \frac{f_K^2}{f_\pi^2} \frac{\tau_{B^0}}{\tau_{B_s^0}} \frac{1}{N_a N_F} \frac{\mathcal{B}(B^0 \to \pi^+D^-)}{\mathcal{B}(B^0 \to K^+D^-)} \frac{\mathcal{B}(D^- \to K^+\pi^-\pi^-)}{\mathcal{B}(D_s^- \to \pi^-\phi)\mathcal{B}(\phi \to K^+K^-)} \frac{N_{\text{corr}}(B_s^0 \to \pi^+D_s^-(\pi^-\phi(K^+K^-)))}{N_{\text{corr}}(B^0 \to \pi^+D^-(K^+\pi^-\pi^-))},
\end{aligned} \quad (1)$$

where $\Phi_{\text{PS}} = 0.97074 \pm 0.00010$ is the ratio of the phase space factors for the two decays [given by inverting the expression on the last line of Eq. (7) in Ref. [31]]; V_{ud} and V_{us} are the corresponding CKM matrix elements; τ_{B^0} and $\tau_{B_s^0}$ are lifetimes of the B^0 and B_s^0 mesons, respectively; f_π and f_K are decay constants for the π and K mesons; N_a and N_F are, respectively, the ratio of Wilson coefficients squared of the D^+K^- and $D_s^+\pi^-$ decays and the ratio of

TABLE II. Inputs for the open-charm PFR measurements.

Input variable	Value	Ref.
$\Phi_{\rm PS}$	0.97074 ± 0.00010	PDG [32]; Ref. [31], Eq. (7)
$\lvert V_{us}\rvert f_K/(\lvert V_{ud}\rvert f_\pi)$	0.27683 ± 0.00035	Ref. [33], Eq. (107)
$\tau_{B^0}/\tau_{B_s^0}$	1.0021 ± 0.0034	HFLAV [10,34]
$1/N_{\rm a}$	$1.0048^{+0.0046}_{-0.0022}$	Ref. [31], Eq. (20)
$1/N_{\rm F}$	1.002 ± 0.042	Ref. [31], Eq. (16)
$\mathcal{B}(B^0 \to K^+D^-)/\mathcal{B}(B^0 \to \pi^+D^-)$	0.0819 ± 0.0020	PDG [32]
$\mathcal{B}(D^- \to K^+\pi^-\pi^-)$	0.0938 ± 0.0016	PDG [32]
$\mathcal{B}(D_s^- \to \pi^-\phi)\mathcal{B}(\phi \to K^+K^-)$	0.0225 ± 0.0005	PDG [32]
$\mathcal{B}(B^+ \to \pi^+\bar{D}^0)$	0.00461 ± 0.00010	PDG [32]
$\mathcal{B}(D^0 \to K^-\pi^+)$	0.03945 ± 0.00030	PDG [32]

form factors squared for the $B^0 \to K^+D^-$ and $B_s^0 \to \pi^+D_s^-$ decays; and $N_{\rm corr}$ (X) is the efficiency- and acceptance-corrected event yield for process X. The last equality in Eq. (1) uses a theoretical calculation for the ratio of branching fractions of the $B^0 \to K^+D^-$ to $B_s^0 \to \pi^+D_s^-$ decays from Ref. [31].

For the f_d/f_u extraction, no theoretical calculations are needed and the following formula is used:

$$\frac{f_d}{f_u} = \frac{\mathcal{B}(B^+ \to \pi^+\bar{D}^0)}{\mathcal{B}(B^0 \to \pi^+D^-)}\frac{\mathcal{B}(D^0 \to K^-\pi^+)}{\mathcal{B}(D^- \to K^+\pi^-\pi^-)} \times \frac{N_{\rm corr}(B^0 \to \pi^+D^-(K^+\pi^-\pi^-))}{N_{\rm corr}(B^+ \to \pi^+\bar{D}^0(K^+\pi^-))}. \tag{2}$$

Finally, f_s/f_u can be obtained from the product of Eqs. (1) and (2) as

$$f_s/f_u = \Phi_{\rm PS}\frac{\lvert V_{us}\rvert^2}{\lvert V_{ud}\rvert^2}\frac{f_K^2}{f_\pi^2}\frac{\tau_{B^0}}{\tau_{B_s^0}}\frac{1}{N_{\rm a}N_{\rm F}}\frac{\mathcal{B}(B^+ \to \pi^+\bar{D}^0)}{\mathcal{B}(B^0 \to K^+D^-)} \times \frac{\mathcal{B}(\bar{D}^0 \to K^+\pi^-)}{\mathcal{B}(D_s^- \to \pi^-\phi)\mathcal{B}(\phi \to K^+K^-)} \times \frac{N_{\rm corr}(B_s^0 \to \pi^+D_s^-(\pi^-\phi(K^+K^-)))}{N_{\rm corr}(B^+ \to \pi^+\bar{D}^0(K^+\pi^-))}. \tag{3}$$

Utilizing the same measurements as in the average values of $\mathcal{B}(B^+ \to \pi^+\bar{D}^0)$ and $\mathcal{B}(B^0 \to \pi^+D^-)$ in Ref. [32], but updating the charm branching fractions and converting to $r^{\pm,0} = 1.057 \pm 0.023$, we obtain a value of $\mathcal{B}(B^+ \to \pi^+\bar{D}^0)/\mathcal{B}(B^0 \to \pi^+D^-) = 1.763 \pm 0.066$ (not including the $r^{\pm,0}$ uncertainty). The other values used in Eqs. (1)–(3) are collected in Table II.

B. Charmonium measurement

In the charmonium channel, we use $B^+ \to J/\psi(\mu^+\mu^-)K^+$, $B^0 \to J/\psi(\mu^+\mu^-)K^{*0}(K^+\pi^-)$, and $B_s^0 \to J/\psi(\mu^+\mu^-)\phi(K^+K^-)$ decays to measure the $\mathcal{R}_s$ and $\mathcal{R}_s^d$ parameters, which are determined as follows:

$$\mathcal{R}_s = \frac{N_{\rm corr}(B_s^0 \to J/\psi(\mu^+\mu^-)\phi(K^+K^-))}{N_{\rm corr}(B^+ \to J/\psi(\mu^+\mu^-)K^+)} = \frac{f_s}{f_u}\frac{\mathcal{B}(B_s^0 \to J/\psi\phi)\mathcal{B}(\phi \to K^+K^-)}{\mathcal{B}(B^+ \to J/\psi K^+)} \tag{4}$$

and

$$\mathcal{R}_s^d = \frac{N_{\rm corr}(B_s^0 \to J/\psi(\mu^+\mu^-)\phi(K^+K^-))}{N_{\rm corr}(B^0 \to J/\psi(\mu^+\mu^-)K^{*0}(K^+\pi^-))} = \frac{f_s}{f_d}\frac{\mathcal{B}(B_s^0 \to J/\psi\phi)\mathcal{B}(\phi \to K^+K^-)}{\mathcal{B}(B^0 \to J/\psi K^{*0})\mathcal{B}(K^{*0} \to K^+\pi^-)}. \tag{5}$$

The ratio f_d/f_u can be determined directly as

$$\frac{f_d}{f_u} = \frac{N_{\rm corr}(B^0 \to J/\psi(\mu^+\mu^-)K^{*0}(K^+\pi^-))}{N_{\rm corr}(B^+ \to J/\psi(\mu^+\mu^-)K^+)} \times \frac{\mathcal{B}(B^+ \to J/\psi K^+)}{\mathcal{B}(B^0 \to J/\psi K^{*0})\mathcal{B}(K^{*0} \to K^+\pi^-)}. \tag{6}$$

As for the open-charm states, the branching fractions used to obtain $\mathcal{R}_s$ and $\mathcal{R}_s^d$ are from Ref. [32]. For the determination of f_d/f_u, we use the same measurements as in the average values of $\mathcal{B}(B^+ \to J/\psi K^+)$ and $\mathcal{B}(B^0 \to J/\psi K^{*0})$ from Ref. [32], but scaling the results to $r^{\pm,0} = 1.057 \pm 0.023$ [11] to obtain $\mathcal{B}(B^+ \to J/\psi K^+)/\mathcal{B}(B^0 \to J/\psi K^{*0}) = 0.769 \pm 0.033$ (not including the $r^{\pm,0}$ uncertainty). The existing measurements of $\mathcal{B}(B^0 \to J/\psi K^{*0})$ include one angular analysis, which results in a pure branching fraction measurement [35], and the remainder, which select events in a mass region around the K^{*0} mass. Using the model from Ref. [35] to estimate the S-wave contribution in the other measurements and scaling all of the measured branching fractions to correspond to the mass region used in our analysis results in a negligible change.

V. EVENT RECONSTRUCTION AND B CANDIDATE SELECTION

Since the events used in this analysis are collected with the B parking triggers, we require that the muon which triggered the event readout (μ_{trig}) is reconstructed offline. The z position of the point of closest approach of the triggering muon to the beamline is used to select the primary vertex (PV) of the hard interaction. Tracks are required to pass the "high-purity" quality criteria [36,37].

A. Open-charm analysis

The B candidate selection relies on the probe side of the event. We require the tracks used to build the B candidate to be separated from the triggering muon by $\Delta R(\text{track}, \mu_{\text{trig}}) > 0.4$, where $\Delta R = \sqrt{(\Delta\eta)^2 + (\Delta\phi)^2}$, and ϕ is the azimuthal angle in radians. To reduce pileup, the tracks are also required to originate from the vicinity of the PV, with $\Delta z(\text{track}, \text{PV}) < 0.5$ cm. Tracks are further selected to have $|\eta| < 2.4$ and $p_{\text{T}} > 1$ GeV. Since the B mesons result in displaced secondary vertices (SVs) due to their sizable decay distance, we only consider tracks with $\text{IP}_{\text{sig}} > 1$, where IP_{sig} is defined as the transverse distance of closest approach of a track to the PV divided by its uncertainty.

Depending on the final state, B candidates have either three (B^+) or four (B^0 and B_s^0) tracks originating from the final-state particles. We create B candidates out of all combinations of pion and kaon mass assignments to these tracks. Since the D meson from the B candidate decay will be displaced from the B meson decay SV, we start the B candidate reconstruction by finding a tertiary vertex (TV) of a decay of the corresponding D meson. The $\bar{D}^0 \to K^+\pi^-$, $D^- \to K^+\pi^-\pi^-$, and $D_s^- \to \pi^-K^+K^-$ candidates are reconstructed by selecting the correct number of tracks with the correct charge and an invariant mass within 20, 20, and 15 MeV of the world-average D meson masses $m(D^0)$, $m(D^-)$, and $m(D_s^-)$ [32], respectively. In all three decay channels, the highest p_{T} (leading) track of the pair or triplet is required to have $p_{\text{T}} > 1.5$ GeV. The tracks of the D candidate are then fitted to a TV, and the D candidate is accepted if the fit probability exceeds 0.01 and the significance of the displacement of the TV from the PV in the plane transverse to the beams $S_{xy,\text{TV}}$, defined as the distance between the two vertices in the x-y plane divided by its uncertainty, exceeds 5. The SV position is then obtained by fitting the remaining track with $p_{\text{T}} > 1.5$ GeV and correct charge, and the D candidate momentum vector to a common vertex. The B candidate is then accepted if the significance of the transverse displacement of the SV from the PV, $S_{xy,\text{SV}}$, defined in a similar way as $S_{xy,\text{TV}}$, exceeds 7, and the cosine of the angle between the line connecting the PV and SV and the B candidate momentum vector, $\cos\alpha_B$, exceeds 0.999.

In the B_s^0 channel, an additional requirement on the invariant mass of the K^+K^- pair to be within 10 MeV of the world-average ϕ mass [32] is applied. This is crucial to remove the copious background from $B^0 \to \pi^+D^-(K^+\pi^-\pi^-)$ decays with one of the pions being misassigned a kaon mass, which results in the shift of the four-track invariant mass peak into the B_s^0 region. The narrowness of the ϕ resonance ensures that this background is negligible (rejection power of over 200) after this extra selection, while retaining about 85% of the signal. The contribution from the K^+K^- continuum in the D_s^- decay mode within the ϕ meson mass window can be estimated from a Dalitz plot analysis of this decay mode by *BABAR* [38]. The parametrization of the invariant mass distribution for the ϕ and nonresonant components, as described in Ref. [38], is applied to fit the K^+K^- invariant mass distribution in data. Based on the fit results, the nonresonant contribution in the B_s^0 channel, which amounts to about 5%, is subsequently subtracted using the $_s\mathit{Plot}$ technique [39].

The summary of the preselection requirements to identify B candidates is given in Table III. While multiple B candidates per event are allowed, ≈98% of events have only a single candidate per event.

To further improve signal purity, we perform a multivariate analysis (MVA) based on boosted decision trees (BDTs). One BDT is trained for each of the three channels. The preselection described above improves the BDT performance, as it reduces the bulk of backgrounds with easily distinguishable topology, thus allowing for the BDT to optimize the rejection against the remaining backgrounds, which are topologically much closer to the signal.

The BDTs are trained on simulated signal events with the B candidate mass in a signal region (SR), centered on the corresponding B meson mass, against the background, which is taken from the upper sideband (SB) of the data. This SB is dominated by the combinatorial background, mainly composed of combinations of a D meson and a random track, similar to the background in the SR. In contrast, the lower sideband is dominated by partially reconstructed B decays, which do not populate the SR and are therefore not used for the BDT training. Signal samples are weighted so that their normalization corresponds to the signal yield in data after the preselection. The SR is defined using the invariant mass of the B candidate as 5.20–5.35 GeV (5.30–5.45 GeV), while the SB is defined as 5.40–5.55 GeV (5.50–5.65 GeV) in the $B^+ \to \pi^+\bar{D}^0$ and $B^0 \to \pi^+D^-$ ($B_s^0 \to \pi^+D_s^-$) channels. The following variables are used as inputs to the BDTs: IP_{sig} of all three or four tracks of the B candidate; invariant mass of the D candidate (and of the ϕ candidate in the $B_s^0 \to \pi^+D_s^-$ channel) before the TV fit; fit probabilities for the SV and TV; $\cos\alpha_B$; and displacement significances in the x-y plane of the SV with respect to the PV and of the TV with respect to the SV. The BDTs are trained using the XGBOOST

TABLE III. Summary of the preselection requirements for B candidates in the open-charm analysis. The ⋯ entries indicate that the selection does not apply to this channel.

Variable	Selection		
	B^+	B^0	B_s^0
General track selection			
Track p_T		>1 GeV	
Track $\lvert\eta\rvert$		>2.4	
$\Delta z(\text{track}, \mu_{\text{trig}})$		<0.5 cm	
Track IP_{sig}		>1	
D candidate selection			
D candidate leading track p_T		>1.5 GeV	
TV fit probability		>0.01	
$S_{xy,\text{TV}}$		>5	
D candidate mass window	± 20 MeV	± 20 MeV	± 15 MeV
$\lvert M(K^+K^-) - m(\phi)\rvert$	⋯	⋯	<10 MeV
B candidate selection			
p_T of the remaining B candidate track		>1.5 GeV	
$S_{xy,\text{SV}}$		>7	
$\cos\alpha_B$		>0.999	

[40] 0.72 package, with gradient boosting. Hyperparameters are optimized via a Bayesian optimization procedure using the SCIKIT-OPTIMIZE [41] 0.9.0 package. The cutoffs on the BDT discriminants were optimized using the $S/\sqrt{S+B}$ figure of merit (FOM), where S and B denote signal and background yields, respectively. The FOM after the BDT selection is increased by about a factor of 2 with respect to the preselection. For an optimized cutoff-based analysis using the same input variables and FOM as the BDT, the FOM is about 20% lower than for the BDT selection. Consequently, the BDT analysis is chosen as the default approach for the signal extraction and the PFR measurement. It was checked that the output BDT variables in data obtained from background-subtracted B candidates after the BDT selection are well described by the signal simulation. The BDT was also checked for a potential mass bias ("sculpting"), and none was found.

B. Charmonium analysis

In the charmonium channel, given the higher purity of the signal, no significant improvement is expected from an MVA, so a cutoff-based analysis is used instead. The selection of the B candidates starts with a requirement of an opposite-sign (OS) muon pair with each muon passing the *soft* identification requirements [17] and having a distance of closest approach to the PV in the z direction of $\Delta z < 1$ cm. Each muon is required to have $p_T > 3.5$ GeV in the barrel ($\lvert\eta\rvert < 1.1$), $p_T > 1.5$ GeV in the end cap ($1.5 < \lvert\eta\rvert < 2.4$), and $p_T > 3.5 + \frac{(1.5-3.5)}{(1.5-1.1)}(\lvert\eta\rvert - 1.1)$ GeV in the transition region. The variable muon p_T threshold reflects the muon detector acceptance in the barrel and end cap, which reduces the sensitivity to potential mismodeling at the edges of the detector acceptance. The muon pair is then fit to a common vertex, with its invariant mass required to be within ± 150 MeV of the nominal J/ψ meson mass [32]. For the $B^0 \to J/\psi K^{*0}$ ($B_s^0 \to J/\psi\phi$) channel, we require two OS tracks with leading track $p_T > 0.85$ GeV, subleading track $p_T > 0.6$ GeV, $\lvert\eta\rvert < 2.4$, and $\Delta z < 1$ cm fitted to a common vertex, with the invariant mass consistent with the world-average K^{*0} (ϕ) mass [32] under the assignment of one kaon and one pion (two kaon) masses to the two tracks: 0.842–0.942 GeV (1.01–1.03 GeV). In the K^{*0} case, both possible mass assignment permutations are tried, and in case both pass the invariant mass requirement, only the combination with the mass closest to the nominal K^{*0} mass [32] is retained. For the $B^+ \to J/\psi K^+$ channel, a single track with $p_T > 0.85$ GeV, $\lvert\eta\rvert < 2.4$, and $\Delta z < 1$ cm is required. The pair of muons and a track ($B^+ \to J/\psi K^+$ channel) or a pair of tracks ($B^0 \to J/\psi K^{*0}$ and $B_s^0 \to J/\psi\phi$ channels) are fit to a common SV, with the J/ψ meson mass constraint on the pair of muons, and the SV χ^2 fit probability is required to exceed 0.07. We further require $\cos\alpha_B > 0.997$, $S_{xy,\text{SV}} > 4$, and the B candidate mass within 4.5–6.0 GeV.

The summary of the selection requirements is presented in Table IV. These optimized selections are applied for all three charmonium channels, with the exception of the mass windows for the ϕ selection and the K^{*0} veto: they are inverted for the $B^0 \to J/\psi K^{*0}$ channel and are not used in the

TABLE IV. Summary of the selection requirements for B candidates in the charmonium analysis. The $\cdots$ entries indicate that the selection does not apply to this channel.

Variable	Selection		
	B^+	B^0	B_s^0
General track selection			
Leading (subleading) track p_T	>0.85 GeV	>0.85 (0.6) GeV	>0.85 (0.6) GeV
Track $\lvert\eta\rvert$	>2.4		
$\Delta z(\mathrm{track, PV})$	<1 cm		
Muon candidate selection			
Muon p_T	$p_\mathrm{T} > \begin{cases} 3.5\ \mathrm{GeV}: \lvert\eta\rvert < 1.1 \\ 3.5 + \frac{1.5-3.5}{1.5-1.1}(\lvert\eta\rvert - 1.1)\ \mathrm{GeV}: 1.1 < \lvert\eta\rvert < 1.5 \\ 1.5\ \mathrm{GeV}: \lvert\eta\rvert > 1.5 \end{cases}$		
Muon identification	Soft ID [17]		
$\lvert M(\mu\mu) - m(J/\psi)\rvert$	<150 MeV		
B candidate selection			
SV fit probability	>0.07		
$S_{xy,\mathrm{SV}}$	>4		
$\cos\alpha_B$	>0.997		
Intermediate resonance masses			
$\lvert M(K^+K^-) - m(\phi)\rvert$	$\cdots$	>10 MeV	<10 MeV
$\lvert M(K^+\pi^-) - m(K^{*0})\rvert$	$\cdots$	<50 MeV, Closest permutation	>50 MeV, Both permutations

$B^+ \to J/\psi K^+$ channel. The ϕ (K^{*0}) veto ensures that there is no overlap between the $B^0 \to J/\psi K^{*0}$ ($B_s^0 \to J/\psi\phi$) candidates and the $B_s^0 \to J/\psi\phi$ ($B^0 \to J/\psi K^{*0}$) candidates.

In the charmonium channel, we further split the analysis into the "tag-side" and "probe-side" categories. The tag-side category requires one of the muons from a J/ψ meson decay to trigger the event, while for the probe-side category, an additional muon that does not belong to the J/ψ candidate is required to trigger the event. If one event falls into both the tag-side and probe-side categories, it is classified as a probe side; thus, the two categories are mutually exclusive. Given that a charmonium analysis based on a significantly larger dataset obtained with dimuon triggers has already been published by CMS [7] to test the kinematic dependence of PFRs, the goal of the present charmonium analysis is to examine the dependence of PFRs with minimal trigger bias, which is achievable by using the probe side. The translation factors between the $\mathcal{R}_s$ ($\mathcal{R}_s^d$) and f_s/f_u (f_s/f_d) variables are also measured on the probe side, as in the open-charm analysis, to minimize systematic uncertainties. The tag-side category is primarily used to verify the consistency of the present analysis with previous measurements.

VI. SIGNAL EXTRACTION

Since the main goal of the analysis is to measure f_s/f_d as a function of p_T and $\lvert y\rvert$ of the B candidates, we extract the signal by performing a binned maximum likelihood fit to the B candidate mass spectrum for each p_T or $\lvert y\rvert$ bin with a sum of several functions describing signal and background components.

A. Open-charm analysis

For the open-charm analysis, there are seven $p_\mathrm{T}(B)$ bins with the lower boundaries of 8, 10, 13, 18, 23, 28, and 33 GeV, with the last bin extending up to 60 GeV, and six bins in $\lvert y(B)\rvert$ with the first five covering 0–1.25 in 0.25-wide bins and the last bin covering 1.25–2.25.

To improve the B candidate mass resolution, we use the D meson mass correction defined as follows for the $B^+ \to \pi^+\bar{D}^0(K^+\pi^-)$, $B^0 \to \pi^+D^-(K^+\pi^-\pi^-)$, and $B_s^0 \to \pi^+D_s^-(\pi^-\phi(K^+K^-))$ channels, respectively:

$$M(B^+) = M(K^+\pi^-\pi^+) - M(K^+\pi^-) + m(D^0),$$
$$M(B^0) = M(K^+\pi^-\pi^-\pi^+) - M(K^+\pi^-\pi^-) + m(D^-),$$
$$M(B_s^0) = M(K^+K^-\pi^-\pi^+) - M(K^+K^-\pi^-) + m(D_s^-).$$

We use a sum of two Gaussian functions with a common mean (double-Gaussian function) to describe the signal template, with the mean, two widths, and the relative normalization parameter constrained via a Gaussian probability density function to the values and the uncertainties obtained from a fit to simulated distributions.

The Cabibbo-suppressed background where the pion is replaced with a kaon is described with the Johnson function [42], given by

$$\frac{\delta}{\lambda\sqrt{2\pi}}\frac{1}{\sqrt{1+(\frac{x-\mu}{\lambda})^2}}e^{-\frac{1}{2}(\gamma+\delta\sinh^{-1}(\frac{x-\mu}{\lambda}))^2},$$

where μ and λ are the mean and the width parameters, while γ and δ are the parameters describing the tails. All of these parameters are also Gaussian constrained to the values obtained from a fit to simulation. The normalization of this background is fixed relative to the Cabibbo-favored signal normalization. Specifically, we calculate the ratio of the signal efficiencies for the Cabibbo-suppressed and Cabibbo-favored channels in each bin and multiply them by the ratio of the corresponding branching fractions. The ratio of the efficiencies is found to be flat in both p_T and $|y|$, so we use a single number per channel: $\epsilon(K/\pi) = 1.040^{+0.014}_{-0.021}$, $0.994^{+0.036}_{-0.040}$, and $1.007^{+0.079}_{-0.053}$ for the $B^+ \to \pi^+\bar{D}^0$, $B^0 \to \pi^+D^-$, and $B^0_s \to \pi^+D^-_s$ channels, respectively. While these ratios are all consistent with unity, we nevertheless propagate them into the ratio of the corresponding branching fractions [32], which yields the following normalization ratios between the expected yields in the Cabibbo-suppressed and Cabibbo-favored channels: $R_{K/\pi} = 0.0806 \pm 0.0023$, 0.0817 ± 0.0056, and 0.0760 ± 0.0064, respectively. In the fits, both the relative normalization of the Cabibbo-suppressed background and the parameters of the Johnson function are constrained within their Gaussian uncertainties using the above $R_{K/\pi}$ numbers and the shape parameters (μ, λ, γ, δ) determined from the fits to simulated samples.

All the open-charm channels have contributions from partially reconstructed backgrounds stemming from processes similar to the signal one, but with an additional pion that is not reconstructed, such as $B_{(s)} \to \pi D^*_{(s)}$ and $B_{(s)} \to \rho D_{(s)}$. This background is small and also shifted to lower masses, and it is described via an error function with the shape parameters and normalization being free parameters of the fit.

The combinatorial background is present in all channels and is modeled using an exponential function with both the normalization and slope as free parameters of the fit. Typical fits in the open-charm channels are presented in Fig. 2.

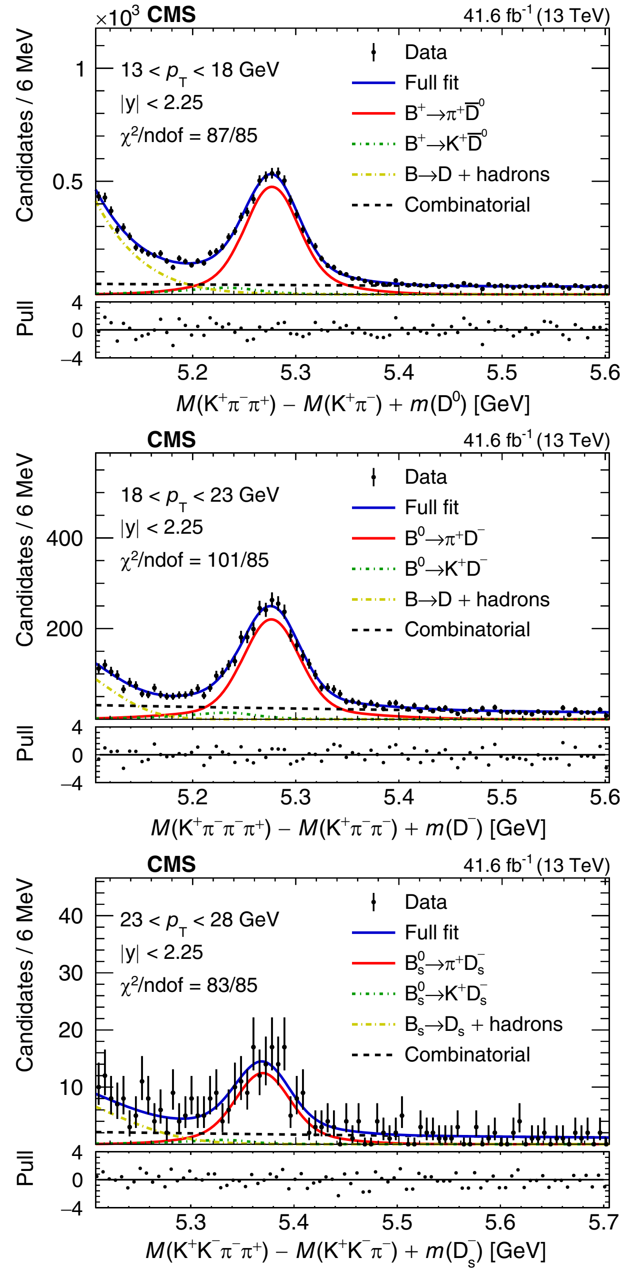

FIG. 2. Examples of fits to the B candidate mass distribution (corrected by the D meson mass) used to extract the signal in the open-charm channels. The upper, middle, and lower plots correspond to the B^+, B^0, and B^0_s decays, respectively. The χ^2 per degree of freedom (χ^2/ndof) of the fit is shown in each plot. The lower panels illustrate the pull, defined as the deviation of data from the fit function, normalized by the statistical uncertainty in each bin.

B. Charmonium analysis

For the charmonium analysis, the binning and the $|y|$ range are different for the tag- and probe-side categories. For the tag-side analysis, there are 13 $p_\mathrm{T}(B)$ bins: five 1-GeV-wide bins spanning the 11–16 GeV range, two 2-GeV-wide bins spanning the 16–20 GeV range, three 3-GeV-wide bins spanning the 20–29 GeV range, and three high-p_T bins: 29–34, 34–45, and 45–60 GeV. For the probe-side analysis, we have fewer bins as there are fewer probe-side events.

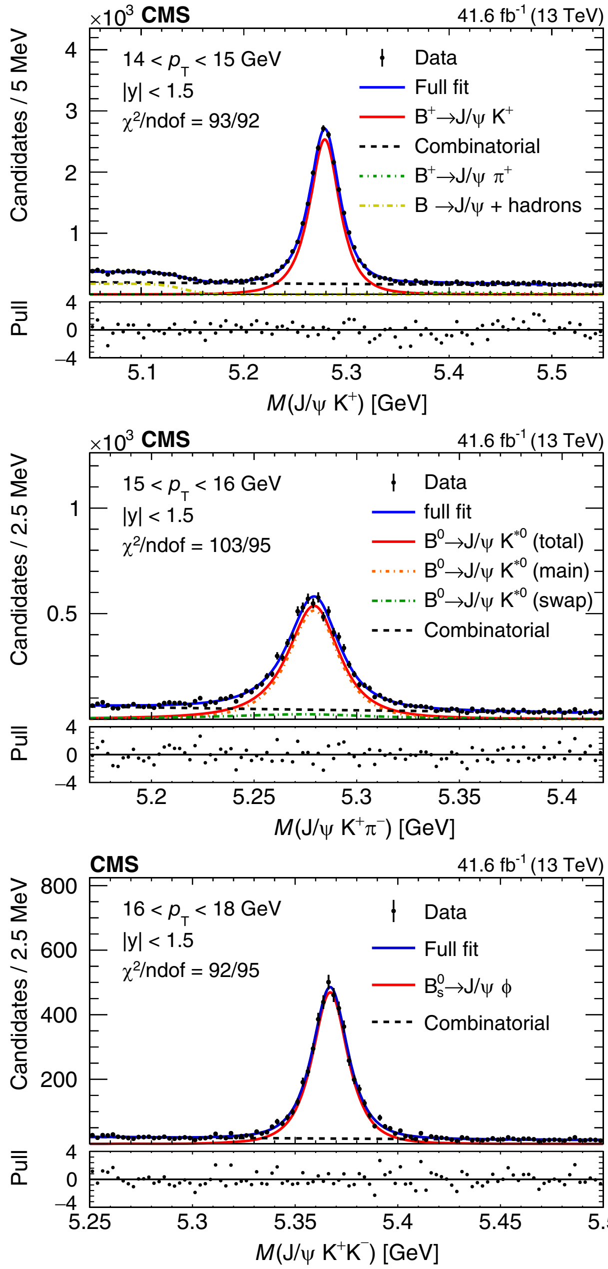

FIG. 3. Examples of fits to the B candidate mass distribution used to extract the signal in the charmonium channels of the tag-side analysis. The upper, middle, and lower plots correspond to the B^+, B^0, and B_s^0 decays, respectively. The χ^2/ndof of the fit is shown in each plot. The lower panels illustrate the pull, defined as the deviation of data from the fit function, normalized by the statistical uncertainty in each bin.

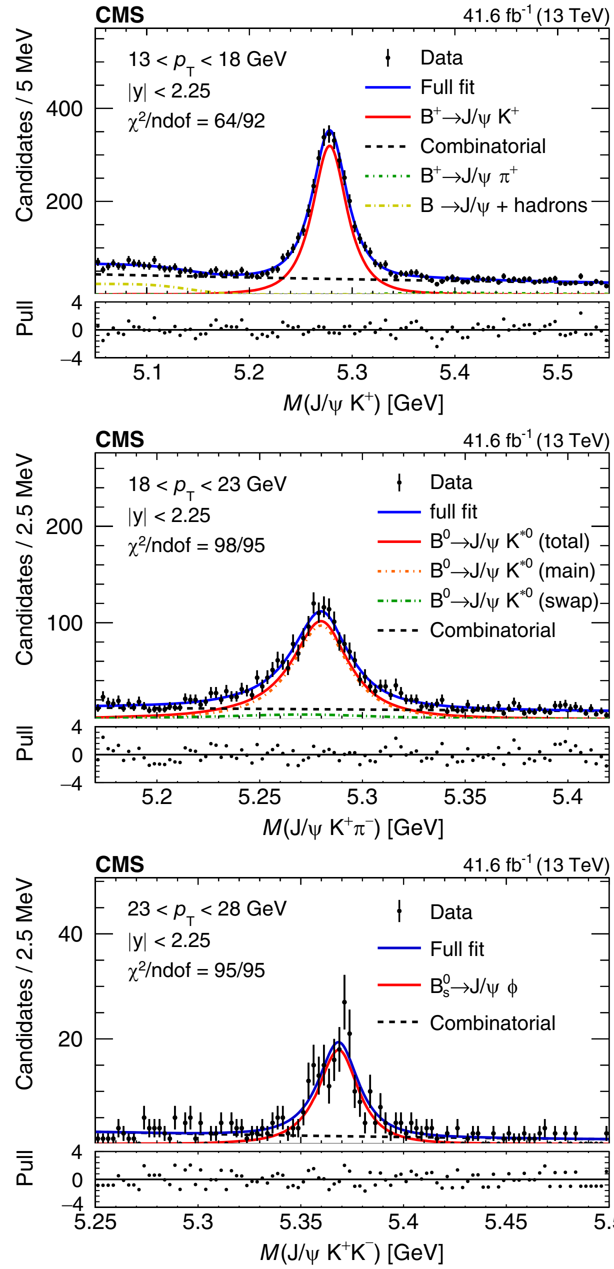

FIG. 4. Examples of fits to the B candidate mass distribution used to extract the signal in the charmonium channels of the probe-side analysis. The upper, middle, and lower plots correspond to the B^+, B^0, and B_s^0 decays, respectively. The χ^2/ndof of the fit is shown in each plot. The lower panels illustrate the pull, defined as the deviation of data from the fit function, normalized by the statistical uncertainty in each bin.

There are 6 $p_{\mathrm{T}}(B)$ bins: five bins with a width of 5 GeV each, covering the 8–33 GeV range, and a sixth bin covering the 33–50 GeV range. The tag-side analysis has six $|y|$ bins of 0.25 width each, spanning the 0–1.5 range, while the probe-side analysis has nine bins of the same width, spanning the 0–2.25 range. The reason the tag-side analysis is more restricted in $|y|$ is the requirement of μ_{trig} to have $|\eta| < 1.5$ for the low-threshold B parking triggers. Finer binning in $|y|$ for the tag side is not considered, as the absence of $|y|$ dependence of PFRs has been well verified in previous studies by both LHCb [5] and CMS [7].

Since the kinematic fit already constrains the $\mu^+\mu^-$ pair mass to the J/ψ meson mass, the invariant mass of the B

TABLE V. Fit functions used in the open-charm and charmonium analyses. The ⋯ entries indicate that the background does not apply to this channel.

	Open-charm analysis		Charmonium analysis	
Source	Function	Constraint	Function	Constraint
Signal	Double Gaussian	Gaussian	Johnson	μ, λ: free; δ, γ: Gaussian
Cabibbo-supp. bkg.	Johnson	Gaussian	Crystal Ball + Gaussian	Fixed
Partially rec. bkg.	Error function	Free	Error function	Free
Combinatorial	Exponential	Free	Exponential	Free
π/K swap signal	⋯		Johnson	Fixed

candidate is directly used for signal extraction instead of correcting it with the J/ψ meson mass.

In the charmonium channel, signal shapes are modeled with Johnson functions, with the means and widths as free parameters of the fit, while the γ and δ tail parameters are constrained by a fit to simulated signal events.

The Cabibbo-suppressed background from $B^+ \to J/\psi(\mu^+\mu^-)\pi^+$ decays only enters in the $B^+ \to J/\psi K^+$ channel. It is described by a sum of Crystal Ball (CB) [43] and Gaussian functions with a common mean. Given that the contribution from this background is small, we fix its relative normalization to $R_{K/\pi} = 0.0385$ [32], and the tail parameters for the CB function, as well as the common mean, and the widths of both the CB and Gaussian functions, to the values obtained from a fit to a sample of simulated events.

The $B^+ \to J/\psi K^+$ channel of the charmonium analysis has contributions from partially reconstructed backgrounds from the $B \to J/\psi K^*$ process with one of the two tracks from the $K^{*0} \to K^+\pi^-$ decay, or a neutral meson in the $K^{*+} \to K^+\pi^0$ or $K^{*+} \to K^0\pi^+$ decay lost. As in the open-charm channels, this background is small and shifted to lower masses, so it is similarly described by an error function with the shape parameters and normalization as free parameters of the fit.

The combinatorial background is modeled across all channels using an exponential function with both the normalization and slope as free parameters in the fit.

Finally, for the $B^0 \to J/\psi K^{*0}$ channel, the π/K-swap component [i.e., the contribution to the signal shape when the swapped (incorrect) mass assignments of the π and K tracks are used] is considered a signal component and described via a Johnson function with the shape parameters and the relative normalization to the signal (i.e., the nonswapped case) yield fixed from a fit to a sample of simulated signal events.

Figures 3 and 4 show typical fits in the charmonium channels for the tag- and probe-side analyses, respectively. Table V summarizes the functions used to describe the signal and background components in each channel.

VII. EFFICIENCY DETERMINATION

As shown in Eqs. (1)–(6), the ratios of efficiency-corrected yields (N_{corr}) are used to obtain $\mathcal{R}_s$, $\mathcal{R}_s^d$, and the PFRs. Therefore, only the corresponding efficiency ratios, $\epsilon_{B^+}/\epsilon_{B_s^0}$, $\epsilon_{B^0}/\epsilon_{B_s^0}$, and $\epsilon_{B^0}/\epsilon_{B^+}$, are required to correct the signal event yields in this analysis. These efficiency ratios are determined from samples of simulated events and reflect the trigger, reconstruction, and selection processes, as well as the detector acceptance.

While the efficiency ratios of the open-charm analysis and the probe-side charmonium analysis are minimally affected by the triggers, the tag-side charmonium analysis relies on a trigger muon. The difference in the trigger response between simulation and data on the tag side is corrected via muon trigger scale factors (SFs). The SFs for the B parking triggers used in this analysis are measured using the "tag-and-probe" method [44] based on the $J/\psi \to \mu^+\mu^-$ decays across different muon p_{T} and $\mathrm{IP}_{\mathrm{sig}}$ ranges.

The remaining difference between simulation and data on the tag side of the charmonium analysis is mitigated by using higher-order corrections at the generator level. The leading-order PYTHIA simulation is reweighted so that the B meson's p_{T} and $|y|$ spectra match fixed-order plus next-to-leading logarithmic (FONLL) accuracy calculations, which are known to reproduce these spectra in data with high accuracy [45].

For the probe side, both in the open-charm and charmonium analyses, since the FONLL calculations cannot properly capture potential correlations between the probe side and the trigger muon, simulated distributions of p_{T} and $|y|$ are reweighted to match the measured ones at the reconstructed level. The weights are extracted for each $B^+ \to \pi^+\bar{D}^0(K^+\pi^-)$, $B^0 \to \pi^+D^-$, and $B_s^0 \to \pi^+D_s^-(\pi^-\phi(K^+K^-))$ decay by comparing simulation and background-subtracted data distributions, obtained using the ${}_s\mathcal{P}lot$ technique [39], and are parametrized via a second-order polynomial, as functions of p_{T} and $|y|$. Table VI summarizes the corrections applied to the simulated samples for the open-charm and charmonium channels.

TABLE VI. Summary of MC corrections for the open-charm and charmonium channels.

Channel	MC correction
Open-charm	Reweight to data
Charmonium (probe)	Reweight to data
Charmonium (tag)	Muon trigger SF
	Reweighting to FONLL

VIII. SYSTEMATIC UNCERTAINTIES

In this analysis, systematic uncertainties are split into two categories. The first category is a bin-to-bin uncorrelated systematic uncertainty, which depends on the B meson's p_T and $|y|$, and affects the shape of the measured PFR or $\mathcal{R}$ values. The second type is bin-to-bin correlated uncertainty, or global uncertainty, which does not affect the shape but impacts the central values of the measured PFRs. In the charmonium analysis, the uncertainties that affect only the global scale of the PFRs are not included in the measurement of $\mathcal{R}_s$ and $\mathcal{R}_s^d$, since this analysis only measures the shape versus p_T and $|y|$. Both types of uncertainties are included in the open-charm analysis and in the translation of the shape-only measurement of the PFRs in the charmonium analysis to an absolute normalization.

A. Open-charm analysis

The primary sources of systematic uncertainties and their effects on the PFR measurement in the open-charm analysis are summarized in Table VII. Sources of systematic uncertainties correlated bin-to-bin and global uncertainties affecting only the central values of PFR are listed below. In this analysis, the systematic uncertainty related to the triggers is negligible, as their impact is found to cancel out in the PFRs for the probe-side analysis.

The following global uncertainties are considered:

(i) Uncertainties in the external inputs to the PFR equations presented in Table II.

(ii) The uncertainty associated with the track reconstruction efficiency. Because B_s^0 and B^0 meson decays have one more track than the B^+ decay, an uncertainty from a single-track reconstruction efficiency is assigned to the efficiency ratios, $\epsilon_{B^+}/\epsilon_{B_s^0}$ and $\epsilon_{B^0}/\epsilon_{B^+}$. This uncertainty of 2.1% [46] is treated as independent of p_T and $|y|$ in this analysis and therefore is considered a global uncertainty.

(iii) The uncertainty associated with the BDT selection procedure. Differences in the BDT efficiencies between simulation and data in each open-charm decay channel range from 1.2% to 2.2%. Since this uncertainty is small compared to the statistical and other systematic uncertainties, we assign the difference as the corresponding uncertainty but do not apply a correction. This uncertainty is found to be independent of p_T and $|y|$.

(iv) The uncertainty in the B_s^0 background subtraction to account for nonresonant K^+K^- contribution to the D_s^- decay. The expected amount of the nonresonant contribution within the ± 10 MeV mass window around the nominal ϕ meson mass is found to be $5.6 \pm 0.9\%$ [38], independent of p_T and $|y|$.

(v) The measurement of f_d/f_u includes a 2.2% uncertainty from the evaluation of $r^{\pm,0} = \mathcal{B}(\Upsilon(4S) \to B^+B^-)/\mathcal{B}(\Upsilon(4S) \to B^0\bar{B}^0) = 1.057 \pm 0.023$ [11].

The overall bin-to-bin correlated systematic uncertainty, calculated as the sum in quadrature of the individual components, ranges from 5.6% to 7.4%, depending on the PFR.

TABLE VII. Sources and values of the systematic uncertainties affecting the measured PFRs in the open-charm analysis. The bin-to-bin uncorrelated uncertainties are presented as ranges, which indicate the range of uncertainties across different p_T and $|y|$ bins. The $\cdots$ entries indicate that the uncertainty does not apply. The reported values are the relative systematic uncertainties in percent.

Source	f_s/f_u (%)	f_s/f_d (%)	f_d/f_u (%)
$\Phi_{PS}, \lvert V_{us}\rvert f_K/(\lvert V_{ud}\rvert f_\pi), \tau_{B^0}/\tau_{B_s^0}, N_a, N_F$	4.2	4.2	⋯
Branching fractions	5.4	4.0	4.2
Tracking efficiency	2.1	⋯	2.1
BDT performance	1.2	2.2	2.2
B_s^0 nonresonant subtraction	0.9	0.9	⋯
$r^{\pm,0}$	⋯	⋯	2.2
Total global systematic uncertainty	7.4	6.3	5.6
Statistical uncertainty in simulation	2.2–3.7	2.2–3.7	2.1–3.6
Signal and background shapes	0.8–2.4	0.8–2.8	0.7–2.8
Reweighting in p_T and $\lvert y\rvert$	0.0–1.4	0.0–1.6	0.1–1.1
Total systematic uncertainty	<7.9	<7.7	<7.2

TABLE VIII. Sources of bin-to-bin uncorrelated systematic uncertainty affecting the measured $\mathcal{R}_s$, $\mathcal{R}_s^d$, and f_d/f_u values for the tag- and probe-side categories in the charmonium analysis. The uncertainties are presented as ranges, which indicate the range of the uncertainties across different p_T and $|y|$ bins. The $\cdots$ entries indicate that the uncertainty does not apply. The reported values are the relative systematic uncertainty in percent.

	Tag			Probe		
Source	$\mathcal{R}_s$ (%)	$\mathcal{R}_s^d$ (%)	f_d/f_u (%)	$\mathcal{R}_s$ (%)	$\mathcal{R}_s^d$ (%)	f_d/f_u (%)
Stat. uncert. in simulation	1.1–5.1	1.3–7.1	1.1–5.6	2.7–5.7	2.6–5.5	2.3–4.9
Signal and bkg. shapes	0.8–4.4	0.6–4.7	0.5–4.2	1.3–10.1	0.9–9.4	0.9–6.6
Trigger SF	1.9–2.6	1.9–2.7	1.9–2.7	$\cdots$	$\cdots$	$\cdots$
Reweighting in p_T and $|y|$	0.2–1.6	0.1–1.2	0.2–1.9	0.1–1.8	0.3–2.2	0.2–1.7
Total syst. uncertainty	<7.5	<7.8	<7.7	<11.7	<11.1	<8.3

For bin-to-bin uncorrelated systematic uncertainties, the following sources are considered:

(i) The uncertainty in the signal efficiency arising from the limited number of simulated events is 1.7%–3.7% depending on the bin and the channel.

(ii) The uncertainty in the signal yields due to the parametrization of signal and background shapes is estimated by varying the functional forms presented in Table V to their alternative shapes and independently comparing the results obtained with the nominal function to those from the alternatives. A Johnson function is considered as an alternative shape for the signal, a Student-t distribution [47] for the Cabibbo-suppressed background, a hyperbolic tangent function for the partially reconstructed background, and a first-order Chebyshev polynomial for the combinatorial backgrounds. The corresponding uncertainties vary between 0.7% and 2.8%, depending on the channel and the bin.

(iii) The uncertainty in the signal efficiency associated with the correction factors applied to simulated events. For the probe-side analysis, the p_T and $|y|$ distributions from simulation are reweighted to match the measured distributions. The uncertainty is estimated by comparing the efficiency ratios $\epsilon_{B^+}/\epsilon_{B_s^0}$, $\epsilon_{B^0}/\epsilon_{B_s^0}$, and $\epsilon_{B^0}/\epsilon_{B^+}$ before and after applying the weights in p_T and $|y|$ bins and is less than 1.6% for all processes and bins.

The overall bin-to-bin uncorrelated systematic uncertainties range from 2.0%–4.7%, depending on the channel and the bin.

B. Charmonium analysis

For the charmonium analysis, the dominant bin-to-bin uncorrelated systematic uncertainties in the tag- and probe-side categories are listed in Table VIII. Several potential sources of systematic uncertainty, including those related to the muon reconstruction and selection efficiencies, are neglected in this analysis because they are found to cancel out in the efficiency ratios. For the probe-side category, as in the open-charm analysis, systematic uncertainty related to the triggers is not included, as its impact on the ratios is negligible.

The following sources of systematic uncertainty in the $\mathcal{R}_s$, $\mathcal{R}_s^d$, and f_d/f_u values are considered:

(i) The uncertainty in the signal efficiency from the limited number of simulated events.

(ii) The uncertainty in the signal yields due to the parametrization of signal and background shapes. As in the open-charm analysis, the uncertainty is estimated by varying the functional forms presented in Table V to alternative shapes. For the charmonium analysis, a triple-Gaussian function with a common mean is considered as an alternative shape for the signal and a first-order Chebyshev polynomial for the combinatorial backgrounds. Uncertainties associated with the Cabibbo-suppressed and partially reconstructed backgrounds are found to be negligible and therefore not included.

(iii) The uncertainty in the signal efficiency associated with the trigger SF for the tag-side category. The uncertainty is computed by varying the SF up and down by its uncertainty and determining the impact on the signal yields.

(iv) The uncertainty in the signal efficiency associated with the correction factors applied to the simulated events. For the tag-side events, simulated p_T and $|y|$ distributions are reweighted based on the FONLL calculations, while for the probe side they are reweighted to match the measured distributions. In both cases, the uncertainty is computed by comparing the efficiency ratios $\epsilon_{B^+}/\epsilon_{B_s^0}$ and $\epsilon_{B^0}/\epsilon_{B_s^0}$ before and after applying the weights.

The overall uncertainties vary from about 2% to 10%, depending on the channel and whether the events are from the tag side or probe side. Significant uncertainties on the tag side are mainly associated with the low-p_T bins, where a fine binning of 1 GeV is used. On the probe side, large uncertainties are primarily associated with the high-rapidity region. The charmonium analysis employs a finer binning in $|y|$, splitting into nine bins, compared to the six bins in the open-charm analysis.

For the measurement of f_d/f_u, the following global uncertainties are considered:

(i) An uncertainty of 2.1% associated with the track reconstruction efficiency [46]. Because B^0 decays have one more track than the B^+ process, the 2.1% uncertainty is assigned to the efficiency ratio, $\epsilon_{B^0}/\epsilon_{B^+}$. This uncertainty is treated as a global uncertainty.

(ii) An uncertainty of 4.3% associated with the branching fraction ratio between the $B^+ \to J/\psi K^+$ and $B^0 \to J/\psi K^{*0}$ channels.

(iii) An uncertainty of 2.2% from $r^{\pm,0} = 1.057 \pm 0.023$ [11].

IX. RESULTS

In this section, we describe the following main measurements performed in this analysis:

(i) Measurement of the B meson PFRs (f_s/f_u and f_s/f_d), using the open-charm decays $B^+ \to \pi^+\bar{D}^0$, $B^0 \to \pi^+ D^-$, and $B_s^0 \to \pi^+ D_s^-$.

(ii) Measurement of the relative PFR ($\mathcal{R}_s$ and $\mathcal{R}_s^d$) using the charmonium decays $B^+ \to J/\psi K^+$, $B^0 \to J/\psi K^{*0}$, and $B^0 \to J/\psi K^{*0}$.

(iii) Measurement of f_d/f_u in both open-charm and charmonium channels without the assumption of isospin invariance.

(iv) Measurement of the normalization factors needed for translation of the $\mathcal{R}_s^d$ and $\mathcal{R}_s$ values to the corresponding PFRs.

In the open-charm decay channels, the PFRs f_s/f_u and f_s/f_d are directly measured using the theoretical calculations of the ratio of the open-charm branching fractions for the B^0 and B_s^0 mesons, as discussed in Sec. IV. For the charmonium decay channels, the relative production fraction ratios $\mathcal{R}_s^d$ and $\mathcal{R}_s$ are measured to determine the trend of the PFRs in p_{T} or $|y|$ with an improved statistical precision compared to previous analyses. The value of f_d/f_u is also directly determined both in the open-charm and charmonium channels to probe isospin invariance in B meson production.

Finally, the results obtained from the probe-side category in the charmonium channels are combined with those derived from the open-charm channels. This combination allows for the estimation of the absolute normalization of the $\mathcal{R}_s^d$ and $\mathcal{R}_s$ values relative to f_s/f_d and f_s/f_u. The normalization is derived using precise measurements of the ratios of branching fractions from charmonium to open-charm decays, which improve upon several world-average values [32]. With this absolute normalization established on the probe side, the PFRs are extracted from the charmonium decays on the tag side. The details of which channels are used for each measurement are summarized in Table IX.

In addition to measuring the PFRs versus p_{T} and $|y|$, we also determine average values, which come from averaging the values in bins of p_T, using the inverse of the squared uncertainties as weights. The statistical uncertainties for each average are obtained by calculating the weighted average using the statistical uncertainties only. The central values of the averages come from the weighted average in which the weights come from summing the statistical and uncorrelated bin-by-bin systematic uncertainties in quadrature. The global uncertainty is added, in quadrature, to the uncertainty of this result to obtain the total uncertainty. The systematic uncertainty is obtained by subtracting, in quadrature, the statistical uncertainty from the total uncertainty. Angle brackets are used to indicate an average in a p_{T} range where a p_{T} dependence is expected.

TABLE IX. Summary of the channels employed in each measurement of f_s/f_u, f_s/f_d, $\mathcal{R}_s$, $\mathcal{R}_s^d$, f_d/f_u and in determining the absolute normalizations for $\mathcal{R}_s$ and $\mathcal{R}_s^d$. The $\cdots$ entries indicate the channel is not included.

Measurements	Open charm	Charmonium	
		Probe	Tag
$f_s/f_u, f_s/f_d$	Included	$\cdots$	$\cdots$
$\mathcal{R}_s, \mathcal{R}_s^d$	$\cdots$	Included	Included
f_d/f_u	Included	Included	Included
$\mathcal{R}_s$, $\mathcal{R}_s^d$ norm.	Included	Included	$\cdots$

A. Measurement of *B* meson PFRs using open-charm decays

The measured PFRs, f_s/f_u and f_s/f_d, are shown as functions of p_{T} and $|y|$ in Fig. 5. For each measured PFR, hypotheses regarding both a linear dependence and no dependence on the B meson kinematics are tested. The results indicate that there is no evidence of a linear dependence of the PFRs on either p_{T} or $|y|$ within the range of this measurement.

The averages over the full reconstructed kinematic range of $8 < p_{\mathrm{T}} < 60$ GeV and $|y| < 2.25$ from the PFR p_{T} values are

$$\langle f_s/f_d \rangle = 0.219 \pm 0.008(\mathrm{stat}) \pm 0.014(\mathrm{syst}),$$
$$\langle f_s/f_u \rangle = 0.218 \pm 0.008(\mathrm{stat}) \pm 0.015(\mathrm{syst}).$$

Due to the previously observed low-p_{T} trend in the PFRs [5,7], any values of f_s/f_d or f_s/f_u obtained from integrating over the full p_{T} range are considered to be *effective* values. However, the trend of the PFRs in the $|y|$ distribution remains unaffected, as the $|y|$ distributions are not correlated with the p_{T} distributions within the kinematic range of this study.

The recent CMS study of B meson PFRs in charmonium decays [7] showed that there exists a p_{T} dependence of f_s/f_u and f_s/f_d at low p_T, followed by a plateau for $p_{\mathrm{T}} \gtrsim 18$ GeV. The present measurement does not have

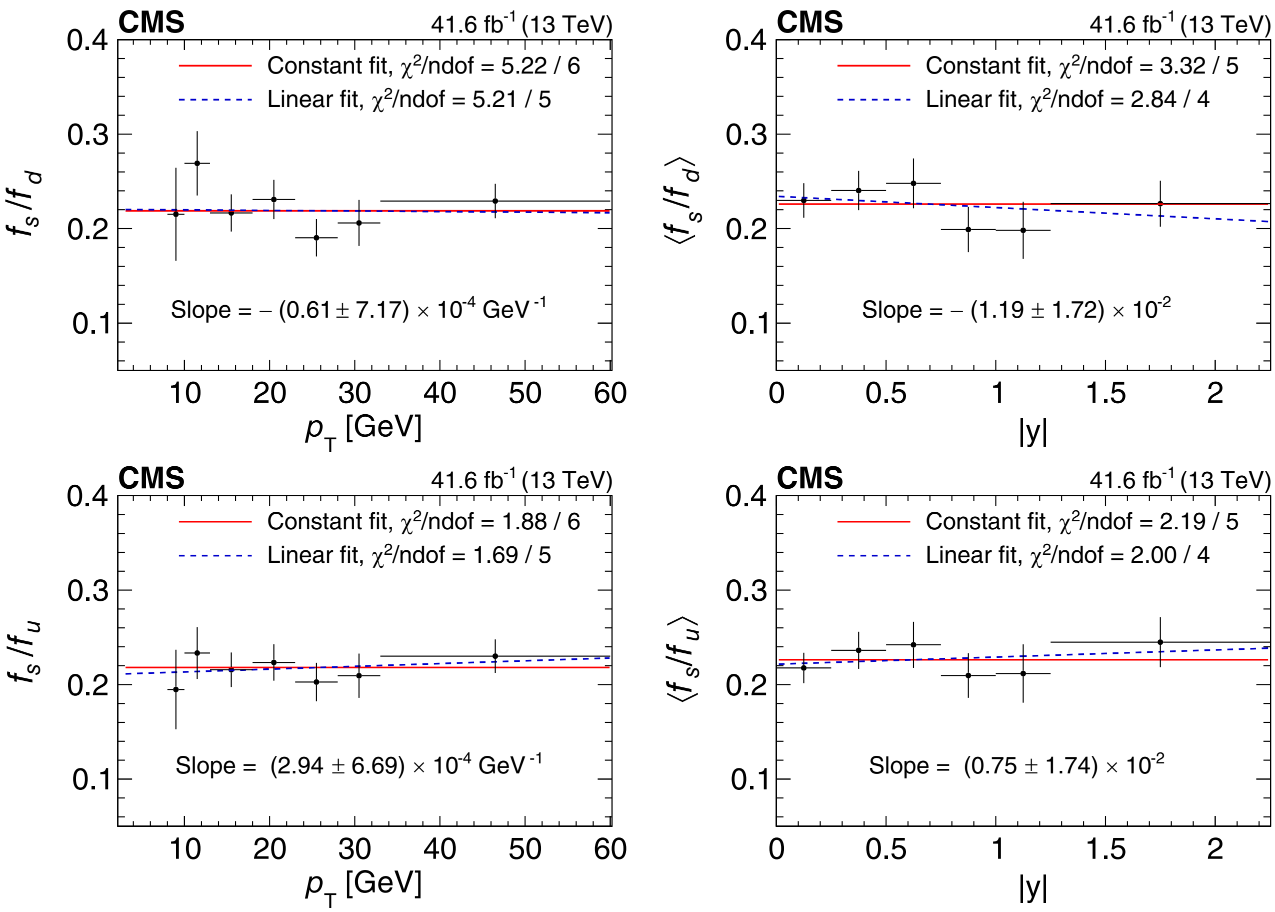

FIG. 5. The production fraction ratios f_s/f_d (upper row) and f_s/f_u (lower row) as functions of p_T (left column) and $|y|$ (right column), measured using open-charm decays. The vertical error bars show the combined statistical and bin-to-bin uncorrelated systematic uncertainty. The global uncertainties are not included. The red line is the average over the full reconstructed kinematic range, and the blue dashed line is the linear fit result. The χ^2/ndof values for the constant fit and linear fit are given. Parameters inside angle brackets are averages over p_T where the absolute normalization may be affected by the p_T dependence.

sufficient precision to probe the low-p_T dependence because of the lower event count in the relevant p_T bins compared to the charmonium decay mode of the previous CMS study, which is based on a larger dataset collected with regular triggers. However, in the high-p_T region, where the PFRs are observed to be independent of *B* meson kinematics, they can be measured with high precision. The average over the $p_T > 18$ GeV region yields

$$f_s/f_d = 0.215 \pm 0.010(\mathrm{stat}) \pm 0.014(\mathrm{syst}),$$
$$f_s/f_u = 0.218 \pm 0.009(\mathrm{stat}) \pm 0.016(\mathrm{syst}).$$

The measured high-p_T value of f_s/f_d is within one standard deviation of the corresponding LEP measurement of $f_s/f_d = 0.249 \pm 0.023$ [48] at high p_T (around 40 GeV).

B. Measurement of $\mathcal{R}_s$ and $\mathcal{R}_s^d$ using charmonium decays

The results of the measurements of $\mathcal{R}_s$ and $\mathcal{R}_s^d$ are presented in bins of p_T and $|y|$ in Fig. 6 for both tag- and probe-side categories. While the measured $\mathcal{R}_s$ and $\mathcal{R}_s^d$ values do not exhibit any statistically significant dependence on either p_T or $|y|$, they are consistent within the uncertainties with the p_T dependence at low p_T, followed by a flat high-p_T trend in both $\mathcal{R}_s$ and $\mathcal{R}_s^d$ observed in earlier analyses [4,7].

C. Measurement of f_d/f_u using both the open-charm and charmonium decays

The measured values of f_d/f_u obtained from Eq. (2) for the open-charm analysis and Eq. (6) for the charmonium analysis are presented as functions of p_T and $|y|$ in Fig. 7. The results from each of the three analyses are consistent

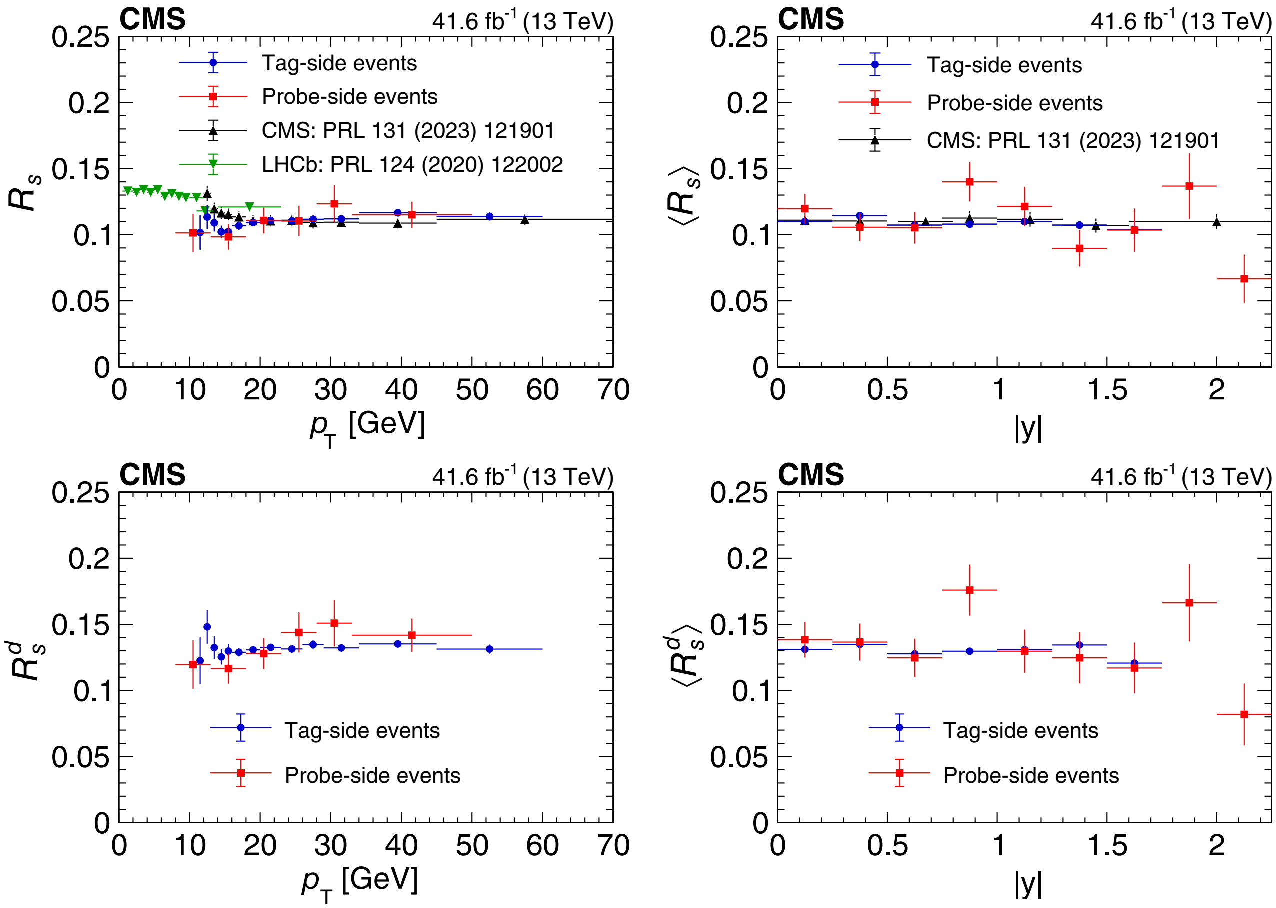

FIG. 6. The relative production fraction ratios $\mathcal{R}_s$ (upper row) and $\mathcal{R}_s^d$ (lower row) as functions of p_T (left column) and $|y|$ (right column), measured using charmonium decays. For comparison, the recent CMS [7] and LHCb [4] measurements are also presented. The error bars include both statistical and bin-to-bin uncorrelated systematic uncertainties. Values enclosed in angle brackets represent averages over p_T, where the absolute normalization may be affected by the p_T dependence.

with each other and show no dependence on p_T or $|y|$. The results are also consistent with a previous CMS analysis [7], which covered the range of $12 < p_T < 70$ GeV and $|y| < 2.4$. The average values are calculated to be

$$f_d/f_u(\text{open charm}) = 0.946 \pm 0.016 \pm 0.055,$$
$$f_d/f_u(\text{charmonium, tag}) = 0.965 \pm 0.002 \pm 0.047,$$
$$f_d/f_u(\text{charmonium, probe}) = 0.949 \pm 0.019 \pm 0.047,$$

where the first and second uncertainties are statistical and systematic, respectively.

We calculate a weighted average of the open-charm and charmonium f_d/f_u values, accounting for correlations within each analysis, including systematic uncertainties from external inputs and the BDT, as well as correlations between the two analyses, such as the uncertainties from the tracking efficiency and $r^{\pm,0}$. The combined f_d/f_u value is

$$f_d/f_u = 0.956 \pm 0.043.$$

The f_d/f_u value is compatible with unity within a 5% precision, consistent with isospin invariance in B meson production at hadron colliders. Figure 8 summarizes the CMS f_d/f_u measurements across decay channels, with the uncertainties including significant contributions from common systematic uncertainties.

We also measure f_d/f_u for particles and antiparticles separately. Combining the results from the open charm and both charmonium analyses, we obtain

$$f_{B^+}/f_{B^0} = 0.947 \pm 0.044,$$
$$f_{B^-}/f_{\bar{B}^0} = 0.957 \pm 0.044.$$

Taking the ratio of the two ratios returns 0.989 ± 0.015, where the uncertainty does not include any global systematic uncertainties as they cancel out in this double ratio.

D. Measurement of *B* branching fractions

The ratio of the efficiency-corrected yields between the charmonium and open-charm decays corresponds to the

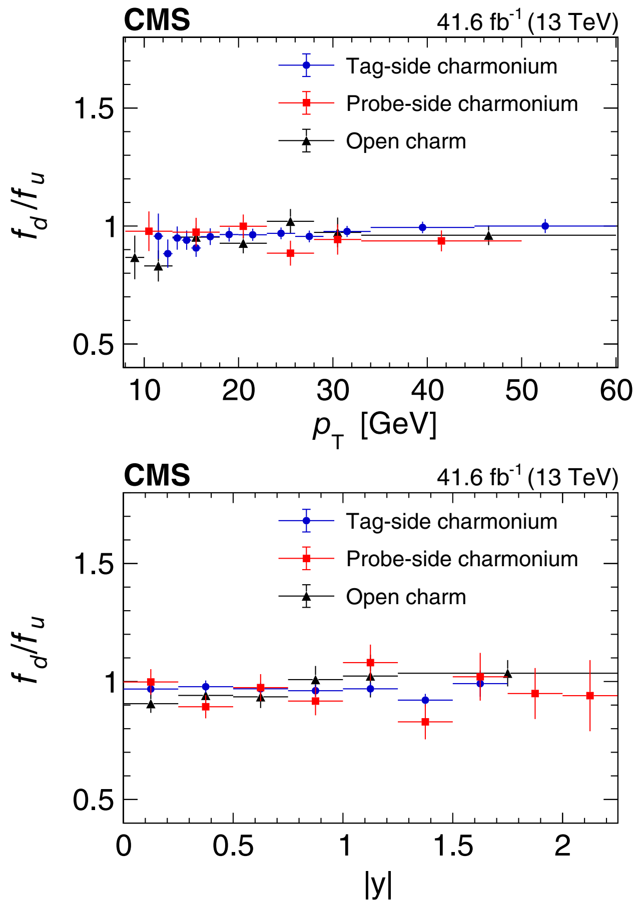

FIG. 7. The production fraction ratios f_d/f_u as functions of p_T (left) and $|y|$ (right) measured using both the open-charm and charmonium decays, without an assumption of isospin invariance. The error bars include both statistical and bin-to-bin uncorrelated systematic uncertainties. The global uncertainties of 5.7% for the open-charm analysis and 4.8% for both charmonium analyses are not shown.

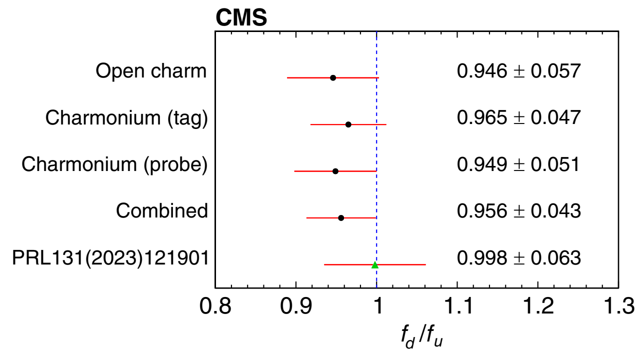

FIG. 8. Comparison of the f_d/f_u measurements across different channels. The "combined" value, shown above the black dashed line, is obtained from a combined χ^2 fit of the measurements from two statistically independent channels: the open charm and tag-side charmonium. Additionally, the plot presents the previous CMS result [7] for comparison. The blue dashed line at unity corresponds to $f_d = f_u$.

ratio of the branching fractions of the charmonium to open-charm decays. We use the probe-side charmonium sample to minimize bias from the triggers and match the p_T binning of the open-charm sample to that of the probe-side charmonium sample to remove the effect of any p_T dependence. The weighted averages of the ratios of the corrected yields in the p_T bins are used to extract the ratios of the branching fractions:

$$\frac{\mathcal{B}(B^+ \to J/\psi K^+)}{\mathcal{B}(B^+ \to \pi^+ \bar{D}^0)} = \frac{N_{\rm corr}(B^+ \to J/\psi(\mu^+\mu^-)K^+)}{N_{\rm corr}(B^+ \to \pi^+ \bar{D}^0(K^+\pi^-))} \times \frac{\mathcal{B}(\bar{D}^0 \to K^+\pi^-)}{\mathcal{B}(J/\psi \to \mu^+\mu^-)} = 0.213 \pm 0.007, \quad (7)$$

$$\frac{\mathcal{B}(B_s^0 \to J/\psi\phi)}{\mathcal{B}(B_s^0 \to \pi^+ D_s^-)} = \frac{N_{\rm corr}(B_s^0 \to J/\psi(\mu^+\mu^-)\phi(K^+K^-))}{N_{\rm corr}(B_s^0 \to \pi^+ D_s^-(\pi^-\phi(K^+K^-)))} \times \frac{\mathcal{B}(D_s^- \to \pi^-\phi)}{\mathcal{B}(J/\psi \to \mu^+\mu^-)} = 0.354 \pm 0.019, \quad (8)$$

$$\frac{\mathcal{B}(B^0 \to J/\psi K^{*0})}{\mathcal{B}(B^0 \to \pi^+ D^-)} = \frac{N_{\rm corr}(B^0 \to J/\psi(\mu^+\mu^-)K^{*0}(K^+\pi^-))}{N_{\rm corr}(B^0 \to \pi^+ D^-(K^+\pi^-\pi^-))} \times \frac{\mathcal{B}(D^- \to K^+\pi^-\pi^-)}{\mathcal{B}(K^{*0} \to K^+\pi^-)\mathcal{B}(J/\psi \to \mu^+\mu^-)} = 0.468 \pm 0.021, \quad (9)$$

where the results in Eqs. (8) and (9) have been corrected to remove the S-wave contributions in the mass ranges used to select the ϕ and K^{*0} decays, respectively. The S-wave contributions are estimated as $(1.0 \pm 0.2)\%$ for Eq. (8) [5] and $(2.2 \pm 0.2)\%$ for Eq. (9), with the latter obtained from considering the $K^*(892)^0$ and $K_0^*(700)$ contributions in the model of Ref. [35], including the uncertainty from varying these two fit fractions. The uncertainties in Eqs. (7)–(9) include both statistical and systematic components. The global uncertainties included are those from the branching fractions appearing in Eqs. (7)–(9), the BDT performance and B_s^0 nonresonant component subtraction (Table VII), and a 2.1% tracking efficiency uncertainty. While each branching fraction ratio measurement consists of the same number of charged particles in the numerator and the denominator, two of the charged particles are muons for the charmonium channels while all of the charged particles are hadrons for the open-charm channels. This leads to only a partial cancellation of the tracking efficiency uncertainty and the value of 2.1% is selected as the midpoint between full cancellation and no cancellation.

Our measured branching fraction ratios are consistent with the world-average values of $\mathcal{B}(B^+ \to J/\psi K^+)/\mathcal{B}(B^+ \to \pi^+\bar{D}^0) = 0.221 \pm 0.006$, $\mathcal{B}(B_s^0 \to J/\psi\phi)/\mathcal{B}(B_s^0 \to \pi^+ D_s^-) = 0.346 \pm 0.021$, and $\mathcal{B}(B^0 \to J/\psi K^{*0})/\mathcal{B}(B^0 \to \pi^+ D^-) = 0.496 \pm 0.025$ [32], with similar precision.

E. Measurement of the normalization for the efficiency-corrected yield ratios $\mathcal{R}$

The branching fractions measured in Eqs. (7)–(9) can be used to extract the factors necessary to translate $\mathcal{R}_s$ and $\mathcal{R}_s^d$ to the absolute PFRs, f_s/f_u and f_s/f_d. These normalization factors, c_{sd} and c_{su}, are calculated as

$$\begin{aligned} c_{sd} &= (f_s/f_d)(\text{open-charm})/\mathcal{R}_s^d(\text{charmonium}) \\ &= \Phi_{\mathrm{PS}} \frac{|V_{us}|^2}{|V_{ud}|^2} \frac{f_K^2}{f_\pi^2} \frac{\tau_{B^0}}{\tau_{B_s^0}} \frac{1}{N_{\mathrm{a}} N_{\mathrm{F}}} \\ &\times \frac{\mathcal{B}(B^0 \to \pi^+ D^-)}{\mathcal{B}(B^0 \to K^+ D^-)} \frac{\mathcal{B}(D^- \to K^+\pi^-\pi^-)}{\mathcal{B}(D_s^- \to \pi^-\phi)\mathcal{B}(\phi \to K^+K^-)} \\ &\times \frac{N_{\mathrm{corr}}(B_s^0 \to \pi^+ D_s^-(\pi^-\phi(K^+K^-)))}{N_{\mathrm{corr}}(B_s^0 \to J/\psi(\mu^+\mu^-)\phi(K^+K^-))} \\ &\times \frac{N_{\mathrm{corr}}(B^0 \to J/\psi(\mu^+\mu^-)K^{*0}(K^+\pi^-))}{N_{\mathrm{corr}}(B^0 \to \pi^+ D^-(K^+\pi^-\pi^-))} \\ &= \Phi_{\mathrm{PS}} \frac{|V_{us}|^2}{|V_{ud}|^2} \frac{f_K^2}{f_\pi^2} \frac{\tau_{B^0}}{\tau_{B_s^0}} \frac{1}{N_{\mathrm{a}} N_{\mathrm{F}}} \\ &\times \frac{\mathcal{B}(B^0 \to \pi^+ D^-)}{\mathcal{B}(B^0 \to K^+ D^-)} \frac{\mathcal{B}(K^{*0} \to K^+\pi^-)}{\mathcal{B}(\phi \to K^+K^-)} \\ &\times \frac{\mathcal{B}(B_s^0 \to \pi^+ D_s^-)}{\mathcal{B}(B_s^0 \to J/\psi\phi)} \frac{\mathcal{B}(B^0 \to J/\psi K^{*0})}{\mathcal{B}(B^0 \to \pi^+ D^-)}, \end{aligned} \tag{10}$$

$$\begin{aligned} c_{su} &= (f_s/f_u)(\text{open-charm})/\mathcal{R}_s(\text{charmonium}) \\ &= \Phi_{\mathrm{PS}} \frac{|V_{us}|^2}{|V_{ud}|^2} \frac{f_K^2}{f_\pi^2} \frac{\tau_{B^0}}{\tau_{B_s^0}} \frac{1}{N_{\mathrm{a}} N_{\mathrm{F}}} \\ &\times \frac{\mathcal{B}(B^+ \to \pi^+ \bar{D}^0)}{\mathcal{B}(B^0 \to K^+ D^-)} \frac{\mathcal{B}(\bar{D}^0 \to K^+\pi^-)}{\mathcal{B}(D_s^- \to \pi^-\phi)\mathcal{B}(\phi \to K^+K^-)} \\ &\times \frac{N_{\mathrm{corr}}(B_s^0 \to \pi^+ D_s^-(\pi^-\phi(K^+K^-)))}{N_{\mathrm{corr}}(B_s^0 \to J/\psi(\mu^+\mu^-)\phi(K^+K^-))} \\ &\times \frac{N_{\mathrm{corr}}(B^+ \to J/\psi(\mu^+\mu^-)K^+)}{N_{\mathrm{corr}}(B^+ \to \pi^+ \bar{D}^0(K^+\pi^-))} \\ &= \Phi_{\mathrm{PS}} \frac{|V_{us}|^2}{|V_{ud}|^2} \frac{f_K^2}{f_\pi^2} \frac{\tau_{B^0}}{\tau_{B_s^0}} \frac{1}{N_{\mathrm{a}} N_{\mathrm{F}}} \\ &\times \frac{\mathcal{B}(B^+ \to \pi^+ \bar{D}^0)}{\mathcal{B}(B^0 \to K^+ D^-)} \frac{1}{\mathcal{B}(\phi \to K^+K^-)} \\ &\times \frac{\mathcal{B}(B_s^0 \to \pi^+ D_s^-)}{\mathcal{B}(B_s^0 \to J/\psi\phi)} \frac{\mathcal{B}(B^+ \to J/\psi K^+)}{\mathcal{B}(B^+ \to \pi^+ \bar{D}^0)}, \end{aligned} \tag{11}$$

where the branching fractions from the last line of each equation are obtained from Eqs. (7)–(9), while the branching fractions in the next-to-last line of each equation are from Ref. [32] and reproduced in Table II. The results are

$$c_{sd} = 1.64 \pm 0.14,$$
$$c_{su} = 2.02 \pm 0.18.$$

The uncertainties include both statistical and systematic components. The global uncertainties included in the calculation of Eqs. (7)–(9) are included except for those from $\mathcal{B}(J/\psi \to \mu^+\mu^-)$, $\mathcal{B}(\phi \to K^+K^-)$, and the tracking efficiency, as these all cancel out. Additional global

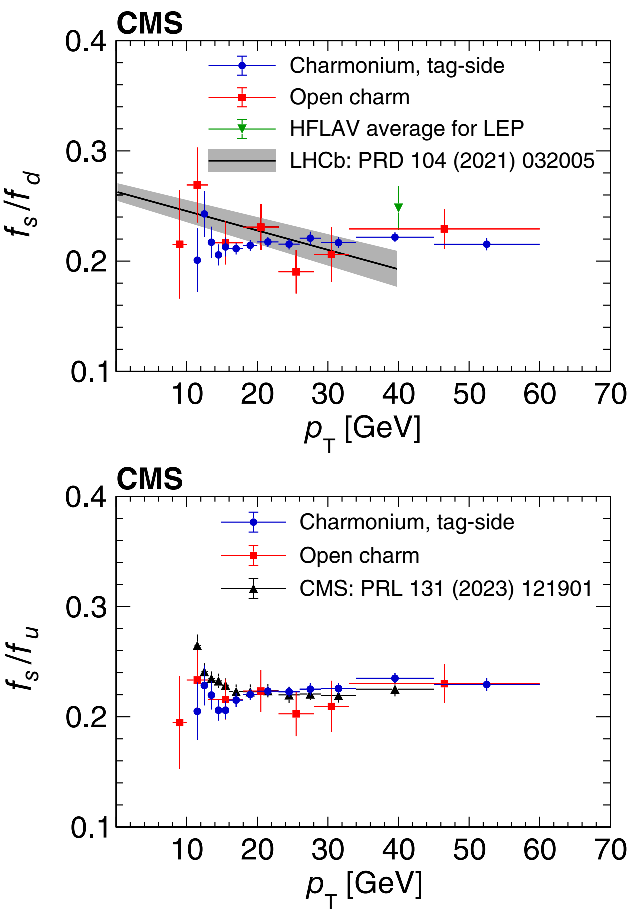

FIG. 9. The $\mathcal{R}_s^d$ and $\mathcal{R}_s$ values measured in the charmonium analysis, converted to f_s/f_d (upper)and f_s/f_u (lower) using the normalization factors c_{sd} and c_{su}, respectively. The error bars include both statistical and bin-to-bin uncorrelated systematic uncertainties. For comparison, PFR measurements from the open-charm analysis, LEP [48], and CMS [7] (converted to f_s/f_u using c_{su}) are overlaid, along with the p_{T} trend of f_s/f_d observed by LHCb [5] with its uncertainties displayed as the gray band. The f_s/f_d (f_s/f_u) global uncertainties are 6.3% (7.4%) for the open-charm channel and 8.4% (8.9%) for both the charmonium channel and the previous CMS result.

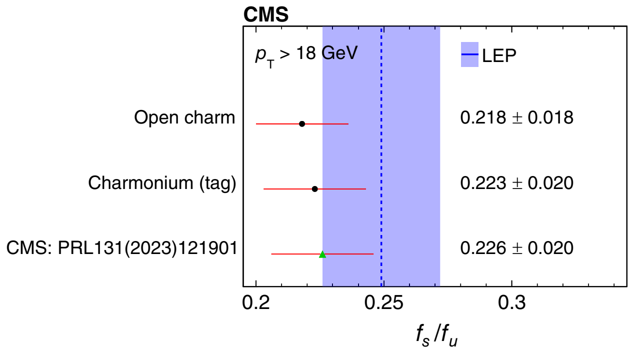

FIG. 10. Comparison of the f_s/f_u measurements at high p_T ($p_T > 18$ GeV) across different channels. The blue dashed line and shaded band represent the LEP measurement and its uncertainty [48], respectively, included for comparison. The $\mathcal{R}_s$ values obtained in the charmonium analysis in the tag-side category and the previous CMS measurement [7] are converted to f_s/f_u using the normalization factor c_{su}.

uncertainties associated with all of the values on the two next-to-last lines of each equation are also included.

The $\mathcal{R}$ values obtained in the tag-side charmonium analysis, as well as in an earlier CMS charmonium analysis [7], are converted to f_s/f_d and f_s/f_u using these normalization factors and are compared in Fig. 9 with the open-charm results, the LHCb [5] linear fit function, and the LEP high-p_T value [48]. The measured PFR values f_s/f_d and f_s/f_u are consistent with previous measurements from LHCb, CMS, and LEP, including the observed p_T dependence at low p_T. The converted PFR measurements from the charmonium analysis for the tag-side category over the full reconstructed kinematic range yield $\langle f_s/f_d \rangle = 0.216 \pm 0.018$ and $\langle f_s/f_u \rangle = 0.223 \pm 0.020$. Restricting to the region of $p_T > 18$ GeV, where the PFRs are observed to be independent of B meson kinematics, gives $f_s/f_d = 0.217 \pm 0.019$ and $f_s/f_u = 0.226 \pm 0.020$. Figure 10 provides a summary of CMS f_s/f_u measurements in the high-p_T region, with the uncertainties dominated by systematic effects that are common to all measurements.

X. SUMMARY

In summary, the relative production fractions of B^+, B^0, and B_s^0 mesons have been measured in proton-proton collisions at $\sqrt{s} = 13$ TeV using a special dataset recorded in 2018 with the CMS experiment at the LHC, corresponding to an integrated luminosity of 41.6 fb^{-1}. This dataset, collected with high-rate triggers, provided an unprecedented unbiased sample of 10^{10} b hadrons.

The production fraction ratios f_s/f_d, f_s/f_u, and f_d/f_u were measured as functions of B meson transverse momentum and absolute rapidity in the range of $8 < p_T < 60$ GeV and $|y| < 2.25$ using the corrected yield of open-charm decays combined with known branching fractions and precise theoretical calculations. These ratios were also measured in the charmonium decay channels, with the normalization of f_s/f_d and f_s/f_u in these channels obtained from the open-charm results. These normalization factors were extracted as a double ratio of the decay modes, thereby canceling any potential p_T dependence of the production fraction ratios. This makes these quantities universal constants that can be applied to any charmonium analysis.

In addition to measuring the production fraction ratios as a function of the B meson kinematics, we also reported average values of these quantities, with the f_d/f_u result being a test of isospin invariance of B meson production. The measurements were also used to extract B^+, B_s^0, and B^0 branching fraction ratios of open-charm decays to charmonium decays, with precision similar to the current world-average values.

ACKNOWLEDGMENTS

We congratulate our colleagues in the CERN accelerator departments for the excellent performance of the LHC and thank the technical and administrative staffs at CERN and at other CMS institutes for their contributions to the success of the CMS effort. In addition, we gratefully acknowledge the computing centers and personnel of the Worldwide LHC Computing Grid and other centers for delivering so effectively the computing infrastructure essential to our analyses. Finally, we acknowledge the enduring support for the construction and operation of the LHC, the CMS detector, and the supporting computing infrastructure provided by the following funding agencies: SC (Armenia), BMBWF and FWF (Austria); FNRS and FWO (Belgium); CNPq, CAPES, FAPERJ, FAPERGS, and FAPESP (Brazil); MES and BNSF (Bulgaria); CERN; CAS, MoST, and NSFC (China); MINCIENCIAS (Colombia); MSES and CSF (Croatia); RIF (Cyprus); SENESCYT (Ecuador); ERC PRG and PSG, TARISTU24-TK10, and MoER TK202 (Estonia); Academy of Finland, MEC, and HIP (Finland); CEA and CNRS/IN2P3 (France); SRNSF (Georgia); BMFTR, DFG, and HGF (Germany); GSRI (Greece); NKFIH (Hungary); DAE and DST (India); IPM (Iran); SFI (Ireland); INFN (Italy); MSIT and NRF (Republic of Korea); MES (Latvia); LMTLT (Lithuania); MOE and UM (Malaysia); BUAP, CINVESTAV, CONACYT, LNS, SEP, and UASLP-FAI (Mexico); MOS (Montenegro); MBIE (New Zealand); PAEC (Pakistan); MES, NSC, and NAWA (Poland); FCT (Portugal); MESTD (Serbia); MICIU/AEI and PCTI (Spain); MOSTR (Sri Lanka); Swiss Funding Agencies (Switzerland); MST (Taipei); MHESI (Thailand); TUBITAK and TENMAK (Türkiye); NASU (Ukraine); STFC (United Kingdom); DOE and NSF (U.S.). Individuals have received support from the Marie-Curie program and the European Research Council and Horizon 2020 Grant, Contracts No. 675440, No. 724704, No. 752730, No. 758316, No. 765710, No. 824093, No. 101115353, No. 101002207, No. 101001205, and COST Action CA16108 (European Union); the Leventis Foundation; the Alfred P. Sloan Foundation; the Alexander von Humboldt Foundation; the Science Committee, project no. 22rl-037 (Armenia); the Fonds pour la Formation *à la* Recherche dans l'Industrie et dans l'Agriculture (FRIA) and Fonds voor Wetenschappelijk Onderzoek Contract No. 1228724N (Belgium); the Beijing Municipal Science & Technology Commission, No. Z191100007219010, the Fundamental Research Funds for the Central Universities, the Ministry of Science and Technology of China under Grant No. 2023YFA1605804, the Natural Science Foundation of China under Grant No. 12535004, and USTC Research Funds of the Double First-Class Initiative No. YD2030002017 (China); the Ministry of Education, Youth and Sports (MEYS) of the Czech Republic; the Shota Rustaveli National Science Foundation, Grant No. FR-22-985 (Georgia); the Deutsche Forschungsgemeinschaft (DFG), among others, under Germany's Excellence Strategy—EXC 2121 "Quantum Universe"—390833306, and under project no. 400140256—GRK2497; the Hellenic Foundation for Research and Innovation (HFRI), project no. 2288 (Greece); the Hungarian Academy of Sciences, the New National Excellence Program—ÚNKP, the NKFIH research Grants No. K 131991, No. K 133046, No. K 138136, No. K 143460, No. K 143477, No. K 146913, No. K 146914, No. K 147048, No. 2020-2.2.1-ED-2021-00181, No. TKP2021-NKTA-64, and No. 2025-1.1.5-NEMZ_KI-2025-00004 (Hungary); the Council of Science and Industrial Research, India; ICSC—National Research Center for High Performance Computing, Big Data and Quantum Computing, FAIR—Future Artificial Intelligence Research, and CUP I53D23001070006 (Mission 4 Component 1), funded by the NextGenerationEU program (Italy); the Latvian Council of Science; the Ministry of Education and Science, project no. 2022/WK/14, and the National Science Center, contracts Opus 2021/41/B/ST2/01369, 2021/43/B/ST2/01552, 2023/49/B/ST2/03273, and the NAWA Contract No. BPN/PPO/2021/1/00011 (Poland); the Fundação para a Ciência e a Tecnologia (Portugal); the National Priorities Research Program by Qatar National Research Fund; MICIU/AEI/10.13039/501100011033, ERDF/EU, "European Union NextGenerationEU/PRTR," and Programa Severo Ochoa del Principado de Asturias (Spain); the Chulalongkorn Academic into Its 2nd Century Project Advancement Project, the National Science, Research and Innovation Fund program IND_FF_68_369_2300_097, and the Program Management Unit for Human Resources & Institutional Development, Research and Innovation, Grant No. B39G680009 (Thailand); the Eric and Wendy Schmidt Fund for Strategic Innovation through the CERN Next Generation Triggers project under Grant Agreement No. SIF-2023-004; the Kavli Foundation; the Nvidia Corporation; the SuperMicro Corporation; the Welch Foundation, Contract No. C-1845; and the Weston Havens Foundation (U.S.).

DATA AVAILABILITY

Release and preservation of data used by the CMS Collaboration as the basis for publications is guided by the CMS data preservation, reuse, and open access policy [49].

[1] LHCb Collaboration, Measurement of b-hadron production fractions in 7 TeV pp collisions, Phys. Rev. D **85**, 032008 (2012).

[2] LHCb Collaboration, Measurement of the fragmentation fraction ratio f_s/f_d and its dependence on B meson kinematics, J. High Energy Phys. 04 (2013) 001.

[3] LHCb Collaboration, Measurement of b hadron fractions in 13 TeV pp collisions, Phys. Rev. D **100**, 031102 (2019).

[4] LHCb Collaboration, Measurement of f_s/f_u variation with proton-proton collision energy and B-meson kinematics, Phys. Rev. Lett. **124**, 122002 (2020).

[5] LHCb Collaboration, Precise measurement of the f_s/f_d ratio of fragmentation fractions and of B_s^0 decay branching fractions, Phys. Rev. D **104**, 032005 (2021).

[6] ATLAS Collaboration, Determination of the ratio of b-quark fragmentation fractions f_s/f_d in pp collisions at $\sqrt{s} = 7$ TeV with the ATLAS detector, Phys. Rev. Lett. **115**, 262001 (2015).

[7] CMS Collaboration, Measurement of the dependence of the hadron production fraction ratio f_s/f_u and f_d/f_u on B meson kinematic variables in proton-proton collisions at $\sqrt{s} = 13$ TeV, Phys. Rev. Lett. **131**, 121901 (2023).

[8] S. Esen *et al.* (Belle Collaboration), Precise measurement of the branching fractions for $B_s^0 \to D_s{}^{(*)+} D_s{}^{(*)-}$ and first measurement of the $D_s{}^{*+} D_s{}^{*-}$ polarization using e^+e^- collisions, Phys. Rev. D **87**, 031101 (2013).

[9] CMS Collaboration, Measurement of the $B_s^0 \to \mu^+\mu^-$ decay properties and search for the $B^0 \to \mu^+\mu^-$ decay in proton-proton collisions at $\sqrt{s} = 13$ TeV, Phys. Lett. B **842**, 137955 (2023).

[10] S. Banerjee *et al.* (HFLAV Collaboration), Averages of b-hadron, c-hadron, and τ-lepton properties as of 2023, Phys. Rev. D **113**, 012008 (2026).

[11] F. Bernlochner, M. Jung, M. Khan, G. Landsberg, and Z. Ligeti, Novel approaches to determine $B^\pm$ and B^0 meson production fractions, Phys. Rev. D **110**, 014007 (2024).

[12] CMS Collaboration, Enriching the physics program of the CMS experiment via data scouting and data parking, Phys. Rep. **1115**, 678 (2025).

[13] CMS Collaboration, CMS luminosity measurements for the 2018 data-taking period at $\sqrt{s} = 13$ TeV, CMS Physics Analysis Summary, Report No. CMS-PAS-LUM-18-001, 2018, https://cds.cern.ch/record/2676164.

[14] HEPDATA record for this analysis (2026), 10.17182/hepdata.158357.

[15] W. Adam *et al.*, The CMS Phase-1 pixel detector upgrade, J. Instrum. **16**, P02027 (2021).

[16] CMS Collaboration, Track impact parameter resolution for the full pseudo rapidity coverage in the 2017 dataset with the CMS Phase-1 Pixel detector, CMS Detector Performance Note, Report No. CMS-DP-2020-049, 2020.

[17] CMS Collaboration, Performance of the CMS muon detector and muon reconstruction with proton-proton collisions at $\sqrt{s} = 13$ TeV, J. Instrum. **13**, P06015 (2018).

[18] CMS Collaboration, Performance of the CMS Level-1 trigger in proton-proton collisions at $\sqrt{s} = 13$ TeV, J. Instrum. **15**, P10017 (2020).

[19] CMS Collaboration, The CMS trigger system, J. Instrum. **12**, P01020 (2017).

[20] CMS Collaboration, The CMS experiment at the CERN LHC, J. Instrum. **3**, S08004 (2008).

[21] CMS Collaboration, Development of the CMS detector for the CERN LHC Run 3, J. Instrum. **19**, P05064 (2024).

[22] T. Sjöstrand, S. Ask, J. R. Christiansen, R. Corke, N. Desai, P. Ilten, S. Mrenna, S. Prestel, C. O. Rasmussen, and P. Z. Skands, An introduction to PYTHIA 8.2, Comput. Phys. Commun. **191**, 159 (2015).

[23] CMS Collaboration, Extraction and validation of a new set of CMS PYTHIA8 tunes from underlying-event measurements, Eur. Phys. J. C **80**, 4 (2020).

[24] R. D. Ball *et al.* (NNPDF Collaboration), Parton distributions from high-precision collider data, Eur. Phys. J. C **77**, 663 (2017).

[25] D. J. Lange, The EvtGen particle decay simulation package, Nucl. Instrum. Methods Phys. Res., Sect. A **462**, 152 (2001).

[26] E. Barberio and Z. Was, PHOTOS: A universal Monte Carlo for QED radiative corrections. Version 2.0, Comput. Phys. Commun. **79**, 291 (1994).

[27] S. Agostinelli *et al.* (GEANT4 Collaboration), GEANT4—a simulation toolkit, Nucl. Instrum. Methods Phys. Res., Sect. A **506**, 250 (2003).

[28] M. Beneke, G. Buchalla, M. Neubert, and C. T. Sachrajda, QCD factorization for exclusive, nonleptonic B meson decays: General arguments and the case of heavy light final states, Nucl. Phys. B **591**, 313 (2000).

[29] R. Fleischer, N. Serra, and N. Tuning, Tests of factorization and SU(3) relations in B decays into heavy-light final states, Phys. Rev. D **83**, 014017 (2011).

[30] T. Huber, S. Kränkl, and X.-Q. Li, Two-body non-leptonic heavy-to-heavy decays at NNLO in QCD factorization, J. High Energy Phys. 09 (2016) 112.

[31] M. Bordone, N. Gubernari, T. Huber, M. Jung, and D. van Dyk, A puzzle in $\bar{B}^0_{(s)} \to D^{(*)+}_{(s)}\{\pi^-, K^-\}$ decays and extraction of the f_s/f_d fragmentation fraction, Eur. Phys. J. C **80**, 951 (2020).

[32] S. Navas *et al.* (Particle Data Group Collaboration), Review of particle physics, Phys. Rev. D **110**, 030001 (2024).

[33] M. Di Carlo, D. Giusti, V. Lubicz, G. Martinelli, C. T. Sachrajda, F. Sanfilippo, S. Simula, and N. Tantalo, Light-meson leptonic decay rates in lattice QCD + QED, Phys. Rev. D **100**, 034514 (2019).

[34] Heavy Flavor Averaging Group, PDG 2025 averages, averages for the 2025 edition of the Review of Particle Physics, https://hflav-eos.web.cern.ch/hflav-eos/osc/PDG_2025.

[35] K. Chilikin *et al.* (Belle Collaboration), Observation of a new charged charmoniumlike state in $\bar{B}^0 \to J/\psi K^-\pi^+$ decays, Phys. Rev. D **90**, 112009 (2014).

[36] CMS Collaboration, CMS tracking performance results from early LHC operation, Eur. Phys. J. C **70**, 1165 (2010).

[37] CMS Collaboration, Particle-flow reconstruction and global event description with the CMS detector, J. Instrum. **12**, P10003 (2017).

[38] P. del Amo Sanchez *et al.* (*BABAR* Collaboration), Dalitz plot analysis of $D_s^+ \to K^+K^-\pi^+$, Phys. Rev. D **83**, 052001 (2011).

[39] M. Pivk and F. R. Le Diberder, ${}_sPlot$: A Statistical tool to unfold data distributions, Nucl. Instrum. Methods Phys. Res., Sect. A **555**, 356 (2005).

[40] T. Chen and C. Guestrin, XGBoost: A scalable tree boosting system, in *Proc. 22nd ACM SIGKDD Int. Conf. on Knowledge Discovery and Data Mining* (2016), 10.1145/2939672.2939785.

[41] F. Pedregosa *et al.*, Scikit-learn: Machine learning in Python, J. Mach. Learn. Res. **12**, 2825 (2011), https://www.slac.stanford.edu/pubs/slacreports/reports13/slac-r-236.pdf.

[42] N. L. Johnson, Systems of frequency curves generated by methods of translation, Biometrika **36**, 149 (1949).

[43] M. J. Oreglia, A study of the reactions $\psi' \to \gamma\gamma\psi$, Ph.D. thesis, Stanford University, 1980 [SLAC Report No. SLAC-R-236].

[44] CMS Collaboration, Measurements of inclusive W and Z cross sections in pp collisions at $\sqrt{s} = 7$ TeV, J. High Energy Phys. 01 (2011) 080.

[45] M. Cacciari, M. Greco, and P. Nason, The p_T spectrum in heavy-flavour hadroproduction, J. High Energy Phys. 05 (1998) 007.

[46] CMS Collaboration, Tracking performances for charged pions with Run2 Legacy data, CMS Detector Performance Note, Report No. CMS-DP-2022-012, 2022, https://cds.cern.ch/record/2810814.

[47] S. Jackman, *Bayesian Analysis for the Social Sciences* (John Wiley & Sons, New Jersey, USA, 2009).

[48] Y. S. Amhis *et al.* (HFLAV Collaboration), Averages of b-hadron, c-hadron, and τ-lepton properties as of 2018, Eur. Phys. J. C **81**, 226 (2021).

[49] CMS data availability statement, 10.7483/OPENDATA.CMS.1BNU.8V1W.

A. Hayrapetyan,[1] V. Makarenko,[1] A. Tumasyan,[1,b] W. Adam,[2] J. W. Andrejkovic,[2] L. Benato,[2] T. Bergauer,[2] M. Dragicevic,[2] C. Giordano,[2] P. S. Hussain,[2] M. Jeitler,[2,c] N. Krammer,[2] A. Li,[2] D. Liko,[2] I. Mikulec,[2] J. Schieck,[2,c] R. Schöfbeck,[2,c] D. Schwarz,[2] M. Shooshtari,[2] M. Sonawane,[2] W. Waltenberger,[2] C.-E. Wulz,[2,c] T. Janssen,[3] H. Kwon,[3] D. Ocampo Henao,[3] T. Van Laer,[3] P. Van Mechelen,[3] J. Bierkens,[4] N. Breugelmans,[4] J. D'Hondt,[4] S. Dansana,[4] A. De Moor,[4] M. Delcourt,[4] F. Heyen,[4] Y. Hong,[4] P. Kashko,[4] S. Lowette,[4] I. Makarenko,[4] D. Müller,[4] J. Song,[4] S. Tavernier,[4] M. Tytgat,[4,d] G. P. Van Onsem,[4] S. Van Putte,[4] D. Vannerom,[4] B. Bilin,[5] B. Clerbaux,[5] A. K. Das,[5] I. De Bruyn,[5] G. De Lentdecker,[5] H. Evard,[5] L. Favart,[5] P. Gianneios,[5] A. Khalilzadeh,[5] F. A. Khan,[5] A. Malara,[5] M. A. Shahzad,[5] L. Thomas,[5] M. Vanden Bemden,[5] C. Vander Velde,[5] P. Vanlaer,[5] F. Zhang,[5] M. De Coen,[6] D. Dobur,[6] G. Gokbulut,[6] J. Knolle,[6] L. Lambrecht,[6] D. Marckx,[6] K. Skovpen,[6] N. Van Den Bossche,[6] J. van der Linden,[6] J. Vandenbroeck,[6] L. Wezenbeek,[6] S. Bein,[7] A. Benecke,[7] A. Bethani,[7] G. Bruno,[7] A. Cappati,[7] J. De Favereau De Jeneret,[7] C. Delaere,[7] A. Giammanco,[7] A. O. Guzel,[7] V. Lemaitre,[7] J. Lidrych,[7] P. Malek,[7] P. Mastrapasqua,[7] S. Turkcapar,[7] G. A. Alves,[8] M. Barroso Ferreira Filho,[8] E. Coelho,[8] C. Hensel,[8] T. Menezes De Oliveira,[8] C. Mora Herrera,[8,e] P. Rebello Teles,[8] M. Soeiro,[8] E. J. Tonelli Manganote,[8,f] A. Vilela Pereira,[8,e] W. L. Aldá Júnior,[9] H. Brandao Malbouisson,[9] W. Carvalho,[9] J. Chinellato,[9,g] M. Costa Reis,[9] E. M. Da Costa,[9] G. G. Da Silveira,[9,h] D. De Jesus Damiao,[9] S. Fonseca De Souza,[9] R. Gomes De Souza,[9] S. S. Jesus,[9] T. Laux Kuhn,[9,h] M. Macedo,[9] K. Mota Amarilo,[9] L. Mundim,[9] H. Nogima,[9] J. P. Pinheiro,[9] A. Santoro,[9] A. Sznajder,[9] M. Thiel,[9] F. Torres Da Silva De Araujo,[9,i] C. A. Bernardes,[10,h] T. R. Fernandez Perez Tomei,[10] E. M. Gregores,[10] B. Lopes Da Costa,[10] I. Maietto Silverio,[10] P. G. Mercadante,[10] S. F. Novaes,[10] B. Orzari,[10] Sandra S. Padula,[10] V. Scheurer,[10] A. Aleksandrov,[11] G. Antchev,[11] P. Danev,[11] R. Hadjiiska,[11] P. Iaydjiev,[11] M. Misheva,[11] M. Shopova,[11] G. Sultanov,[11] A. Dimitrov,[12] L. Litov,[12] B. Pavlov,[12] P. Petkov,[12] A. Petrov,[12] S. Keshri,[13] D. Laroze,[13] S. Thakur,[13] W. Brooks,[14] T. Cheng,[15] T. Javaid,[15] L. Wang,[15] L. Yuan,[15] Z. Hu,[16] Z. Liang,[16] J. Liu,[16] X. Wang,[16] G. M. Chen,[17,j] H. S. Chen,[17,j] M. Chen,[17,j] Y. Chen,[17] Q. Hou,[17] X. Hou,[17] F. Iemmi,[17] C. H. Jiang,[17] A. Kapoor,[17,k] H. Liao,[17] G. Liu,[17] Z.-A. Liu,[17,l] J. N. Song,[17,l] S. Song,[17] J. Tao,[17] C. Wang,[17,j] J. Wang,[17] H. Zhang,[17] J. Zhao,[17] A. Agapitos,[18] Y. Ban,[18] A. Carvalho Antunes De Oliveira,[18] S. Deng,[18] B. Guo,[18] Q. Guo,[18] C. Jiang,[18] A. Levin,[18] C. Li,[18] Q. Li,[18] Y. Mao,[18] S. Qian,[18] S. J. Qian,[18] X. Qin,[18] X. Sun,[18] D. Wang,[18] J. Wang,[18] H. Yang,[18] M. Zhang,[18] Y. Zhao,[18] C. Zhou,[18] S. Yang,[19] Z. You,[20] K. Jaffel,[21] N. Lu,[21] G. Bauer,[22,m] B. Li,[22,n] H. Wang,[22] K. Yi,[22,o] J. Zhang,[22] Y. Li,[23] Z. Lin,[24] C. Lu,[24] M. Xiao,[24,p] C. Avila,[25] D. A. Barbosa Trujillo,[25] A. Cabrera,[25] C. Florez,[25] J. Fraga,[25] J. A. Reyes Vega,[25] C. Rendón,[26] M. Rodriguez,[26] A. A. Ruales Barbosa,[26] J. D. Ruiz Alvarez,[26] N. Godinovic,[27] D. Lelas,[27] A. Sculac,[27] M. Kovac,[28] A. Petkovic,[28] T. Sculac,[28] P. Bargassa,[29] V. Brigljevic,[29] B. K. Chitroda,[29] D. Ferencek,[29] K. Jakovcic,[29] A. Starodumov,[29] T. Susa,[29] A. Attikis,[30] K. Christoforou,[30] A. Hadjiagapiou,[30] C. Leonidou,[30] C. Nicolaou,[30] L. Paizanos,[30] F. Ptochos,[30] P. A. Razis,[30] H. Rykaczewski,[30] H. Saka,[30] A. Stepennov,[30] M. Finger,[31,a] M. Finger Jr.,[31] E. Ayala,[32] E. Carrera Jarrin,[33] S. Elgammal,[34,q] A. Ellithi Kamel,[34,r] M. Abdullah Al-Mashad,[35] A. Hussein,[35] H. Mohammed,[35] K. Ehataht,[36] M. Kadastik,[36] T. Lange,[36] C. Nielsen,[36] J. Pata,[36] M. Raidal,[36] N. Seeba,[36] L. Tani,[36] A. Milieva,[37] K. Osterberg,[37] M. Voutilainen,[37] N. Bin Norjoharuddeen,[38] E. Brücken,[38] F. Garcia,[38] P. Inkaew,[38] K. T. S. Kallonen,[38] R. Kumar Verma,[38] T. Lampén,[38] K. Lassila-Perini,[38] B. Lehtela,[38] S. Lehti,[38] T. Lindén,[38] N. R. Mancilla Xinto,[38] M. Myllymäki,[38] M. m. Rantanen,[38] S. Saariokari,[38] N. T. Toikka,[38] J. Tuominiemi,[38] H. Kirschenmann,[39] P. Luukka,[39] H. Petrow,[39] M. Besancon,[40] F. Couderc,[40] M. Dejardin,[40] D. Denegri,[40] P. Devouge,[40] J. L. Faure,[40] F. Ferri,[40] S. Ganjour,[40] P. Gras,[40] G. Hamel de Monchenault,[40] M. Kumar,[40] V. Lohezic,[40] J. Malcles,[40] F. Orlandi,[40] L. Portales,[40] S. Ronchi,[40] M. Ö. Sahin,[40] A. Savoy-Navarro,[40,s] P. Simkina,[40] M. Titov,[40] M. Tornago,[40] F. Beaudette,[41] G. Boldrini,[41] P. Busson,[41] C. Charlot,[41] M. Chiusi,[41] T. D. Cuisset,[41] F. Damas,[41] O. Davignon,[41] A. De Wit,[41] T. Debnath,[41] I. T. Ehle,[41] B. A. Fontana Santos Alves,[41] S. Ghosh,[41] A. Gilbert,[41] R. Granier de Cassagnac,[41] L. Kalipoliti,[41] M. Manoni,[41] M. Nguyen,[41] S. Obraztsov,[41] C. Ochando,[41] R. Salerno,[41] J. B. Sauvan,[41] Y. Sirois,[41] G. Sokmen,[41] L. Urda Gómez,[41] A. Zabi,[41] A. Zghiche,[41] J.-L. Agram,[42,t] J. Andrea,[42] D. Bloch,[42] J.-M. Brom,[42] E. C. Chabert,[42] C. Collard,[42] G. Coulon,[42] S. Falke,[42] U. Goerlach,[42] R. Haeberle,[42] A.-C. Le Bihan,[42] M. Meena,[42] O. Poncet,[42] G. Saha,[42] P. Vaucelle,[42] A. Di Florio,[43] D. Amram,[44] S. Beauceron,[44] B. Blancon,[44] G. Boudoul,[44] N. Chanon,[44] D. Contardo,[44] P. Depasse,[44] C. Dozen,[44,u]

H. El Mamouni,[44] J. Fay,[44] S. Gascon,[44] M. Gouzevitch,[44] C. Greenberg,[44] G. Grenier,[44] B. Ille,[44] E. Jourd'huy,[44] I. B. Laktineh,[44] M. Lethuillier,[44] B. Massoteau,[44] L. Mirabito,[44] A. Purohit,[44] M. Vander Donckt,[44] J. Xiao,[44] G. Adamov,[45] I. Lomidze,[45] Z. Tsamalaidze,[45,v] V. Botta,[46] S. Consuegra Rodríguez,[46] L. Feld,[46] K. Klein,[46] M. Lipinski,[46] D. Meuser,[46] P. Nattland,[46] V. Oppenländer,[46] A. Pauls,[46] D. Pérez Adán,[46] N. Röwert,[46] M. Teroerde,[46] C. Daumann,[47] S. Diekmann,[47] A. Dodonova,[47] N. Eich,[47] D. Eliseev,[47] F. Engelke,[47] J. Erdmann,[47] M. Erdmann,[47] B. Fischer,[47] T. Hebbeker,[47] K. Hoepfner,[47] F. Ivone,[47] A. Jung,[47] N. Kumar,[47] M. y. Lee,[47] F. Mausolf,[47] M. Merschmeyer,[47] A. Meyer,[47] F. Nowotny,[47] A. Pozdnyakov,[47] W. Redjeb,[47] H. Reithler,[47] U. Sarkar,[47] V. Sarkisovi,[47] A. Schmidt,[47] C. Seth,[47] A. Sharma,[47] J. L. Spah,[47] V. Vaulin,[47] S. Zaleski,[47] M. R. Beckers,[48] C. Dziwok,[48] G. Flügge,[48] N. Hoeflich,[48] T. Kress,[48] A. Nowack,[48] O. Pooth,[48] A. Stahl,[48] A. Zotz,[48] H. Aarup Petersen,[49] A. Abel,[49] M. Aldaya Martin,[49] J. Alimena,[49] S. Amoroso,[49] Y. An,[49] I. Andreev,[49] J. Bach,[49] S. Baxter,[49] M. Bayatmakou,[49] H. Becerril Gonzalez,[49] O. Behnke,[49] A. Belvedere,[49] F. Blekman,[49,w] K. Borras,[49,x] A. Campbell,[49] S. Chatterjee,[49] L. X. Coll Saravia,[49] G. Eckerlin,[49] D. Eckstein,[49] E. Gallo,[49,w] A. Geiser,[49] V. Guglielmi,[49] M. Guthoff,[49] A. Hinzmann,[49] L. Jeppe,[49] M. Kasemann,[49] C. Kleinwort,[49] R. Kogler,[49] M. Komm,[49] D. Krücker,[49] W. Lange,[49] D. Leyva Pernia,[49] K.-Y. Lin,[49] K. Lipka,[49,y] W. Lohmann,[49,z] J. Malvaso,[49] R. Mankel,[49] I.-A. Melzer-Pellmann,[49] M. Mendizabal Morentin,[49] A. B. Meyer,[49] G. Milella,[49] K. Moral Figueroa,[49] A. Mussgiller,[49] L. P. Nair,[49] J. Niedziela,[49] A. Nürnberg,[49] J. Park,[49] E. Ranken,[49] A. Raspereza,[49] D. Rastorguev,[49] L. Rygaard,[49] M. Scham,[49,aa,x] S. Schnake,[49,x] P. Schütze,[49] C. Schwanenberger,[49,w] D. Selivanova,[49] K. Sharko,[49] M. Shchedrolosiev,[49] D. Stafford,[49] M. Torkian,[49] F. Vazzoler,[49] A. Ventura Barroso,[49] R. Walsh,[49] D. Wang,[49] Q. Wang,[49] K. Wichmann,[49] L. Wiens,[49,x] C. Wissing,[49] Y. Yang,[49] S. Zakharov,[49] A. Zimermmane Castro Santos,[49] A. Albrecht,[50] A. R. Alves Andrade,[50] M. Antonello,[50] S. Bollweg,[50] M. Bonanomi,[50] K. El Morabit,[50] Y. Fischer,[50] M. Frahm,[50] E. Garutti,[50] A. Grohsjean,[50] A. A. Guvenli,[50] J. Haller,[50] D. Hundhausen,[50] H. R. Jabusch,[50] G. Kasieczka,[50] P. Keicher,[50] R. Klanner,[50] W. Korcari,[50] T. Kramer,[50] C. c. Kuo,[50] V. Kutzner,[50] F. Labe,[50] J. Lange,[50] A. Lobanov,[50] L. Moureaux,[50] M. Mrowietz,[50] A. Nigamova,[50] K. Nikolopoulos,[50] Y. Nissan,[50] A. Paasch,[50] K. J. Pena Rodriguez,[50] N. Prouvost,[50] T. Quadfasel,[50] B. Raciti,[50] M. Rieger,[50] D. Savoiu,[50] J. Schindler,[50] P. Schleper,[50] M. Schröder,[50] J. Schwandt,[50] M. Sommerhalder,[50] H. Stadie,[50] G. Steinbrück,[50] A. Tews,[50] R. Ward,[50] B. Wiederspan,[50] M. Wolf,[50] S. Brommer,[51] E. Butz,[51] Y. M. Chen,[51] T. Chwalek,[51] A. Dierlamm,[51] G. G. Dincer,[51] U. Elicabuk,[51] N. Faltermann,[51] M. Giffels,[51] A. Gottmann,[51] F. Hartmann,[51,bb] R. Hofsaess,[51] M. Horzela,[51] U. Husemann,[51] J. Kieseler,[51] M. Klute,[51] R. Kunnilan Muhammed Rafeek,[51] O. Lavoryk,[51] J. M. Lawhorn,[51] A. Lintuluoto,[51] S. Maier,[51] M. Mormile,[51] Th. Müller,[51] E. Pfeffer,[51] M. Presilla,[51] G. Quast,[51] K. Rabbertz,[51] B. Regnery,[51] R. Schmieder,[51] N. Shadskiy,[51] I. Shvetsov,[51] H. J. Simonis,[51] L. Sowa,[51] L. Stockmeier,[51] K. Tauqeer,[51] M. Toms,[51] B. Topko,[51] N. Trevisani,[51] C. Verstege,[51] T. Voigtländer,[51] R. F. Von Cube,[51] J. Von Den Driesch,[51] M. Wassmer,[51] R. Wolf,[51] W. D. Zeuner,[51] X. Zuo,[51] G. Anagnostou,[52] G. Daskalakis,[52] A. Kyriakis,[52] A. Papadopoulos,[52,bb] A. Stakia,[52] G. Melachroinos,[53] Z. Painesis,[53] I. Paraskevas,[53] N. Saoulidou,[53] K. Theofilatos,[53] E. Tziaferi,[53] K. Vellidis,[53] I. Zisopoulos,[53] T. Chatzistavrou,[54] G. Karapostoli,[54] K. Kousouris,[54] E. Siamarkou,[54] G. Tsipolitis,[54] I. Bestintzanos,[55] I. Evangelou,[55] C. Foudas,[55] P. Katsoulis,[55] P. Kokkas,[55] P. G. Kosmoglou Kioseoglou,[55] N. Manthos,[55] I. Papadopoulos,[55] J. Strologas,[55] D. Druzhkin,[56] C. Hajdu,[56] D. Horvath,[56,cc,dd] K. Márton,[56] A. J. Rádl,[56,ee] F. Sikler,[56] V. Veszpremi,[56] M. Csanád,[57] K. Farkas,[57] A. Fehérkuti,[57,ff] M. M. A. Gadallah,[57,gg] Á. Kadlecsik,[57] M. León Coello,[57] G. Pásztor,[57] G. I. Veres,[57] B. Ujvari,[58] G. Zilizi,[58] G. Bencze,[59] S. Czellar,[59] J. Molnar,[59] Z. Szillasi,[59] T. Csorgo,[60,ff] F. Nemes,[60,ff] T. Novak,[60] I. Szanyi,[60,hh] S. Bansal,[61] S. B. Beri,[61] V. Bhatnagar,[61] G. Chaudhary,[61] S. Chauhan,[61] N. Dhingra,[61,ii] A. Kaur,[61] A. Kaur,[61] H. Kaur,[61] M. Kaur,[61] S. Kumar,[61] T. Sheokand,[61] J. B. Singh,[61] A. Singla,[61] A. Bhardwaj,[62] A. Chhetri,[62] B. C. Choudhary,[62] A. Kumar,[62] A. Kumar,[62] M. Naimuddin,[62] S. Phor,[62] K. Ranjan,[62] M. K. Saini,[62] S. Acharya,[63,jj] B. Gomber,[63,jj] B. Sahu,[63,jj] S. Mukherjee,[64] S. Baradia,[65] S. Bhattacharya,[65] S. Das Gupta,[65] S. Dutta,[65] S. Dutta,[65] S. Sarkar,[65] M. M. Ameen,[66] P. K. Behera,[66] S. Chatterjee,[66] G. Dash,[66] A. Dattamunsi,[66] P. Jana,[66] P. Kalbhor,[66] S. Kamble,[66] J. R. Komaragiri,[66,kk] T. Mishra,[66] P. R. Pujahari,[66] N. R. Saha,[66] A. K. Sikdar,[66] R. K. Singh,[66] P. Verma,[66] S. Verma,[66] A. Vijay,[66] B. K. Sirasva,[67] L. Bhatt,[68] S. Dugad,[68] G. B. Mohanty,[68] M. Shelake,[68] P. Suryadevara,[68] A. Bala,[69] S. Banerjee,[69] S. Barman,[69,ll] R. M. Chatterjee,[69] M. Guchait,[69] Sh. Jain,[69]

A. Jaiswal,[69] B. M. Joshi,[69] S. Kumar,[69] M. Maity,[69,ll] G. Majumder,[69] K. Mazumdar,[69] S. Parolia,[69] R. Saxena,[69] A. Thachayath,[69] S. Bahinipati,[70,mm] D. Maity,[70,nn] P. Mal,[70] K. Naskar,[70,nn] A. Nayak,[70,nn] S. Nayak,[70] K. Pal,[70] R. Raturi,[70] P. Sadangi,[70] S. K. Swain,[70] S. Varghese,[70,nn] D. Vats,[70,nn] A. Alpana,[71] S. Dube,[71] P. Hazarika,[71] B. Kansal,[71] A. Laha,[71] R. Sharma,[71] S. Sharma,[71] K. Y. Vaish,[71] S. Ghosh,[72] H. Bakhshiansohi,[73,oo] A. Jafari,[73,pp] V. Sedighzadeh Dalavi,[73] M. Zeinali,[73,qq] S. Bashiri,[74] S. Chenarani,[74,rr] S. M. Etesami,[74] Y. Hosseini,[74] M. Khakzad,[74] E. Khazaie,[74] M. Mohammadi Najafabadi,[74] S. Tizchang,[74,ss] M. Felcini,[75] M. Grunewald,[75] M. Abbrescia,[76a,76b] M. Barbieri,[76a,76b] M. Buonsante,[76a,76b] A. Colaleo,[76a,76b] D. Creanza,[76a,76c] B. D'Anzi,[76a,76b] N. De Filippis,[76a,76c] M. De Palma,[76a,76b] W. Elmetenawee,[76a,76b,tt] N. Ferrara,[76a,76c] L. Fiore,[76a] L. Longo,[76a] M. Louka,[76a,76b] G. Maggi,[76a,76c] M. Maggi,[76a] I. Margjeka,[76a] V. Mastrapasqua,[76a,76b] S. My,[76a,76b] F. Nenna,[76a,76b] S. Nuzzo,[76a,76b] A. Pellecchia,[76a,76b] A. Pompili,[76a,76b] G. Pugliese,[76a,76c] R. Radogna,[76a,76b] D. Ramos,[76a] A. Ranieri,[76a] L. Silvestris,[76a] F. M. Simone,[76a,76c] Ü. Sözbilir,[76a] A. Stamerra,[76a,76b] D. Troiano,[76a,76b] R. Venditti,[76a,76b] P. Verwilligen,[76a] A. Zaza,[76a,76b] G. Abbiendi,[77a] C. Battilana,[77a,77b] D. Bonacorsi,[77a,77b] P. Capiluppi,[77a,77b] F. R. Cavallo,[77a] M. Cuffiani,[77a,77b] G. M. Dallavalle,[77a] T. Diotalevi,[77a,77b] F. Fabbri,[77a] A. Fanfani,[77a,77b] D. Fasanella,[77a] C. Grandi,[77a] L. Guiducci,[77a,77b] S. Lo Meo,[77a,uu] M. Lorusso,[77a,77b] L. Lunerti,[77a] S. Marcellini,[77a] G. Masetti,[77a] F. L. Navarria,[77a,77b] G. Paggi,[77a,77b] A. Perrotta,[77a] F. Primavera,[77a,77b] A. M. Rossi,[77a,77b] S. Rossi Tisbeni,[77a,77b] T. Rovelli,[77a,77b] G. P. Siroli,[77a,77b] S. Costa,[78a,78b,vv] A. Di Mattia,[78a] A. Lapertosa,[78a] R. Potenza,[78a,78b] A. Tricomi,[78a,78b,vv] J. Altork,[79a,79b] P. Assiouras,[79a] G. Barbagli,[79a] G. Bardelli,[79a] M. Bartolini,[79a,79b] A. Calandri,[79a,79b] B. Camaiani,[79a,79b] A. Cassese,[79a] R. Ceccarelli,[79a] V. Ciulli,[79a,79b] C. Civinini,[79a] R. D'Alessandro,[79a,79b] L. Damenti,[79a,79b] E. Focardi,[79a,79b] T. Kello,[79a] G. Latino,[79a,79b] P. Lenzi,[79a,79b] M. Lizzo,[79a] M. Meschini,[79a] S. Paoletti,[79a] A. Papanastassiou,[79a,79b] G. Sguazzoni,[79a] L. Viliani,[79a] L. Benussi,[80] S. Colafranceschi,[80] S. Meola,[80,ww] D. Piccolo,[80] M. Alves Gallo Pereira,[81a] F. Ferro,[81a] E. Robutti,[81a] S. Tosi,[81a,81b] A. Benaglia,[82a] F. Brivio,[82a] V. Camagni,[82a,82b] F. Cetorelli,[82a,82b] F. De Guio,[82a,82b] M. E. Dinardo,[82a,82b] P. Dini,[82a] S. Gennai,[82a] R. Gerosa,[82a,82b] A. Ghezzi,[82a,82b] P. Govoni,[82a,82b] L. Guzzi,[82a] M. R. Kim,[82a] G. Lavizzari,[82a,82b] M. T. Lucchini,[82a,82b] M. Malberti,[82a] S. Malvezzi,[82a] A. Massironi,[82a] D. Menasce,[82a] L. Moroni,[82a] M. Paganoni,[82a,82b] S. Palluotto,[82a,82b] D. Pedrini,[82a] A. Perego,[82a,82b] B. S. Pinolini,[82a] G. Pizzati,[82a,82b] S. Ragazzi,[82a,82b] T. Tabarelli de Fatis,[82a,82b] S. Buontempo,[83a] A. Cagnotta,[83a,83b] C. Di Fraia,[83a,83b] F. Fabozzi,[83a,83c] L. Favilla,[83a,83d] A. O. M. Iorio,[83a,83b] L. Lista,[83a,83b,xx] P. Paolucci,[83a,bb] B. Rossi,[83a] P. Azzi,[84a] N. Bacchetta,[84a,yy] D. Bisello,[84a,84b] P. Bortignon,[84a] G. Bortolato,[84a,84b] A. C. M. Bulla,[84a] R. Carlin,[84a,84b] P. Checchia,[84a] T. Dorigo,[84a,zz] F. Fanzago,[84a] F. Gasparini,[84a,84b] U. Gasparini,[84a,84b] S. Giorgetti,[84a] E. Lusiani,[84a] M. Margoni,[84a,84b] J. Pazzini,[84a,84b] P. Ronchese,[84a,84b] R. Rossin,[84a,84b] F. Simonetto,[84a,84b] M. Tosi,[84a,84b] A. Triossi,[84a,84b] S. Ventura,[84a] P. Zotto,[84a,84b] A. Zucchetta,[84a,84b] G. Zumerle,[84a,84b] A. Braghieri,[85a] S. Calzaferri,[85a] P. Montagna,[85a,85b] M. Pelliccioni,[85a] V. Re,[85a] C. Riccardi,[85a,85b] P. Salvini,[85a] I. Vai,[85a,85b] P. Vitulo,[85a,85b] S. Ajmal,[86a,86b] M. E. Ascioti,[86a,86b] G. M. Bilei,[86a] C. Carrivale,[86a,86b] D. Ciangottini,[86a,86b] L. Della Penna,[86a,86b] L. Fanò,[86a,86b] V. Mariani,[86a,86b] M. Menichelli,[86a] F. Moscatelli,[86a,aaa] A. Rossi,[86a,86b] A. Santocchia,[86a,86b] D. Spiga,[86a] T. Tedeschi,[86a,86b] C. Aimè,[87a,87b] C. A. Alexe,[87a,87c] P. Asenov,[87a,87b] P. Azzurri,[87a] G. Bagliesi,[87a] R. Bhattacharya,[87a] L. Bianchini,[87a,87b] T. Boccali,[87a] E. Bossini,[87a] D. Bruschini,[87a,87c] L. Calligaris,[87a,87b] R. Castaldi,[87a] F. Cattafesta,[87a,87c] M. A. Ciocci,[87a,87d] M. Cipriani,[87a,87b] V. D'Amante,[87a,87d] R. Dell'Orso,[87a] S. Donato,[87a,87b] R. Forti,[87a,87b] A. Giassi,[87a] F. Ligabue,[87a,87c] A. C. Marini,[87a,87b] D. Matos Figueiredo,[87a] A. Messineo,[87a,87b] S. Mishra,[87a] V. K. Muraleedharan Nair Bindhu,[87a,87b] S. Nandan,[87a] F. Palla,[87a] M. Riggirello,[87a,87c] A. Rizzi,[87a,87b] G. Rolandi,[87a,87c] S. Roy Chowdhury,[87a,bbb] T. Sarkar,[87a] A. Scribano,[87a] P. Solanki,[87a,87b] P. Spagnolo,[87a] F. Tenchini,[87a,87b] R. Tenchini,[87a] G. Tonelli,[87a,87b] N. Turini,[87a,87d] F. Vaselli,[87a,87c] A. Venturi,[87a] P. G. Verdini,[87a] P. Akrap,[88a,88b] C. Basile,[88a,88b] S. C. Behera,[88a] F. Cavallari,[88a] L. Cunqueiro Mendez,[88a,88b] F. De Riggi,[88a,88b] D. Del Re,[88a,88b] E. Di Marco,[88a] M. Diemoz,[88a] F. Errico,[88a] L. Frosina,[88a,88b] R. Gargiulo,[88a,88b] B. Harikrishnan,[88a,88b] F. Lombardi,[88a,88b] E. Longo,[88a,88b] L. Martikainen,[88a,88b] J. Mijuskovic,[88a,88b] G. Organtini,[88a,88b] N. Palmeri,[88a,88b] R. Paramatti,[88a,88b] C. Quaranta,[88a,88b] S. Rahatlou,[88a,88b] C. Rovelli,[88a] F. Santanastasio,[88a,88b] L. Soffi,[88a] V. Vladimirov,[88a,88b] N. Amapane,[89a,89b] R. Arcidiacono,[89a,89c] S. Argiro,[89a,89b] M. Arneodo,[89a,89c] N. Bartosik,[89a,89c] R. Bellan,[89a,89b] A. Bellora,[89a,89b]

C. Biino,[89a] C. Borca,[89a,89b] N. Cartiglia,[89a] M. Costa,[89a,89b] R. Covarelli,[89a,89b] N. Demaria,[89a] L. Finco,[89a] M. Grippo,[89a,89b] B. Kiani,[89a,89b] F. Legger,[89a] F. Luongo,[89a,89b] C. Mariotti,[89a] S. Maselli,[89a] A. Mecca,[89a,89b] L. Menzio,[89a,89b] P. Meridiani,[89a] E. Migliore,[89a,89b] M. Monteno,[89a] M. M. Obertino,[89a,89b] G. Ortona,[89a] L. Pacher,[89a,89b] N. Pastrone,[89a] M. Ruspa,[89a,89c] F. Siviero,[89a,89b] V. Sola,[89a,89b] A. Solano,[89a,89b] A. Staiano,[89a] C. Tarricone,[89a,89b] D. Trocino,[89a] G. Umoret,[89a,89b] E. Vlasov,[89a,89b] R. White,[89a,89b] J. Babbar,[90a,90b] S. Belforte,[90a] V. Candelise,[90a,90b] M. Casarsa,[90a] F. Cossutti,[90a] K. De Leo,[90a] G. Della Ricca,[90a,90b] R. Delli Gatti,[90a,90b] S. Dogra,[91] J. Hong,[91] J. Kim,[91] T. Kim,[91] D. Lee,[91] H. Lee,[91] J. Lee,[91] S. W. Lee,[91] C. S. Moon,[91] Y. D. Oh,[91] S. Sekmen,[91] B. Tae,[91] Y. C. Yang,[91] M. S. Kim,[92] G. Bak,[93] P. Gwak,[93] H. Kim,[93] D. H. Moon,[93] J. Seo,[93] E. Asilar,[94] F. Carnevali,[94] J. Choi,[94,ccc] T. J. Kim,[94] Y. Ryou,[94] S. Ha,[95] S. Han,[95] B. Hong,[95] K. Lee,[95] K. S. Lee,[95] S. Lee,[95] J. Yoo,[95] J. Goh,[96] J. Shin,[96] S. Yang,[96] Y. Kang,[97] H. S. Kim,[97] Y. Kim,[97] S. Lee,[97] J. Almond,[98] J. H. Bhyun,[98] J. Choi,[98] J. Choi,[98] W. Jun,[98] H. Kim,[98] J. Kim,[98] T. Kim,[98] Y. Kim,[98] Y. W. Kim,[98] S. Ko,[98] H. Lee,[98] J. Lee,[98] J. Lee,[98] B. H. Oh,[98] S. B. Oh,[98] J. Shin,[98] U. K. Yang,[98] I. Yoon,[98] W. Jang,[99] D. Y. Kang,[99] D. Kim,[99] S. Kim,[99] B. Ko,[99] J. S. H. Lee,[99] Y. Lee,[99] J. A. Merlin,[99] I. C. Park,[99] Y. Roh,[99] I. J. Watson,[99] G. Cho,[100] K. Hwang,[100] B. Kim,[100] S. Kim,[100] K. Lee,[100] H. D. Yoo,[100] M. Choi,[101] Y. Lee,[101] I. Yu,[101] T. Beyrouthy,[102] Y. Gharbia,[102] F. Alazemi,[103] K. Dreimanis,[104] O. M. Eberlins,[104] A. Gaile,[104] C. Munoz Diaz,[104] D. Osite,[104] G. Pikurs,[104] R. Plese,[104] A. Potrebko,[104] M. Seidel,[104] D. Sidiropoulos Kontos,[104] N. R. Strautnieks,[105] M. Ambrozas,[106] A. Juodagalvis,[106] S. Nargelas,[106] A. Rinkevicius,[106] G. Tamulaitis,[106] I. Yusuff,[107,ddd] Z. Zolkapli,[107] J. F. Benitez,[108] A. Castaneda Hernandez,[108] A. Cota Rodriguez,[108] L. E. Cuevas Picos,[108] H. A. Encinas Acosta,[108] L. G. Gallegos Maríñez,[108] J. A. Murillo Quijada,[108] A. Sehrawat,[108] L. Valencia Palomo,[108] G. Ayala,[109] H. Castilla-Valdez,[109] H. Crotte Ledesma,[109] R. Lopez-Fernandez,[109] J. Mejia Guisao,[109] R. Reyes-Almanza,[109] A. Sánchez Hernández,[109] C. Oropeza Barrera,[110] D. L. Ramirez Guadarrama,[110] M. Ramírez García,[110] I. Bautista,[111] F. E. Neri Huerta,[111] I. Pedraza,[111] H. A. Salazar Ibarguen,[111] C. Uribe Estrada,[111] I. Bubanja,[112] N. Raicevic,[112] P. H. Butler,[113] A. Ahmad,[114] M. I. Asghar,[114] A. Awais,[114] M. I. M. Awan,[114] W. A. Khan,[114] V. Avati,[115] L. Forthomme,[115] L. Grzanka,[115] M. Malawski,[115] K. Piotrzkowski,[115] M. Bluj,[116] M. Górski,[116] M. Kazana,[116] M. Szleper,[116] P. Zalewski,[116] K. Bunkowski,[117] K. Doroba,[117] A. Kalinowski,[117] M. Konecki,[117] J. Krolikowski,[117] A. Muhammad,[117] P. Fokow,[118] K. Pozniak,[118] W. Zabolotny,[118] M. Araujo,[119] D. Bastos,[119] C. Beirão Da Cruz E Silva,[119] A. Boletti,[119] M. Bozzo,[119] T. Camporesi,[119] G. Da Molin,[119] P. Faccioli,[119] M. Gallinaro,[119] J. Hollar,[119] N. Leonardo,[119] G. B. Marozzo,[119] A. Petrilli,[119] M. Pisano,[119] J. Seixas,[119] J. Varela,[119] J. W. Wulff,[119] P. Adzic,[120] L. Markovic,[120] P. Milenovic,[120] V. Milosevic,[120] D. Devetak,[121] M. Dordevic,[121] J. Milosevic,[121] L. Nadderd,[121] V. Rekovic,[121] M. Stojanovic,[121] M. Alcalde Martinez,[122] J. Alcaraz Maestre,[122] Cristina F. Bedoya,[122] J. A. Brochero Cifuentes,[122] Oliver M. Carretero,[122] M. Cepeda,[122] M. Cerrada,[122] N. Colino,[122] J. Cuchillo Ortega,[122] B. De La Cruz,[122] A. Delgado Peris,[122] A. Escalante Del Valle,[122] D. Fernández Del Val,[122] J. P. Fernández Ramos,[122] J. Flix,[122] M. C. Fouz,[122] M. Gonzalez Hernandez,[122] O. Gonzalez Lopez,[122] S. Goy Lopez,[122] J. M. Hernandez,[122] M. I. Josa,[122] J. Llorente Merino,[122] C. Martin Perez,[122] E. Martin Viscasillas,[122] D. Moran,[122] C. M. Morcillo Perez,[122] R. Paz Herrera,[122] C. Perez Dengra,[122] A. Pérez-Calero Yzquierdo,[122] J. Puerta Pelayo,[122] I. Redondo,[122] J. Vazquez Escobar,[122] J. F. de Trocóniz,[123] B. Alvarez Gonzalez,[124] J. Ayllon Torresano,[124] A. Cardini,[124] J. Cuevas,[124] J. Del Riego Badas,[124] D. Estrada Acevedo,[124] J. Fernandez Menendez,[124] S. Folgueras,[124] I. Gonzalez Caballero,[124] P. Leguina,[124] M. Obeso Menendez,[124] E. Palencia Cortezon,[124] J. Prado Pico,[124] A. Soto Rodríguez,[124] C. Vico Villalba,[124] P. Vischia,[124] S. Blanco Fernández,[125] I. J. Cabrillo,[125] A. Calderon,[125] J. Duarte Campderros,[125] M. Fernandez,[125] G. Gomez,[125] C. Lasaosa García,[125] R. Lopez Ruiz,[125] C. Martinez Rivero,[125] P. Martinez Ruiz del Arbol,[125] F. Matorras,[125] P. Matorras Cuevas,[125] E. Navarrete Ramos,[125] J. Piedra Gomez,[125] C. Quintana San Emeterio,[125] L. Scodellaro,[125] I. Vila,[125] R. Vilar Cortabitarte,[125] J. M. Vizan Garcia,[125] B. Kailasapathy,[126,eee] D. D. C. Wickramarathna,[126] W. G. D. Dharmaratna,[127,fff] K. Liyanage,[127] N. Perera,[127] D. Abbaneo,[128] C. Amendola,[128] R. Ardino,[128] E. Auffray,[128] J. Baechler,[128] D. Barney,[128] M. Bianco,[128] A. Bocci,[128] L. Borgonovi,[128] C. Botta,[128] A. Bragagnolo,[128] C. E. Brown,[128] C. Caillol,[128] G. Cerminara,[128] P. Connor,[128] D. d'Enterria,[128] A. Dabrowski,[128] A. David,[128] A. De Roeck,[128] M. M. Defranchis,[128] M. Deile,[128] M. Dobson,[128] W. Funk,[128]

A. Gaddi,[128] S. Giani,[128] D. Gigi,[128] K. Gill,[128] F. Glege,[128] M. Glowacki,[128] A. Gruber,[128] J. Hegeman,[128] J. K. Heikkilä,[128] B. Huber,[128] V. Innocente,[128] T. James,[128] P. Janot,[128] O. Kaluzinska,[128] O. Karacheban,[128,z] G. Karathanasis,[128] L. Lanteri,[128] S. Laurila,[128] P. Lecoq,[128] C. Lourenço,[128] A.-M. Lyon,[128] M. Magherini,[128] L. Malgeri,[128] M. Mannelli,[128] A. Mehta,[128] F. Meijers,[128] S. Mersi,[128] E. Meschi,[128] M. Migliorini,[128] F. Monti,[128] F. Moortgat,[128] M. Mulders,[128] M. Musich,[128] I. Neutelings,[128] S. Orfanelli,[128] F. Pantaleo,[128] M. Pari,[128] G. Petrucciani,[128] A. Pfeiffer,[128] M. Pierini,[128] M. Pitt,[128] H. Qu,[128] D. Rabady,[128] B. Ribeiro Lopes,[128] F. Riti,[128] P. Rosado,[128] M. Rovere,[128] H. Sakulin,[128] R. Salvatico,[128] S. Sanchez Cruz,[128] S. Scarfi,[128] M. Selvaggi,[128] A. Sharma,[128] K. Shchelina,[128] P. Silva,[128] P. Sphicas,[128,ggg] A. G. Stahl Leiton,[128] A. Steen,[128] S. Summers,[128] D. Treille,[128] P. Tropea,[128] E. Vernazza,[128] J. Wanczyk,[128,hhh] J. Wang,[128] S. Wuchterl,[128] M. Zarucki,[128] P. Zehetner,[128] P. Zejdl,[128] G. Zevi Della Porta,[128] T. Bevilacqua,[129,iii] L. Caminada,[129,iii] W. Erdmann,[129] R. Horisberger,[129] Q. Ingram,[129] H. C. Kaestli,[129] D. Kotlinski,[129] C. Lange,[129] U. Langenegger,[129] M. Missiroli,[129,iii] L. Noehte,[129,iii] T. Rohe,[129] A. Samalan,[129] T. K. Aarrestad,[130] M. Backhaus,[130] G. Bonomelli,[130] C. Cazzaniga,[130] K. Datta,[130] P. De Bryas Dexmiers D'archiacchiac,[130,hhh] A. De Cosa,[130] G. Dissertori,[130] M. Dittmar,[130] M. Donegà,[130] F. Eble,[130] K. Gedia,[130] F. Glessgen,[130] C. Grab,[130] N. Härringer,[130] T. G. Harte,[130] W. Lustermann,[130] M. Malucchi,[130] R. A. Manzoni,[130] M. Marchegiani,[130] L. Marchese,[130] A. Mascellani,[130,hhh] F. Nessi-Tedaldi,[130] F. Pauss,[130] V. Perovic,[130] B. Ristic,[130] R. Seidita,[130] J. Steggemann,[130,hhh] A. Tarabini,[130] D. Valsecchi,[130] R. Wallny,[130] C. Amsler,[131,jjj] P. Bärtschi,[131] F. Bilandzija,[131] M. F. Canelli,[131] G. Celotto,[131] K. Cormier,[131] M. Huwiler,[131] W. Jin,[131] A. Jofrehei,[131] B. Kilminster,[131] T. H. Kwok,[131] S. Leontsinis,[131] V. Lukashenko,[131] A. Macchiolo,[131] F. Meng,[131] J. Motta,[131] A. Reimers,[131] P. Robmann,[131] M. Senger,[131] E. Shokr,[131] F. Stäger,[131] R. Tramontano,[131] D. Bhowmik,[132] C. M. Kuo,[132] P. K. Rout,[132] S. Taj,[132] P. C. Tiwari,[132,kk] L. Ceard,[133] K. F. Chen,[133] Z. g. Chen,[133] A. De Iorio,[133] W.-S. Hou,[133] T. h. Hsu,[133] Y. w. Kao,[133] S. Karmakar,[133] G. Kole,[133] Y. y. Li,[133] R.-S. Lu,[133] E. Paganis,[133] X. f. Su,[133] J. Thomas-Wilsker,[133] L. s. Tsai,[133] D. Tsionou,[133] H. y. Wu,[133] E. Yazgan,[133] C. Asawatangtrakuldee,[134] N. Srimanobhas,[134] Y. Maghrbi,[135] D. Agyel,[136] F. Boran,[136] F. Dolek,[136] I. Dumanoglu,[136,kkk] Y. Guler,[136,lll] E. Gurpinar Guler,[136,lll] C. Isik,[136] O. Kara,[136] A. Kayis Topaksu,[136] Y. Komurcu,[136] G. Onengut,[136] K. Ozdemir,[136,mmm] B. Tali,[136,nnn] U. G. Tok,[136] E. Uslan,[136] I. S. Zorbakir,[136] M. Yalvac,[137,ooo] B. Akgun,[138] I. O. Atakisi,[138,ppp] E. Gülmez,[138] M. Kaya,[138,qqq] O. Kaya,[138,rrr] M. A. Sarkisla,[138,sss] S. Tekten,[138,ttt] A. Cakir,[139] K. Cankocak,[139,kkk,uuu] S. Sen,[139,vvv] O. Aydilek,[140,www] B. Hacisahinoglu,[140] I. Hos,[140,xxx] B. Kaynak,[140] S. Ozkorucuklu,[140] O. Potok,[140] H. Sert,[140] C. Simsek,[140] C. Zorbilmez,[140] S. Cerci,[141] B. Isildak,[141,yyy] D. Sunar Cerci,[141] T. Yetkin,[141,u] A. Boyaryntsev,[142] O. Dadazhanova,[142] B. Grynyov,[142] L. Levchuk,[143] J. J. Brooke,[144] A. Bundock,[144] F. Bury,[144] E. Clement,[144] D. Cussans,[144] D. Dharmender,[144] H. Flacher,[144] J. Goldstein,[144] H. F. Heath,[144] M.-L. Holmberg,[144] L. Kreczko,[144] S. Paramesvaran,[144] L. Robertshaw,[144] M. S. Sanjrani,[144] J. Segal,[144] V. J. Smith,[144] A. H. Ball,[145] K. W. Bell,[145] A. Belyaev,[145,zzz] C. Brew,[145] R. M. Brown,[145] D. J. A. Cockerill,[145] C. Cooke,[145] A. Elliot,[145] K. V. Ellis,[145] J. Gajownik,[145] K. Harder,[145] S. Harper,[145] J. Linacre,[145] K. Manolopoulos,[145] M. Moallemi,[145] D. M. Newbold,[145] E. Olaiya,[145] D. Petyt,[145] T. Reis,[145] A. R. Sahasransu,[145] G. Salvi,[145] T. Schuh,[145] C. H. Shepherd-Themistocleous,[145] I. R. Tomalin,[145] K. C. Whalen,[145] T. Williams,[145] I. Andreou,[146] R. Bainbridge,[146] P. Bloch,[146] O. Buchmuller,[146] C. A. Carrillo Montoya,[146] D. Colling,[146] J. S. Dancu,[146] I. Das,[146] P. Dauncey,[146] G. Davies,[146] M. Della Negra,[146] S. Fayer,[146] G. Fedi,[146] G. Hall,[146] H. R. Hoorani,[146] A. Howard,[146] G. Iles,[146] C. R. Knight,[146] P. Krueper,[146] J. Langford,[146] K. H. Law,[146] J. León Holgado,[146] E. Leutgeb,[146] L. Lyons,[146] A.-M. Magnan,[146] B. Maier,[146] S. Mallios,[146] A. Mastronikolis,[146] M. Mieskolainen,[146] J. Nash,[146,aaaa] M. Pesaresi,[146] P. B. Pradeep,[146] B. C. Radburn-Smith,[146] A. Richards,[146] A. Rose,[146] L. Russell,[146] K. Savva,[146] C. Seez,[146] R. Shukla,[146] A. Tapper,[146] K. Uchida,[146] G. P. Uttley,[146] T. Virdee,[146,bb] M. Vojinovic,[146] N. Wardle,[146] D. Winterbottom,[146] J. E. Cole,[147] A. Khan,[147] P. Kyberd,[147] I. D. Reid,[147] S. Abdullin,[148] A. Brinkerhoff,[148] E. Collins,[148] M. R. Darwish,[148] J. Dittmann,[148] K. Hatakeyama,[148] V. Hegde,[148] J. Hiltbrand,[148] B. McMaster,[148] J. Samudio,[148] S. Sawant,[148] C. Sutantawibul,[148] J. Wilson,[148] J. M. Hogan,[149,bbbb] R. Bartek,[150] A. Dominguez,[150] S. Raj,[150] A. E. Simsek,[150] S. S. Yu,[150] B. Bam,[151] A. Buchot Perraguin,[151] S. Campbell,[151] R. Chudasama,[151] S. I. Cooper,[151] C. Crovella,[151] G. Fidalgo,[151] S. V. Gleyzer,[151]

A. Khukhunaishvili,[151] K. Matchev,[151] E. Pearson,[151] C. U. Perez,[151] P. Rumerio,[151,cccc] E. Usai,[151] R. Yi,[151] S. Cholak,[152] G. De Castro,[152] Z. Demiragli,[152] C. Erice,[152] C. Fangmeier,[152] C. Fernandez Madrazo,[152] E. Fontanesi,[152] J. Fulcher,[152] F. Golf,[152] S. Jeon,[152] J. O'Cain,[152] I. Reed,[152] J. Rohlf,[152] K. Salyer,[152] D. Sperka,[152] D. Spitzbart,[152] I. Suarez,[152] A. Tsatsos,[152] E. Wurtz,[152] A. G. Zecchinelli,[152] G. Barone,[153] G. Benelli,[153] D. Cutts,[153] S. Ellis,[153] L. Gouskos,[153] M. Hadley,[153] U. Heintz,[153] K. W. Ho,[153] T. Kwon,[153] G. Landsberg,[153] K. T. Lau,[153] J. Luo,[153] S. Mondal,[153] J. Roloff,[153] T. Russell,[153] S. Sagir,[153,dddd] X. Shen,[153] M. Stamenkovic,[153] N. Venkatasubramanian,[153] S. Abbott,[154] B. Barton,[154] R. Breedon,[154] H. Cai,[154] M. Calderon De La Barca Sanchez,[154] M. Chertok,[154] M. Citron,[154] J. Conway,[154] P. T. Cox,[154] R. Erbacher,[154] O. Kukral,[154] G. Mocellin,[154] S. Ostrom,[154] W. Wei,[154] S. Yoo,[154] K. Adamidis,[155] M. Bachtis,[155] D. Campos,[155] R. Cousins,[155] A. Datta,[155] G. Flores Avila,[155] J. Hauser,[155] M. Ignatenko,[155] M. A. Iqbal,[155] T. Lam,[155] Y. f. Lo,[155] E. Manca,[155] A. Nunez Del Prado,[155] D. Saltzberg,[155] V. Valuev,[155] R. Clare,[156] J. W. Gary,[156] G. Hanson,[156] A. Aportela,[157] A. Arora,[157] J. G. Branson,[157] S. Cittolin,[157] S. Cooperstein,[157] D. Diaz,[157] J. Duarte,[157] L. Giannini,[157] Y. Gu,[157] J. Guiang,[157] V. Krutelyov,[157] R. Lee,[157] J. Letts,[157] H. Li,[157] M. Masciovecchio,[157] F. Mokhtar,[157] S. Mukherjee,[157] M. Pieri,[157] D. Primosch,[157] M. Quinnan,[157] V. Sharma,[157] M. Tadel,[157] E. Vourliotis,[157] F. Würthwein,[157] A. Yagil,[157] Z. Zhao,[157] A. Barzdukas,[158] L. Brennan,[158] C. Campagnari,[158] S. Carron Montero,[158,eeee] K. Downham,[158] C. Grieco,[158] M. M. Hussain,[158] J. Incandela,[158] J. Kim,[158] M. W. K. Lai,[158] A. J. Li,[158] P. Masterson,[158] J. Richman,[158] S. N. Santpur,[158] U. Sarica,[158] R. Schmitz,[158] F. Setti,[158] J. Sheplock,[158] D. Stuart,[158] T. Á. Vámi,[158] X. Yan,[158] D. Zhang,[158] A. Albert,[159] S. Bhattacharya,[159] A. Bornheim,[159] O. Cerri,[159] R. Kansal,[159] J. Mao,[159] H. B. Newman,[159] G. Reales Gutiérrez,[159] T. Sievert,[159] M. Spiropulu,[159] J. R. Vlimant,[159] R. A. Wynne,[159] S. Xie,[159] J. Alison,[160] S. An,[160] M. Cremonesi,[160] V. Dutta,[160] E. Y. Ertorer,[160] T. Ferguson,[160] T. A. Gómez Espinosa,[160] A. Harilal,[160] A. Kallil Tharayil,[160] M. Kanemura,[160] C. Liu,[160] P. Meiring,[160] T. Mudholkar,[160] S. Murthy,[160] P. Palit,[160] K. Park,[160] M. Paulini,[160] A. Roberts,[160] A. Sanchez,[160] W. Terrill,[160] J. P. Cumalat,[161] W. T. Ford,[161] A. Hart,[161] A. Hassani,[161] S. Kwan,[161] J. Pearkes,[161] C. Savard,[161] N. Schonbeck,[161] K. Stenson,[161] K. A. Ulmer,[161] S. R. Wagner,[161] N. Zipper,[161] D. Zuolo,[161] J. Alexander,[162] X. Chen,[162] D. J. Cranshaw,[162] J. Dickinson,[162] J. Fan,[162] X. Fan,[162] J. Grassi,[162] S. Hogan,[162] P. Kotamnives,[162] J. Monroy,[162] G. Niendorf,[162] M. Oshiro,[162] J. R. Patterson,[162] M. Reid,[162] A. Ryd,[162] J. Thom,[162] P. Wittich,[162] R. Zou,[162] L. Zygala,[162] M. Albrow,[163] M. Alyari,[163] O. Amram,[163] G. Apollinari,[163] A. Apresyan,[163] L. A. T. Bauerdick,[163] D. Berry,[163] J. Berryhill,[163] P. C. Bhat,[163] K. Burkett,[163] J. N. Butler,[163] A. Canepa,[163] G. B. Cerati,[163] H. W. K. Cheung,[163] F. Chlebana,[163] C. Cosby,[163] G. Cummings,[163] I. Dutta,[163] V. D. Elvira,[163] J. Freeman,[163] A. Gandrakota,[163] Z. Gecse,[163] L. Gray,[163] D. Green,[163] A. Grummer,[163] S. Grünendahl,[163] D. Guerrero,[163] O. Gutsche,[163] R. M. Harris,[163] T. C. Herwig,[163] J. Hirschauer,[163] B. Jayatilaka,[163] S. Jindariani,[163] M. Johnson,[163] U. Joshi,[163] T. Klijnsma,[163] B. Klima,[163] K. H. M. Kwok,[163] S. Lammel,[163] C. Lee,[163] D. Lincoln,[163] R. Lipton,[163] T. Liu,[163] K. Maeshima,[163] D. Mason,[163] P. McBride,[163] P. Merkel,[163] S. Mrenna,[163] S. Nahn,[163] J. Ngadiuba,[163] D. Noonan,[163] S. Norberg,[163] V. Papadimitriou,[163] N. Pastika,[163] K. Pedro,[163] C. Pena,[163,ffff] C. E. Perez Lara,[163] F. Ravera,[163] A. Reinsvold Hall,[163,gggg] L. Ristori,[163] M. Safdari,[163] E. Sexton-Kennedy,[163] N. Smith,[163] A. Soha,[163] L. Spiegel,[163] S. Stoynev,[163] J. Strait,[163] L. Taylor,[163] S. Tkaczyk,[163] N. V. Tran,[163] L. Uplegger,[163] E. W. Vaandering,[163] C. Wang,[163] I. Zoi,[163] C. Aruta,[164] P. Avery,[164] D. Bourilkov,[164] P. Chang,[164] V. Cherepanov,[164] R. D. Field,[164] C. Huh,[164] E. Koenig,[164] M. Kolosova,[164] J. Konigsberg,[164] A. Korytov,[164] N. Menendez,[164] G. Mitselmakher,[164] K. Mohrman,[164] A. Muthirakalayil Madhu,[164] N. Rawal,[164] S. Rosenzweig,[164] V. Sulimov,[164] Y. Takahashi,[164] J. Wang,[164] T. Adams,[165] A. Al Kadhim,[165] A. Askew,[165] S. Bower,[165] R. Hashmi,[165] R. S. Kim,[165] T. Kolberg,[165] G. Martinez,[165] M. Mazza,[165] H. Prosper,[165] P. R. Prova,[165] M. Wulansatiti,[165] R. Yohay,[165] B. Alsufyani,[166] S. Butalla,[166] S. Das,[166] M. Hohlmann,[166] M. Lavinsky,[166] E. Yanes,[166] M. R. Adams,[167] N. Barnett,[167] A. Baty,[167] C. Bennett,[167] R. Cavanaugh,[167] R. Escobar Franco,[167] O. Evdokimov,[167] C. E. Gerber,[167] H. Gupta,[167] M. Hawksworth,[167] A. Hingrajiya,[167] D. J. Hofman,[167] J. h. Lee,[167] D. S. Lemos,[167] C. Mills,[167] S. Nanda,[167] G. Nigmatkulov,[167] B. Ozek,[167] T. Phan,[167] D. Pilipovic,[167] R. Pradhan,[167] E. Prifti,[167] P. Roy,[167] T. Roy,[167] N. Singh,[167] M. B. Tonjes,[167] N. Varelas,[167] M. A. Wadud,[167] J. Yoo,[167] M. Alhusseini,[168] D. Blend,[168] K. Dilsiz,[168,hhhh] O. K. Köseyan,[168] A. Mestvirishvili,[168,iiii] O. Neogi,[168] H. Ogul,[168,jjjj] Y. Onel,[168]

A. Penzo,[168] C. Snyder,[168] E. Tiras,[168,kkkk] B. Blumenfeld,[169] J. Davis,[169] A. V. Gritsan,[169] L. Kang,[169] S. Kyriacou,[169] P. Maksimovic,[169] M. Roguljic,[169] S. Sekhar,[169] M. V. Srivastav,[169] M. Swartz,[169] A. Abreu,[170] L. F. Alcerro Alcerro,[170] J. Anguiano,[170] S. Arteaga Escatel,[170] P. Baringer,[170] A. Bean,[170] Z. Flowers,[170] D. Grove,[170] J. King,[170] G. Krintiras,[170] M. Lazarovits,[170] C. Le Mahieu,[170] J. Marquez,[170] M. Murray,[170] M. Nickel,[170] S. Popescu,[170,llll] C. Rogan,[170] C. Royon,[170] S. Rudrabhatla,[170] S. Sanders,[170] C. Smith,[170] G. Wilson,[170] B. Allmond,[171] R. Gujju Gurunadha,[171] N. Islam,[171] A. Ivanov,[171] K. Kaadze,[171] Y. Maravin,[171] J. Natoli,[171] D. Roy,[171] G. Sorrentino,[171] A. Baden,[172] A. Belloni,[172] J. Bistany-riebman,[172] S. C. Eno,[172] N. J. Hadley,[172] S. Jabeen,[172] R. G. Kellogg,[172] T. Koeth,[172] B. Kronheim,[172] S. Lascio,[172] P. Major,[172] A. C. Mignerey,[172] C. Palmer,[172] C. Papageorgakis,[172] M. M. Paranjpe,[172] E. Popova,[172,mmmm] A. Shevelev,[172] L. Zhang,[172] C. Baldenegro Barrera,[173] J. Bendavid,[173] H. Bossi,[173] S. Bright-Thonney,[173] I. A. Cali,[173] Y. c. Chen,[173] P. c. Chou,[173] M. D'Alfonso,[173] J. Eysermans,[173] C. Freer,[173] G. Gomez-Ceballos,[173] M. Goncharov,[173] G. Grosso,[173] P. Harris,[173] D. Hoang,[173] G. M. Innocenti,[173] D. Kovalskyi,[173] J. Krupa,[173] L. Lavezzo,[173] Y.-J. Lee,[173] K. Long,[173] C. Mcginn,[173] A. Novak,[173] M. I. Park,[173] C. Paus,[173] C. Reissel,[173] C. Roland,[173] G. Roland,[173] S. Rothman,[173] T. a. Sheng,[173] G. S. F. Stephans,[173] D. Walter,[173] Z. Wang,[173] B. Wyslouch,[173] T. J. Yang,[173] B. Crossman,[174] W. J. Jackson,[174] C. Kapsiak,[174] M. Krohn,[174] D. Mahon,[174] J. Mans,[174] B. Marzocchi,[174] R. Rusack,[174] O. Sancar,[174] R. Saradhy,[174] N. Strobbe,[174] K. Bloom,[175] D. R. Claes,[175] G. Haza,[175] J. Hossain,[175] C. Joo,[175] I. Kravchenko,[175] A. Rohilla,[175] J. E. Siado,[175] W. Tabb,[175] A. Vagnerini,[175] A. Wightman,[175] F. Yan,[175] H. Bandyopadhyay,[176] L. Hay,[176] H. w. Hsia,[176] I. Iashvili,[176] A. Kalogeropoulos,[176] A. Kharchilava,[176] A. Mandal,[176] M. Morris,[176] D. Nguyen,[176] S. Rappoccio,[176] H. Rejeb Sfar,[176] A. Williams,[176] P. Young,[176] D. Yu,[176] G. Alverson,[177] E. Barberis,[177] J. Bonilla,[177] B. Bylsma,[177] M. Campana,[177] J. Dervan,[177] Y. Haddad,[177] Y. Han,[177] I. Israr,[177] A. Krishna,[177] M. Lu,[177] N. Manganelli,[177] R. Mccarthy,[177] D. M. Morse,[177] T. Orimoto,[177] A. Parker,[177] L. Skinnari,[177] C. S. Thoreson,[177] E. Tsai,[177] D. Wood,[177] S. Dittmer,[178] K. A. Hahn,[178] Y. Liu,[178] M. Mcginnis,[178] Y. Miao,[178] D. G. Monk,[178] M. H. Schmitt,[178] A. Taliercio,[178] M. Velasco,[178] J. Wang,[178] G. Agarwal,[179] R. Band,[179] R. Bucci,[179] S. Castells,[179] A. Das,[179] A. Ehnis,[179] R. Goldouzian,[179] M. Hildreth,[179] K. Hurtado Anampa,[179] T. Ivanov,[179] C. Jessop,[179] A. Karneyeu,[179] K. Lannon,[179] J. Lawrence,[179] N. Loukas,[179] L. Lutton,[179] J. Mariano,[179] N. Marinelli,[179] I. Mcalister,[179] T. McCauley,[179] C. Mcgrady,[179] C. Moore,[179] Y. Musienko,[179,mmmm] H. Nelson,[179] M. Osherson,[179] A. Piccinelli,[179] R. Ruchti,[179] A. Townsend,[179] Y. Wan,[179] M. Wayne,[179] H. Yockey,[179] A. Basnet,[180] M. Carrigan,[180] R. De Los Santos,[180] L. S. Durkin,[180] C. Hill,[180] M. Joyce,[180] M. Nunez Ornelas,[180] D. A. Wenzl,[180] B. L. Winer,[180] B. R. Yates,[180] H. Bouchamaoui,[181] K. Coldham,[181] P. Das,[181] G. Dezoort,[181] P. Elmer,[181] A. Frankenthal,[181] M. Galli,[181] B. Greenberg,[181] N. Haubrich,[181] K. Kennedy,[181] G. Kopp,[181] Y. Lai,[181] D. Lange,[181] A. Loeliger,[181] D. Marlow,[181] I. Ojalvo,[181] J. Olsen,[181] F. Simpson,[181] D. Stickland,[181] C. Tully,[181] S. Malik,[182] R. Sharma,[182] A. S. Bakshi,[183] S. Chandra,[183] R. Chawla,[183] A. Gu,[183] L. Gutay,[183] M. Jones,[183] A. W. Jung,[183] D. Kondratyev,[183] M. Liu,[183] M. Matthewman,[183] G. Negro,[183] N. Neumeister,[183] G. Paspalaki,[183] S. Piperov,[183] J. F. Schulte,[183] F. Wang,[183] A. Wildridge,[183] W. Xie,[183] Y. Yao,[183] Y. Zhong,[183] N. Parashar,[184] A. Pathak,[184] E. Shumka,[184] D. Acosta,[185] A. Agrawal,[185] C. Arbour,[185] T. Carnahan,[185] K. M. Ecklund,[185] P. J. Fernández Manteca,[185] S. Freed,[185] P. Gardner,[185] F. J. M. Geurts,[185] T. Huang,[185] I. Krommydas,[185] N. Lewis,[185] W. Li,[185] J. Lin,[185] O. Miguel Colin,[185] B. P. Padley,[185] R. Redjimi,[185] J. Rotter,[185] E. Yigitbasi,[185] Y. Zhang,[185] O. Bessidskaia Bylund,[186] A. Bodek,[186] P. de Barbaro,[186,a] R. Demina,[186] J. L. Dulemba,[186] A. Garcia-Bellido,[186] H. S. Hare,[186] O. Hindrichs,[186] N. Parmar,[186] P. Parygin,[186,mmmm] H. Seo,[186] R. Taus,[186] B. Chiarito,[187] J. P. Chou,[187] S. V. Clark,[187] S. Donnelly,[187] D. Gadkari,[187] Y. Gershtein,[187] E. Halkiadakis,[187] M. Heindl,[187] C. Houghton,[187] D. Jaroslawski,[187] S. Konstantinou,[187] I. Laflotte,[187] A. Lath,[187] J. Martins,[187] B. Rand,[187] J. Reichert,[187] P. Saha,[187] S. Salur,[187] S. Schnetzer,[187] S. Somalwar,[187] R. Stone,[187] S. A. Thayil,[187] S. Thomas,[187] J. Vora,[187] D. Ally,[188] A. G. Delannoy,[188] S. Fiorendi,[188] J. Harris,[188] S. Higginbotham,[188] T. Holmes,[188] A. R. Kanuganti,[188] N. Karunarathna,[188] J. Lawless,[188] L. Lee,[188] E. Nibigira,[188] B. Skipworth,[188] S. Spanier,[188] D. Aebi,[189] M. Ahmad,[189] T. Akhter,[189] K. Androsov,[189] A. Bolshov,[189] O. Bouhali,[189,nnnn] R. Eusebi,[189] P. Flanagan,[189] J. Gilmore,[189] Y. Guo,[189] T. Kamon,[189] S. Luo,[189] R. Mueller,[189] A. Safonov,[189] N. Akchurin,[190] J. Damgov,[190] Y. Feng,[190] N. Gogate,[190] Y. Kazhykarim,[190] K. Lamichhane,[190] S. W. Lee,[190]

C. Madrid,[190] A. Mankel,[190] T. Peltola,[190] I. Volobouev,[190] E. Appelt,[191] Y. Chen,[191] S. Greene,[191] A. Gurrola,[191] W. Johns,[191] R. Kunnawalkam Elayavalli,[191] A. Melo,[191] D. Rathjens,[191] F. Romeo,[191] P. Sheldon,[191] S. Tuo,[191] J. Velkovska,[191] J. Viinikainen,[191] J. Zhang,[191] B. Cardwell,[192] H. Chung,[192] B. Cox,[192] J. Hakala,[192] R. Hirosky,[192] M. Jose,[192] A. Ledovskoy,[192] C. Mantilla,[192] C. Neu,[192] C. Ramón Álvarez,[192] S. Bhattacharya,[193] P. E. Karchin,[193] A. Aravind,[194] S. Banerjee,[194] K. Black,[194] T. Bose,[194] E. Chavez,[194] S. Dasu,[194] P. Everaerts,[194] C. Galloni,[194] H. He,[194] M. Herndon,[194] A. Herve,[194] C. K. Koraka,[194] S. Lomte,[194] R. Loveless,[194] A. Mallampalli,[194] A. Mohammadi,[194] S. Mondal,[194] T. Nelson,[194] G. Parida,[194] L. Pétré,[194] D. Pinna,[194] A. Savin,[194] V. Shang,[194] V. Sharma,[194] W. H. Smith,[194] D. Teague,[194] H. F. Tsoi,[194] W. Vetens,[194] A. Warden,[194] S. Afanasiev,[195] V. Alexakhin,[195] Yu. Andreev,[195] T. Aushev,[195] D. Budkouski,[195] R. Chistov,[195,mmmm] M. Danilov,[195,mmmm] T. Dimova,[195,mmmm] A. Ershov,[195,mmmm] S. Gninenko,[195] I. Gorbunov,[195] A. Gribushin,[195,mmmm] A. Kamenev,[195] V. Karjavine,[195] M. Kirsanov,[195] V. Klyukhin,[195,mmmm] O. Kodolova,[195,oooo] V. Korenkov,[195] A. Kozyrev,[195,mmmm] N. Krasnikov,[195] A. Lanev,[195] A. Malakhov,[195] V. Matveev,[195,mmmm] A. Nikitenko,[195,pppp,oooo] V. Palichik,[195] V. Perelygin,[195] S. Petrushanko,[195,mmmm] S. Polikarpov,[195,mmmm] O. Radchenko,[195,mmmm] M. Savina,[195] V. Shalaev,[195] S. Shmatov,[195] S. Shulha,[195] Y. Skovpen,[195,mmmm] V. Smirnov,[195] O. Teryaev,[195] I. Tlisova,[195,mmmm] A. Toropin,[195] N. Voytishin,[195] B. S. Yuldashev,[195,a,qqqq] A. Zarubin,[195] I. Zhizhin,[195] L. Dudko,[196] K. Ivanov,[196] V. Kim,[196,mmmm] V. Murzin,[196] V. Oreshkin,[196] D. Sosnov,[196] E. Boos,[196] V. Bunichev,[196] M. Dubinin,[196,ffff] V. Savrin,[196] and A. Snigirev[196]

(CMS Collaboration)

[1]*Yerevan Physics Institute, Yerevan, Armenia*
[2]*Institut für Hochenergiephysik, Vienna, Austria*
[3]*Universiteit Antwerpen, Antwerpen, Belgium*
[4]*Vrije Universiteit Brussel, Brussel, Belgium*
[5]*Université Libre de Bruxelles, Bruxelles, Belgium*
[6]*Ghent University, Ghent, Belgium*
[7]*Université Catholique de Louvain, Louvain-la-Neuve, Belgium*
[8]*Centro Brasileiro de Pesquisas Fisicas, Rio de Janeiro, Brazil*
[9]*Universidade do Estado do Rio de Janeiro, Rio de Janeiro, Brazil*
[10]*Universidade Estadual Paulista, Universidade Federal do ABC, São Paulo, Brazil*
[11]*Institute for Nuclear Research and Nuclear Energy, Bulgarian Academy of Sciences, Sofia, Bulgaria*
[12]*University of Sofia, Sofia, Bulgaria*
[13]*Instituto De Alta Investigación, Universidad de Tarapacá, Casilla 7 D, Arica, Chile*
[14]*Universidad Tecnica Federico Santa Maria, Valparaiso, Chile*
[15]*Beihang University, Beijing, China*
[16]*Department of Physics, Tsinghua University, Beijing, China*
[17]*Institute of High Energy Physics, Beijing, China*
[18]*State Key Laboratory of Nuclear Physics and Technology, Peking University, Beijing, China*
[19]*State Key Laboratory of Nuclear Physics and Technology, Institute of Quantum Matter, South China Normal University, Guangzhou, China*
[20]*Sun Yat-Sen University, Guangzhou, China*
[21]*University of Science and Technology of China, Hefei, China*
[22]*Nanjing Normal University, Nanjing, China*
[23]*Institute of Modern Physics and Key Laboratory of Nuclear Physics and Ion-beam Application (MOE) - Fudan University, Shanghai, China*
[24]*Zhejiang University, Hangzhou, Zhejiang, China*
[25]*Universidad de Los Andes, Bogota, Colombia*
[26]*Universidad de Antioquia, Medellin, Colombia*
[27]*University of Split, Faculty of Electrical Engineering, Mechanical Engineering and Naval Architecture, Split, Croatia*
[28]*University of Split, Faculty of Science, Split, Croatia*
[29]*Institute Rudjer Boskovic, Zagreb, Croatia*
[30]*University of Cyprus, Nicosia, Cyprus*
[31]*Charles University, Prague, Czech Republic*
[32]*Escuela Politecnica Nacional, Quito, Ecuador*
[33]*Universidad San Francisco de Quito, Quito, Ecuador*

[34]Academy of Scientific Research and Technology of the Arab Republic of Egypt,
Egyptian Network of High Energy Physics, Cairo, Egypt
[35]Center for High Energy Physics (CHEP-FU), Fayoum University, El-Fayoum, Egypt
[36]National Institute of Chemical Physics and Biophysics, Tallinn, Estonia
[37]Department of Physics, University of Helsinki, Helsinki, Finland
[38]Helsinki Institute of Physics, Helsinki, Finland
[39]Lappeenranta-Lahti University of Technology, Lappeenranta, Finland
[40]IRFU, CEA, Université Paris-Saclay, Gif-sur-Yvette, France
[41]Laboratoire Leprince-Ringuet, CNRS/IN2P3, Ecole Polytechnique,
Institut Polytechnique de Paris, Palaiseau, France
[42]Université de Strasbourg, CNRS, IPHC UMR 7178, Strasbourg, France
[43]Centre de Calcul de l'Institut National de Physique Nucleaire et de Physique des Particules,
CNRS/IN2P3, Villeurbanne, France
[44]Institut de Physique des 2 Infinis de Lyon (IP2I), Villeurbanne, France
[45]Georgian Technical University, Tbilisi, Georgia
[46]RWTH Aachen University, I. Physikalisches Institut, Aachen, Germany
[47]RWTH Aachen University, III. Physikalisches Institut A, Aachen, Germany
[48]RWTH Aachen University, III. Physikalisches Institut B, Aachen, Germany
[49]Deutsches Elektronen-Synchrotron, Hamburg, Germany
[50]University of Hamburg, Hamburg, Germany
[51]Karlsruher Institut fuer Technologie, Karlsruhe, Germany
[52]Institute of Nuclear and Particle Physics (INPP), NCSR Demokritos, Aghia Paraskevi, Greece
[53]National and Kapodistrian University of Athens, Athens, Greece
[54]National Technical University of Athens, Athens, Greece
[55]University of Ioánnina, Ioánnina, Greece
[56]HUN-REN Wigner Research Centre for Physics, Budapest, Hungary
[57]MTA-ELTE Lendület CMS Particle and Nuclear Physics Group, Eötvös Loránd University,
Budapest, Hungary
[58]Faculty of Informatics, University of Debrecen, Debrecen, Hungary
[59]HUN-REN ATOMKI - Institute of Nuclear Research, Debrecen, Hungary
[60]Karoly Robert Campus, MATE Institute of Technology, Gyongyos, Hungary
[61]Panjab University, Chandigarh, India
[62]University of Delhi, Delhi, India
[63]University of Hyderabad, Hyderabad, India
[64]Indian Institute of Technology Kanpur, Kanpur, India
[65]Saha Institute of Nuclear Physics, HBNI, Kolkata, India
[66]Indian Institute of Technology Madras, Madras, India
[67]IISER Mohali, India, Mohali, India
[68]Tata Institute of Fundamental Research-A, Mumbai, India
[69]Tata Institute of Fundamental Research-B, Mumbai, India
[70]National Institute of Science Education and Research, An OCC of Homi Bhabha National Institute,
Bhubaneswar, Odisha, India
[71]Indian Institute of Science Education and Research (IISER), Pune, India
[72]Indian Institute of Technology Hyderabad, Telangana, India
[73]Isfahan University of Technology, Isfahan, Iran
[74]Institute for Research in Fundamental Sciences (IPM), Tehran, Iran
[75]University College Dublin, Dublin, Ireland
[76a]INFN Sezione di Bari, Bari, Italy
[76b]Università di Bari , Bari, Italy
[76c]Politecnico di Bari, Bari, Italy
[77a]INFN Sezione di Bologna, Bologna, Italy
[77b]Università di Bologna , Bologna, Italy
[78a]INFN Sezione di Catania, Catania, Italy
[78b]Università di Catania , Catania, Italy
[79a]INFN Sezione di Firenze, Firenze, Italy
[79b]Università di Firenze , Firenze, Italy
[80]INFN Laboratori Nazionali di Frascati, Frascati, Italy
[81a]INFN Sezione di Genova, Genova, Italy
[81b]Università di Genova , Genova, Italy
[82a]INFN Sezione di Milano-Bicocca, Milano, Italy

[82b]*Università di Milano-Bicocca , Milano, Italy*
[83a]*INFN Sezione di Napoli, Napoli, Italy*
[83b]*Università di Napoli 'Federico II' , Napoli, Italy*
[83c]*Università della Basilicata , Potenza, Italy*
[83d]*Scuola Superiore Meridionale (SSM), Napoli, Italy*
[84a]*INFN Sezione di Padova, Padova, Italy*
[84b]*Università di Padova , Padova, Italy*
[84c]*Universita degli Studi di Cagliari , Cagliari, Italy*
[85a]*INFN Sezione di Pavia, Pavia, Italy*
[85b]*Università di Pavia , Pavia, Italy*
[86a]*INFN Sezione di Perugia, Perugia, Italy*
[86b]*Università di Perugia , Perugia, Italy*
[87a]*INFN Sezione di Pisa, Pisa, Italy*
[87b]*Università di Pisa , Pisa, Italy*
[87c]*Scuola Normale Superiore di Pisa, Pisa, Italy*
[87d]*Università di Siena , Siena, Italy*
[88a]*INFN Sezione di Roma, Roma, Italy*
[88b]*Sapienza Università di Roma , Roma, Italy*
[89a]*INFN Sezione di Torino, Torino, Italy*
[89b]*Università di Torino , Torino, Italy*
[89c]*Università del Piemonte Orientale , Novara, Italy*
[90a]*INFN Sezione di Trieste, Trieste, Italy*
[90b]*Università di Trieste , Trieste, Italy*
[91]*Kyungpook National University, Daegu, Korea*
[92]*Department of Mathematics and Physics - GWNU, Gangneung, Korea*
[93]*Chonnam National University, Institute for Universe and Elementary Particles, Kwangju, Korea*
[94]*Hanyang University, Seoul, Korea*
[95]*Korea University, Seoul, Korea*
[96]*Kyung Hee University, Department of Physics, Seoul, Korea*
[97]*Sejong University, Seoul, Korea*
[98]*Seoul National University, Seoul, Korea*
[99]*University of Seoul, Seoul, Korea*
[100]*Yonsei University, Department of Physics, Seoul, Korea*
[101]*Sungkyunkwan University, Suwon, Korea*
[102]*College of Engineering and Technology, American University of the Middle East (AUM), Dasman, Kuwait*
[103]*Kuwait University - College of Science - Department of Physics, Safat, Kuwait*
[104]*Riga Technical University, Riga, Latvia*
[105]*University of Latvia (LU), Riga, Latvia*
[106]*Vilnius University, Vilnius, Lithuania*
[107]*National Centre for Particle Physics, Universiti Malaya, Kuala Lumpur, Malaysia*
[108]*Universidad de Sonora (UNISON), Hermosillo, Mexico*
[109]*Centro de Investigacion y de Estudios Avanzados del IPN, Mexico City, Mexico*
[110]*Universidad Iberoamericana, Mexico City, Mexico*
[111]*Benemerita Universidad Autonoma de Puebla, Puebla, Mexico*
[112]*University of Montenegro, Podgorica, Montenegro*
[113]*University of Canterbury, Christchurch, New Zealand*
[114]*National Centre for Physics, Quaid-I-Azam University, Islamabad, Pakistan*
[115]*AGH University of Krakow, Krakow, Poland*
[116]*National Centre for Nuclear Research, Swierk, Poland*
[117]*Institute of Experimental Physics, Faculty of Physics, University of Warsaw, Warsaw, Poland*
[118]*Warsaw University of Technology, Warsaw, Poland*
[119]*Laboratório de Instrumentação e Física Experimental de Partículas, Lisboa, Portugal*
[120]*Faculty of Physics, University of Belgrade, Belgrade, Serbia*
[121]*VINCA Institute of Nuclear Sciences, University of Belgrade, Belgrade, Serbia*
[122]*Centro de Investigaciones Energéticas Medioambientales y Tecnológicas (CIEMAT), Madrid, Spain*
[123]*Universidad Autónoma de Madrid, Madrid, Spain*
[124]*Universidad de Oviedo, Instituto Universitario de Ciencias y Tecnologías Espaciales de Asturias (ICTEA), Oviedo, Spain*
[125]*Instituto de Física de Cantabria (IFCA), CSIC-Universidad de Cantabria, Santander, Spain*

[126]University of Colombo, Colombo, Sri Lanka
[127]University of Ruhuna, Department of Physics, Matara, Sri Lanka
[128]CERN, European Organization for Nuclear Research, Geneva, Switzerland
[129]PSI Center for Neutron and Muon Sciences, Villigen, Switzerland
[130]ETH Zurich - Institute for Particle Physics and Astrophysics (IPA), Zurich, Switzerland
[131]Universität Zürich, Zurich, Switzerland
[132]National Central University, Chung-Li, Taiwan
[133]National Taiwan University (NTU), Taipei, Taiwan
[134]High Energy Physics Research Unit, Department of Physics, Faculty of Science, Chulalongkorn University, Bangkok, Thailand
[135]Tunis El Manar University, Tunis, Tunisia
[136]Çukurova University, Physics Department, Science and Art Faculty, Adana, Turkey
[137]Middle East Technical University, Physics Department, Ankara, Turkey
[138]Bogazici University, Istanbul, Turkey
[139]Istanbul Technical University, Istanbul, Turkey
[140]Istanbul University, Istanbul, Turkey
[141]Yildiz Technical University, Istanbul, Turkey
[142]Institute for Scintillation Materials of National Academy of Science of Ukraine, Kharkiv, Ukraine
[143]National Science Centre, Kharkiv Institute of Physics and Technology, Kharkiv, Ukraine
[144]University of Bristol, Bristol, United Kingdom
[145]Rutherford Appleton Laboratory, Didcot, United Kingdom
[146]Imperial College, London, United Kingdom
[147]Brunel University, Uxbridge, United Kingdom
[148]Baylor University, Waco, Texas, USA
[149]Bethel University, St. Paul, Minnesota, USA
[150]Catholic University of America, Washington, DC, USA
[151]The University of Alabama, Tuscaloosa, Alabama, USA
[152]Boston University, Boston, Massachusetts, USA
[153]Brown University, Providence, Rhode Island, USA
[154]University of California, Davis, Davis, California, USA
[155]University of California, Los Angeles, California, USA
[156]University of California, Riverside, Riverside, California, USA
[157]University of California, San Diego, La Jolla, California, USA
[158]University of California, Santa Barbara - Department of Physics, Santa Barbara, California, USA
[159]California Institute of Technology, Pasadena, California, USA
[160]Carnegie Mellon University, Pittsburgh, Pennsylvania, USA
[161]University of Colorado Boulder, Boulder, Colorado, USA
[162]Cornell University, Ithaca, New York, USA
[163]Fermi National Accelerator Laboratory, Batavia, Illinois, USA
[164]University of Florida, Gainesville, Florida, USA
[165]Florida State University, Tallahassee, Florida, USA
[166]Florida Institute of Technology, Melbourne, Florida, USA
[167]University of Illinois Chicago, Chicago, Illinois, USA
[168]The University of Iowa, Iowa City, Iowa, USA
[169]Johns Hopkins University, Baltimore, Maryland, USA
[170]The University of Kansas, Lawrence, Kansas, USA
[171]Kansas State University, Manhattan, Kansas, USA
[172]University of Maryland, College Park, Maryland, USA
[173]Massachusetts Institute of Technology, Cambridge, Massachusetts, USA
[174]University of Minnesota, Minneapolis, Minnesota, USA
[175]University of Nebraska-Lincoln, Lincoln, Nebraska, USA
[176]State University of New York at Buffalo, Buffalo, New York, USA
[177]Northeastern University, Boston, Massachusetts, USA
[178]Northwestern University, Evanston, Illinois, USA
[179]University of Notre Dame, Notre Dame, Indiana, USA
[180]The Ohio State University, Columbus, Ohio, USA
[181]Princeton University, Princeton, New Jersey, USA
[182]University of Puerto Rico, Mayaguez, Puerto Rico, USA
[183]Purdue University, West Lafayette, Indiana, USA
[184]Purdue University Northwest, Hammond, Indiana, USA

[185]*Rice University, Houston, Texas, USA*
[186]*University of Rochester, Rochester, New York, USA*
[187]*Rutgers, The State University of New Jersey, Piscataway, New Jersey, USA*
[188]*University of Tennessee, Knoxville, Tennessee, USA*
[189]*Texas A&M University, College Station, Texas, USA*
[190]*Texas Tech University, Lubbock, Texas, USA*
[191]*Vanderbilt University, Nashville, Tennessee, USA*
[192]*University of Virginia, Charlottesville, Virginia, USA*
[193]*Wayne State University, Detroit, Michigan, USA*
[194]*University of Wisconsin - Madison, Madison, Wisconsin, USA*
[195]*An institute or international laboratory covered by a cooperation agreement with CERN*
[196]*An institute formerly covered by a cooperation agreement with CERN*

[a]Deceased.
[b]Also at Yerevan State University, Yerevan, Armenia.
[c]Also at TU Wien, Vienna, Austria.
[d]Also at Ghent University, Ghent, Belgium.
[e]Also at Universidade do Estado do Rio de Janeiro, Rio de Janeiro, Brazil.
[f]Also at FACAMP—Faculdades de Campinas, Sao Paulo, Brazil.
[g]Also at Universidade Estadual de Campinas, Campinas, Brazil.
[h]Also at Federal University of Rio Grande do Sul, Porto Alegre, Brazil.
[i]Also at The University of the State of Amazonas, Manaus, Brazil.
[j]Also at University of Chinese Academy of Sciences, Beijing, China.
[k]Also at China Center of Advanced Science and Technology, Beijing, China.
[l]Also at University of Chinese Academy of Sciences, Beijing, China.
[m]Also at Henan Normal University, Xinxiang, China.
[n]Also at University of Shanghai for Science and Technology, Shanghai, China.
[o]Also at The University of Iowa, Iowa City, Iowa, USA.
[p]Also at Center for High Energy Physics, Peking University, Beijing, China.
[q]Also at British University in Egypt, Cairo, Egypt.
[r]Also at Cairo University, Cairo, Egypt.
[s]Also at Purdue University, West Lafayette, Indiana, USA.
[t]Also at Université de Haute Alsace, Mulhouse, France.
[u]Also at Istinye University, Istanbul, Turkey.
[v]Also at Another institute or international laboratory covered by a cooperation agreement with CERN.
[w]Also at University of Hamburg, Hamburg, Germany.
[x]Also at RWTH Aachen University, III. Physikalisches Institut A, Aachen, Germany.
[y]Also at Bergische University Wuppertal (BUW), Wuppertal, Germany.
[z]Also at Brandenburg University of Technology, Cottbus, Germany.
[aa]Also at Forschungszentrum Jülich, Juelich, Germany.
[bb]Also at CERN, European Organization for Nuclear Research, Geneva, Switzerland.
[cc]Also at HUN-REN ATOMKI—Institute of Nuclear Research, Debrecen, Hungary.
[dd]Also at Universitatea Babes-Bolyai—Facultatea de Fizica, Cluj-Napoca, Romania.
[ee]Also at MTA-ELTE Lendület CMS Particle and Nuclear Physics Group, Eötvös Loránd University, Budapest, Hungary.
[ff]Also at HUN-REN Wigner Research Centre for Physics, Budapest, Hungary.
[gg]Also at Physics Department, Faculty of Science, Assiut University, Assiut, Egypt.
[hh]Also at The University of Kansas, Lawrence, Kansas, USA.
[ii]Also at Punjab Agricultural University, Ludhiana, India.
[jj]Also at University of Hyderabad, Hyderabad, India.
[kk]Also at Indian Institute of Science (IISc), Bangalore, India.
[ll]Also at University of Visva-Bharati, Santiniketan, India.
[mm]Also at IIT Bhubaneswar, Bhubaneswar, India.
[nn]Also at Institute of Physics, Bhubaneswar, India.
[oo]Also at Deutsches Elektronen-Synchrotron, Hamburg, Germany.
[pp]Also at Isfahan University of Technology, Isfahan, Iran.
[qq]Also at Sharif University of Technology, Tehran, Iran.
[rr]Also at Department of Physics, University of Science and Technology of Mazandaran, Behshahr, Iran.
[ss]Also at Department of Physics, Faculty of Science, Arak University, ARAK, Iran.
[tt]Also at Helwan University, Cairo, Egypt.
[uu]Also at Italian National Agency for New Technologies, Energy and Sustainable Economic Development, Bologna, Italy.

[vv]Also at Centro Siciliano di Fisica Nucleare e di Struttura Della Materia, Catania, Italy.
[ww]Also at Università degli Studi Guglielmo Marconi, Roma, Italy.
[xx]Also at Scuola Superiore Meridionale, Università di Napoli 'Federico II', Napoli, Italy.
[yy]Also at Fermi National Accelerator Laboratory, Batavia, Illinois, USA.
[zz]Also at Lulea University of Technology, Lulea, Sweden.
[aaa]Also at Consiglio Nazionale delle Ricerche—Istituto Officina dei Materiali, Perugia, Italy.
[bbb]Also at UPES—University of Petroleum and Energy Studies, Dehradun, India.
[ccc]Also at Institut de Physique des 2 Infinis de Lyon (IP2I), Villeurbanne, France.
[ddd]Also at Department of Applied Physics, Faculty of Science and Technology, Universiti Kebangsaan Malaysia, Bangi, Malaysia.
[eee]Also at Trincomalee Campus, Eastern University, Sri Lanka, Nilaveli, Sri Lanka.
[fff]Also at Saegis Campus, Nugegoda, Sri Lanka.
[ggg]Also at National and Kapodistrian University of Athens, Athens, Greece.
[hhh]Also at Ecole Polytechnique Fédérale Lausanne, Lausanne, Switzerland.
[iii]Also at Universität Zürich, Zurich, Switzerland.
[jjj]Also at Stefan Meyer Institute for Subatomic Physics, Vienna, Austria.
[kkk]Also at Near East University, Research Center of Experimental Health Science, Mersin, Turkey.
[lll]Also at Konya Technical University, Konya, Turkey.
[mmm]Also at Izmir Bakircay University, Izmir, Turkey.
[nnn]Also at Adiyaman University, Adiyaman, Turkey.
[ooo]Also at Bozok Universitetesi Rektörlügü, Yozgat, Turkey.
[ppp]Also at Istanbul Sabahattin Zaim University, Istanbul, Turkey.
[qqq]Also at Marmara University, Istanbul, Turkey.
[rrr]Also at Milli Savunma University, Istanbul, Turkey.
[sss]Also at Informatics and Information Security Research Center, Gebze/Kocaeli, Turkey.
[ttt]Also at Kafkas University, Kars, Turkey.
[uuu]Also at Istanbul Okan University, Istanbul, Turkey.
[vvv]Also at Hacettepe University, Ankara, Turkey.
[www]Also at Erzincan Binali Yildirim University, Erzincan, Turkey.
[xxx]Also at Istanbul University—Cerrahpasa, Faculty of Engineering, Istanbul, Turkey.
[yyy]Also at Yildiz Technical University, Istanbul, Turkey.
[zzz]Also at School of Physics and Astronomy, University of Southampton, Southampton, United Kingdom.
[aaaa]Also at Monash University, Faculty of Science, Clayton, Australia.
[bbbb]Also at Bethel University, St. Paul, Minnesota, USA.
[cccc]Also at Università di Torino, Torino, Italy.
[dddd]Also at Karamanoğlu Mehmetbey University, Karaman, Turkey.
[eeee]Also at California Lutheran University;, Thousand Oaks, California, USA.
[ffff]Also at California Institute of Technology, Pasadena, California, USA.
[gggg]Also at United States Naval Academy, Annapolis, Maryland, USA.
[hhhh]Also at Bingol University, Bingol, Turkey.
[iiii]Also at Georgian Technical University, Tbilisi, Georgia.
[jjjj]Also at Sinop University, Sinop, Turkey.
[kkkk]Also at Erciyes University, Kayseri, Turkey.
[llll]Also at Horia Hulubei National Institute of Physics and Nuclear Engineering (IFIN-HH), Bucharest, Romania.
[mmmm]Also at Another institute formerly covered by a cooperation agreement with CERN.
[nnnn]Also at Hamad Bin Khalifa University (HBKU), Doha, Qatar.
[oooo]Also at Yerevan Physics Institute, Yerevan, Armenia.
[pppp]Also at Imperial College, London, United Kingdom.
[qqqq]Also at Institute of Nuclear Physics of the Uzbekistan Academy of Sciences, Tashkent, Uzbekistan.